



UNIVERSITEIT VAN PRETORIA
UNIVERSITY OF PRETORIA
YUNIBESITHI YA PRETORIA

**Dynamic bioinformatics and isotopic evaluation of
the permeome of intraerythrocytic *Plasmodium
falciparum* parasites**

By

Mariska Naude

12063283

Submitted in partial fulfilment of the degree

Magister Scientiae Biochemistry

In the Faculty of Natural and Agricultural Sciences

University of Pretoria

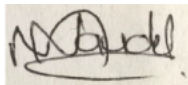
South Africa

May 2018

UNIVERSITY OF PRETORIA

Submission declaration

I, Mariska Naude, declare that the dissertation, which I hereby submit for the degree *Magister Scientiae* in the Department of Biochemistry, at the University of Pretoria, is my own work and has not previously been submitted by me for a degree at this or any other tertiary institution.



SIGNATURE:

DATE:.....11...May...2018.....

DECLARATION OF ORIGINALITY

UNIVERSITY OF PRETORIA

FACULTY OF NATURAL AND AGRICULTURAL SCIENCES

DEPARTMENT OF BIOCHEMISTRY

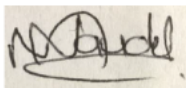
Full name: Mariska Naude

Student number: 12063283

Title of work: Dynamic bioinformatics and isotopic evaluation of the permeome of intraerythrocytic *Plasmodium falciparum* parasites

Declaration

1. I understand what plagiarism is and am aware of the University's policy in this regard.
2. I declare that this dissertation is my own original work. Where other people's work has been used (either from a printed source, Internet or any other source), this has been properly acknowledged and referenced in accordance with departmental requirements.
3. I did not make use of another student's previous work and submit it as my own.
4. I did not allow, and will not allow, anyone to copy my work with the intention of presenting it as his or her own work.



SIGNATURE:.....

DATE:.....11....May....2018.....

Acknowledgements

First and foremost, I am thankful for the Almighty God, who gave me courage and strength and also for His showers of blessings throughout my research to complete this research successfully.

I would like to express my deep and sincere gratitude to my parents, Kallie and Mari Naude, and to my boyfriend, Ruan Hattingh for providing me with unfailing support and continuous encouragement throughout my years of study and through the process of researching and writing this dissertation. This accomplishment would not have been possible without them.

I wish to thank my supervisor Dr. Jandeli Niemand (Department of Biochemistry, University of Pretoria) for giving me the opportunity to do research and providing invaluable guidance throughout this research. I am extremely grateful for what she has offered me. I would also like to thank my co-supervisor, Prof. Lyn-Marie Birkholtz (Department of Biochemistry, University of Pretoria) for her input and assistance during my research.

To all those who have contributed to this work and provided assistance and expertise, you have been extremely kind to me. I would like to especially acknowledge Riëtte van Biljon (Department of Biochemistry, University of Pretoria) who provided the transcriptome dataset of the gametocyte stages. Without her participation and input, the investigation of the transcript expression could not have been successfully conducted.

I would also like to thank my fellow students from the Malaria Parasite Molecular Laboratory (Department of Biochemistry, University of Pretoria) for their kindness and support, as well as assistance with experimental work and data analyses.

Finally, I would like to thank the National Research Foundation by funding this degree through the NRF Master's Innovation Scholarship.

Summary

The *Plasmodium falciparum* parasite is the causative agent of the most severe form of malaria. The increase in resistance against the majority of antimalarial compounds underpins the need for the development of new antimalarial compounds, targeting novel biological activities of the parasite. As the *P. falciparum* parasite develops through its life cycle stages, the parasite is exposed to different environments, resulting in both strategy-specific differences between the asexual (proliferation) and gametocyte (differentiation) stages, as well as stage-specific (i.e. ring – schizont stages; stage I - V gametocytes) differences within each strategy. These strategy- and stage-specific differences might be supported by the presence of different membrane transport proteins (MTPs) in the asexual and gametocyte stages. *P. falciparum*-encoded MTPs (permeome) are promising novel drug targets because they are specific to *P. falciparum* and essential for the survival of the *P. falciparum* parasite as these proteins mediate the uptake and removal of metabolites and waste products. However, to propose parasite-encoded MTPs as potential novel drug targets in the asexual and gametocyte stages, the presence of these MTPs in these stages should be investigated.

The *P. falciparum*-encoded permeome is well characterised in the asexual stages. However, limited knowledge is available about the permeome in the gametocyte stages. Therefore, to address this knowledge gap, the strategy- and stage-specific expression of the entire complement of parasite-encoded MTPs were investigated in the asexual and gametocyte stages to infer the presence of MTP transcripts in the absence of biochemical uptake data.

The transcript expression of the permeome revealed strategy-specific expression, with the entire permeome expressed during asexual stages, as expected, given the metabolic adaptations that support the high proliferation rate. By contrast, the gametocyte stages that are undergoing sexual differentiation towards transmission, as opposed to active proliferation, less than half of the permeome were expressed, indicating a reduced range of MTPs active in the gametocyte stages. Subsequently, stage-specific expression of the permeome was investigated by correlating stage-specific metabolic processes that occur within the asexual and gametocyte stages, to the expression profiles of MTP genes involved in these processes. Most of the MTPs involved in these processes showed stage-specific expression, with a few MTP genes showing no stage-specific expression within the asexual and gametocyte stages, respectively. When comparing the stage-specific expression between the asexual and gametocyte stages, it was observed that during the gametocyte stages, there was an absence of some MTPs (decreased expression) that were expressed during the asexual stages, suggesting that the gametocyte stages require only certain metabolites to maintain the investigated metabolic processes.

In conclusion, these expression profiles of the permeome in the asexual and gametocyte stages suggest the differential expression of the permeome in these stages. The data presented in this study provides the first complete evaluation of expression of the permeome across *P. falciparum* asexual and gametocyte stages and serves as a blueprint for future biochemical investigations of transport in these stages, thereby providing a foundation for identifying novel MTP drug targets in future drug development programmes.

Table of Contents

Acknowledgements	iv
Summary	v
List of Figures	ix
List of Tables	xi
Abbreviations	xii
Chapter 1: Introduction	1
1.1 Malaria	1
1.2 Life cycle of <i>P. falciparum</i>	2
1.3 Control strategies	4
1.3.1 Vector control	4
1.3.2 Parasite control	4
1.4 Metabolite exchange and membrane transport proteins (MTPs) as drug targets	6
1.5 MTPs in <i>P. falciparum</i> intraerythrocytic parasites	9
1.5.1 Membrane transport processes in the asexual stages	9
1.5.2 Membrane transport processes in the gametocyte stages	14
1.6 Metabolic differences between and within asexual and gametocyte stages	15
1.6.1 Strategy-specific metabolic differences between asexual and gametocyte stages	15
1.7 Hypothesis	20
1.8 Aim	20
1.9 Objectives	20
1.10 Outputs	20
Chapter 2: Materials and Methods	22
2.1 <i>In silico</i> analyses of the permeome of <i>P. falciparum</i> parasites	22
2.1.1 Identification of the current permeome encoded by <i>P. falciparum</i> parasites	23
2.1.2 Characterisation of the 11 newly identified MTPs	24
2.1.3 The functional characterisation of the permeome	24
2.2 Analyses of strategy- and stage-specific expression of the permeome	25
2.3 Experimental analysis of metabolite uptake in <i>P. falciparum</i> asexual parasites	26
2.3.1 Erythrocyte collection and storage	26
2.3.2 Asexual parasite cultivation	26
2.3.3 Isotopic evaluation of the permeome in <i>P. falciparum</i> parasites	27
Chapter 3: Results	30
3.1 <i>In silico</i> evaluation and characterisation of the permeome encoded by <i>P. falciparum</i> parasites	30
3.1.1 Identification of the permeome	30

3.1.2	Characterisation of the 11 newly identified MTPs	34
3.1.3	Identification of MTPs essential for <i>P. falciparum</i> intraerythrocytic parasites	38
3.2	The strategy- and stage-specific expression of the permeome	40
3.2.1	Strategy-specific expression of the permeome	41
3.2.2	Stage-specific expression of the permeome	44
3.3	Functional studies of metabolite uptake in <i>P. falciparum</i> parasites	57
3.3.1	<i>In vitro</i> <i>P. falciparum</i> asexual parasite cultivation	57
3.3.2	<i>P. falciparum</i> intraerythrocytic trophozoite stage enrichment	58
3.3.3	Uptake of 2DG into <i>P. falciparum</i> uninfected RBCs and trophozoite iRBCs.....	58
3.3.4	Uptake of amino acids into <i>P. falciparum</i> uninfected RBCs and trophozoite iRBCs.....	60
Chapter 4: Discussion		62
Chapter 5: Concluding Discussion		73
References		75
Supplementary material		102

List of Figures

Figure 1: The life cycle of <i>P. falciparum</i> parasites.....	2
Figure 2: Five stages of <i>P. falciparum</i> gametocyte development.....	3
Figure 3: Classes of integral membrane proteins.....	7
Figure 4: Morphological differences between asexual and gametocyte stages.	14
Figure 5: The workflow that was followed for the identification and characterisation of the current permeome encoded by the <i>P. falciparum</i> genome.....	22
Figure 6: Classification of the <i>P. falciparum</i> -encoded permeome into specific integral membrane protein classes.	35
Figure 7: Comparison of hydropathy plots of the 11 new MTPs to a typical MTP hydropathy plot generated using ProtScale – Kyte & Doolittle hydropathy input.....	37
Figure 8: The phenotype distribution of each MTP gene in the specific integral membrane protein classes.	39
Figure 9: Determination of the optimum number of transcript expression clusters, using elbow plots.....	40
Figure 10: Transcript expression profiles of the MTP genes in <i>P. falciparum</i> asexual stages.	41
Figure 11: Transcript expression profiles of the MTP genes in <i>P. falciparum</i> gametocyte stages..	43
Figure 12: Constitutively expressed MTP genes in both asexual (green) and gametocyte (blue) stages.....	44
Figure 13: Stage-specific transcript expression profiles of six amino acid transporter genes throughout the asexual stages, clustered using Euclidian distance in similar profiles of transcript expression.....	45
Figure 14: Stage-specific transcript expression profiles of MTP genes involved in carbohydrate metabolism (glycolysis and TCA cycle) throughout the asexual stages, clustered using Euclidian distance in similar patterns of transcript expression.....	46
Figure 15: Stage-specific transcript expression profiles of four PfNT genes throughout the asexual stage, clustered using Euclidian distance in similar patterns of transcript expression.	47
Figure 16: Stage-specific transcript expression profiles throughout the asexual stages of lipid-related MTP genes, clustered using Euclidian distance in similar patterns of transcript expression.	48
Figure 17: Stage-specific transcript expression profiles of six amino acid transporter genes throughout the gametocyte stages, clustered using Euclidian distance in similar patterns of transcript expression.	49
Figure 18: Stage-specific transcript expression profiles throughout the gametocyte stages of MTP genes involved in carbohydrate metabolism, clustered using Euclidian distance in similar patterns of transcript expression.	50

Figure 19: Stage-specific transcript expression profile of a nucleoside transporter gene throughout the gametocyte stages, clustered using Euclidian distance in similar patterns of transcript expression.	51
Figure 20: Stage-specific transcript expression profiles throughout the gametocyte stages of lipid-related MTP genes, clustered using Euclidian distance in similar patterns of transcript expression.	52
Figure 21: Stage-specific transcript expression profiles throughout the asexual stages of ion transporting MTP genes grouped according to ions.....	53
Figure 22: Stage-specific transcript expression profiles throughout the gametocyte stages of MTPs transporting ions grouped according to ions.	55
Figure 23: The microscopic evaluation of the cultivation of different stages of <i>P. falciparum</i> asexual parasites.....	57
Figure 24: Microscopic evaluation of the enriched mature trophozoite stages prior and following magnetic enrichment.	58
Figure 25: The uptake of [¹⁴ C]-2DG into uninfected RBCs and trophozoite iRBCs.....	59
Figure 26: The uptake of 1 μCi/ml [¹⁴ C]-leucine, [¹⁴ C]-lysine, [¹⁴ C]-glutamic acid and [¹⁴ C]-aspartic acid into uninfected RBCs (blue) and trophozoite iRBCs (red).	60

List of Tables

Table 1: An overview of target candidate profiles (TCPs) required for molecules that are subsequently developed into therapies with the requisite target product profile (TPPs).....	5
Table 2: The predicted <i>P. falciparum</i> -encoded MTPs across the EPM in asexual parasites.....	10
Table 3: The predicted <i>P. falciparum</i> -encoded MTPs across the PPM in asexual parasites.....	12
Table 4: Putative MTP genes identified with keyword searches and a TMD (2-30 domains) search, using the TMHMM algorithm.	30
Table 5: Overview of the current <i>P. falciparum</i> -encoded permeome.	32
Supplementary Table 1: An overview of the endogenous erythrocyte MTPs, NPP and the MTPs across the PVM in the asexual parasites.	102
Supplementary Table 2: Classification of <i>P. falciparum</i> -encoded MTPs.....	103
Supplementary Table 3: The phenotypic data of the MTP genes identified in <i>P. berghei</i> and <i>P. falciparum</i>	109

Abbreviations

2DG	2-deoxyglucose
2DG6P	2DG-6-phosphate
ABC	ATP-binding cassette transporter
ACT	Artemisinin-based combination therapies
ATP	Adenosine triphosphate
BLASTP	Basic Local Alignment Search Tool Protein
CIC-2	Chloride channel 2
<i>clag3</i>	cytoadherence-linked asexual gene 3
DNA	Deoxyribonucleic acid
EPM	Erythrocyte plasma membrane
EXP2	Exported protein 2
GMAP	Global Malaria Action Plan
GMEP	Global Malaria Eradication Programme
GO	Gene Ontology
GTS	Global Technical Strategy
HEPES	4-(2-hydroxyethyl)-1-piperazineethanesulfonic acid
HMM	Hidden Markov Model
HP1	Heterochromatin protein 1
hpi	h post merozoite invasion
IMC	Inner membrane complex
iRBC	Infected erythrocyte
IRS	Indoor residual spraying
ITNs	Insecticide-treated mosquito nets
IUMBM	International Union of Biochemistry and Molecular Biology
KEGG	Kyoto Encyclopedia of Genes and Genomes
malERA	Malaria Eradication Research Agenda
MPMP	Malaria Parasite Metabolic Pathways
mRNA	messenger RNA
MTP	Membrane transport protein
NADH	Nicotinamide adenine dinucleotide
NPC	Nuclear pore complex

NPP	New permeation pathways
NTF2	Nuclear transport factor 2 protein
PbHT	<i>P. berghei</i> hexose transporter
PbNPT1	<i>P. berghei</i> novel putative transporter 1
PBS	Phosphate buffered saline
PfACT	<i>P. falciparum</i> Acetyl-CoA transporter
PfATP4	<i>P. falciparum</i> Ca ²⁺ transporting P-ATPase
PfCRT	<i>P. falciparum</i> chloroquine-resistant transporter
PfDTC	<i>P. falciparum</i> dicarboxylate/tricarboxylate carrier
PfFNT	<i>P. falciparum</i> formate-nitrite transporter
PfHT	<i>P. falciparum</i> hexose transporter
PfK	<i>P. falciparum</i> K ⁺ ion channel
PfMDR	<i>P. falciparum</i> multidrug resistance protein
PfMIT	<i>P. falciparum</i> CorA-like magnesium transporter
PfMRP	<i>P. falciparum</i> multidrug resistance-associated protein
PfNHE	<i>P. falciparum</i> Na ⁺ /H ⁺ exchanger
PfNPT	<i>P. falciparum</i> novel putative transporter
PfNT	<i>P. falciparum</i> nucleoside transporter
PfPgh1	<i>P. falciparum</i> P-glycoprotein homologue 1
PfPit	<i>P. falciparum</i> sodium-dependent phosphate transporter
PfPPT	<i>P. falciparum</i> phosphoenolpyruvate/phosphate translocator
PfSulP	<i>P. falciparum</i> inorganic anion exchanger
PfTPT	<i>P. falciparum</i> triose phosphate transporter
PfVP	<i>P. falciparum</i> V-type H ⁺ -translocating pyrophosphatase
PPM	Parasite plasma membrane
PSAC	Plasmodial surface anion channel
PTEX	<i>Plasmodium</i> translocon of exported proteins
PVM	Parasitophorous vacuolar membrane
RBC	Erythrocyte
RBM	Roll Back Malaria
RNA	Ribonucleic acid
SSE	Sum of squared error

TCA	Tricarboxylic acid
TCDB	Transport Classification Database
TCPs	Target candidate profiles
TgNPT 1	<i>T. gondii</i> novel putative transporter 1
TMD	Transmembrane domain
TPPs	Target product profiles
WHO	World Health Organisation

Chapter 1: Introduction

1.1 Malaria

Malaria is a major public health problem with 91 countries reporting a total of 216 million malaria cases in 2016, which led to 445 000 deaths, mostly affecting children under 5 years of age (World Health Organisation, 2017). About 90% of these cases and deaths occurred in the World Health Organisation (WHO) African region¹ and 80% of the global malaria burden is carried by 15 countries, including India and all sub-Saharan African countries (World Health Organisation, 2017).

In spite of the prevalence of malaria, the incidence and mortality rates of malaria have decreased in the past decades, which can be largely attributed to global malaria elimination and eradication programmes. The WHO embarked on the Global Malaria Eradication Programme (GMEP) from 1955 – 1969, which achieved a reduction in the geographical distribution of malaria as well as the elimination of malaria in many countries (Nájera *et al.*, 2011; World Health Organisation, 1973). However, in countries such as Venezuela and Thailand, there was a resurgence of malaria, highlighting the fact that no single strategy to either eliminate or eradicate malaria can be applied everywhere and that a long-term commitment to a flexible strategy is needed (Makowski, 2017; Nájera *et al.*, 2011). In 2007, a renewed Global Malaria Action Plan (GMAP) was adopted, supported by the WHO and the Roll Back Malaria (RBM) Partnership, to move from malaria control to elimination and ultimately eradication (Alonso *et al.*, 2011). The GMAP was further complemented by the establishment of the Malaria Eradication Research Agenda (malERA) in 2011, which resulted in an 18% decline in malaria cases and 48% decline in malaria deaths by 2015 (World Health Organisation, 2015b; Alonso *et al.*, 2011). This global initiative has been extended by the WHO Global Technical Strategy (GTS) for Malaria 2016 - 2030, together with the RBM Partnership, to accelerate the progress towards malaria elimination. The GTS aims at a global reduction of at least 90% in malaria case incidence and mortality rates, as well as elimination in 35 countries by 2030 (World Health Organisation, 2015a).

Malaria in humans is caused by five different species of protozoan parasites from the *Plasmodium* family: *Plasmodium falciparum*, *P. vivax*, *P. malariae*, *P. ovale* and *P. knowlesi*. The *P. vivax* and *P. ovale* parasites have dormant liver stages, but the mechanism that drives dormancy and reactivation is still unknown (Wells *et al.*, 2010). *P. knowlesi* parasites typically infect primates, but in 2004, it was found to also infect humans (Jongwutiwes *et al.*, 2004). *P. malariae* infections are not usually life threatening (Marcus and Babcock, 2009), while in contrast, *P. falciparum* parasites

¹ WHO African region includes Algeria, Angola, Benin, Botswana, Burkina Faso, Burundi, Cameroon, Cape Verde, Chad, Central African Republic, Congo, Democratic Republic of Congo, Equatorial Guinea, Eritrea, Ethiopia, Gabon, Gambia, Ghana, Guinea, Guinea-Bissau, Ivory Coast, Kenya, Lesotho, Liberia, Madagascar, Malawi, Mali, Mauritania, Mauritius, Mozambique, Namibia, Niger, Nigeria, Rwanda, Sao Tome and Principe, Senegal, Seychelles, Sierra Leone, South Africa, Swaziland, Togo, Uganda, United Republic of Tanzania, Zambia and Zimbabwe.

are responsible for the majority of malaria deaths and are most prevalent in sub-Saharan Africa (World Health Organisation, 2017). Therefore, *P. falciparum* parasites are the main focus in South African malaria research.

1.2 Life cycle of *P. falciparum*

The life cycle of *P. falciparum* parasites occurs in two hosts: the mosquito vector and the human host (Sherman, 1979) and has distinct phases of development (Fig. 1).

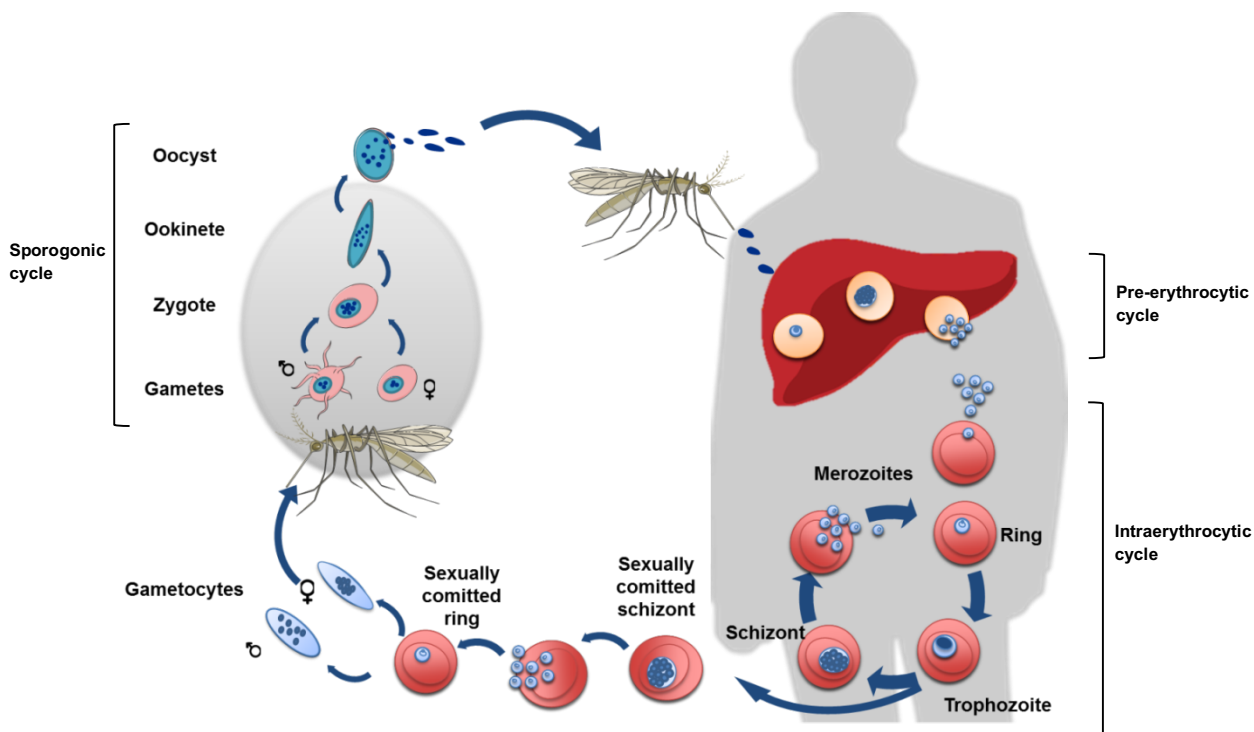


Figure 1: The life cycle of *P. falciparum* parasites During a blood meal of the infected female *Anopheles* mosquito, sporozoites are injected into the human host, where they develop through the pre-erythrocytic cycle in the liver and subsequent intraerythrocytic cycle. In the intraerythrocytic cycle, these parasites develop through the ring, trophozoite, schizont and merozoite stages. A small portion of asexual parasites differentiates into male or female gametocyte stages, which can be taken up by a mosquito, leading to the sporogonic cycle and the repeat of the life cycle of *P. falciparum* parasites. This work “The life cycle of *P. falciparum* parasites” was compiled using graphic components from “Creative Commons Infectiology” by Servier, used under CC BY 3.0.

The pre-erythrocytic cycle begins, when sporozoites from the salivary glands of the mosquito are injected into a human host during a blood meal, and subsequently migrate to the liver, where hepatocytes are invaded within an hour (Shortt *et al.*, 1949). The sporozoites remain for 9 – 16 days in the hepatocytes, developing into multinucleated schizonts. The intraerythrocytic cycle initiates when the hepatic schizonts rupture, releasing thousands of merozoites into the bloodstream, which invade erythrocytes (Miller *et al.*, 2002; Cowman and Crabb, 2006). The intraerythrocytic parasites subsequently develop through the ring, trophozoite and schizont stages that form developmental stages associated with proliferating asexual parasites (Bannister and Mitchell, 2003; Salcedo-Sora *et al.*, 2014).

Following the development of mature schizont stages, the erythrocytes rupture and each schizont stage releases 6 – 32 daughter merozoites (Wipasa *et al.*, 2002) into the blood to invade new erythrocytes. The asexual cycle is then repeated, resulting in an increase in parasitaemia and the development of the symptoms of malaria, including fever, headache, fatigue, muscle pain, diarrhoea and hyperventilation, amongst others (Lagerberg, 2008).

During intraerythrocytic development, a small portion ($\leq 10\%$) of parasites do not undergo asexual proliferation, but differentiates into nearly quiescent non-dividing sexual, gametocyte stages that await reactivation in the mosquito vector (Talman *et al.*, 2004; Dixon *et al.*, 2008). All the merozoites from a single schizont commit to gametocyte development to form sexually - committed ring stages (Drakeley *et al.*, 2006). These subsequently undergo gametocytogenesis (Talman *et al.*, 2004) as characterised by five morphological recognisable stages, early gametocyte stages (stage I – III) and late gametocyte stages (stage IV – V) (Fig. 2) (Sinden, 1982).



Figure 2: Five stages of *P. falciparum* gametocyte development. The morphological differentiation of gametocyte stages happens in about 10 – 14 days, during which the gametocyte matures through five morphological stages. This work “Five stages of *P. falciparum* gametocyte development” was compiled using graphic components from “Creative Commons Infectiology” by Servier, used under CC BY 3.0.

Initially, stage I and IIa gametocytes are morphologically indistinguishable from asexual parasites (early trophozoite stages) (Dixon *et al.*, 2012; Talman *et al.*, 2004), with stage IIb the first morphologically distinguishable stage with a spherical structure that contains only one nucleus, where asexual parasites of the same size will contain four nuclei (Dixon *et al.*, 2012). Stage I – IV gametocytes are absent from blood circulation and sequester in the bone marrow to avoid clearance by the spleen (Meibalan and Marti, 2017). Here, stage III gametocytes will start to develop into D-shaped parasites due to the extension of the one side of these parasites (Dixon *et al.*, 2012; Talman *et al.*, 2004). By stage IV, these parasites have elongated further, and the erythrocytes are only present as a thin layer around these parasites (Dixon *et al.*, 2012). Stage V gametocytes become more rounded at the ends, exhibiting a sausage shape (Dixon *et al.*, 2012), which differentiate into male (microgametocytes – nuclear material is scattered) or female (macrogametocytes – compact nuclear material) gametocytes (Smith *et al.*, 2000; Silvestrini *et al.*, 2000) and reappear in the blood circulation as the only stage that can be transmitted to mosquitoes.

The sporogonic cycle starts, when stage V gametocytes are ingested by the mosquito during a blood meal and migrate to the mosquito gut, where they mature to form male and female gametes (Fig. 1) (Eksi *et al.*, 2006). After fertilisation, the zygote develops into an ookinete, which in turn

develops to an oocyst, from which sporozoites are released that migrate to the salivary glands, leading to the repeat of the *P. falciparum* parasite's life cycle (Wipasa *et al.*, 2002).

In summary, the development of these parasites through their multi-stage life cycle is crucial for the survival and transmission of *P. falciparum* parasites. However, the plasticity of the mosquito vector and *P. falciparum* parasites has made it difficult to control and ultimately eliminate malaria (Smith *et al.*, 2014) by solely targeting either the vector or the parasites. Therefore, for the goal of malaria elimination, integrative control strategies are needed (Birkholtz *et al.*, 2012).

1.3 Control strategies

Integrative control strategies include vector control and parasite control, which can contribute to the treatment and possible eradication of malaria (Hemingway *et al.*, 2016).

1.3.1 Vector control

Vector control can contribute to malaria elimination by (i) reducing the malaria vector capacities (rate at which future infections arise from currently infected vectors), (ii) improving the effectiveness of existing insecticide-based interventions and (iii) targeting vector species not affected by current vector control strategies (malERA, 2011). There are four classes of insecticides that are commonly used in malaria vector control, which include organophosphates, organochlorides, carbamates and pyrethroids (Kelly-Hope *et al.*, 2008). These insecticides are being used for indoor residual spraying (IRS) (Enayati and Hemingway, 2010) and insecticide-treated mosquito nets (ITNs) (Enayati and Hemingway, 2010; Touré, 2001). However, insecticide resistant *Anopheles* mosquitoes limit the efficacy of vector control (Corbel *et al.*, 2007; Ranson *et al.*, 2009), necessitating the use of simultaneous parasite control when combating malaria.

1.3.2 Parasite control

Parasite control aims to target the different life cycle stages of *Plasmodium* parasites with the emphasis on breaking the cycle of parasite development or transmission (Burrows *et al.*, 2017). Parasite control includes vaccine development as well as the use of chemotherapies.

1.3.2.1 Vaccine development

Three different approaches towards the development of antimalarial vaccines have been explored: (i) pre-erythrocytic vaccines (targeting the liver stages that should prevent blood-stage infection), (ii) blood-stage vaccines (targeting the intraerythrocytic stages to ultimately clear parasitaemia and prevent clinical disease) and (iii) transmission-blocking vaccines (targeting the gametocyte stages to prevent the transmission of the parasite to the mosquito vector) (Hemingway *et al.*, 2016). However, vaccine development is challenging due to the adaptable nature of the parasite,

antigenic variation and lack of knowledge about the interaction between the human immune system and *P. falciparum* parasites (Crompton *et al.*, 2010). RTS,S, a pre-erythrocytic vaccine, was developed for the prevention of clinical *Plasmodium* malaria in children and is the first malaria vaccine to complete phase III clinical trials (Hemingway *et al.*, 2016). However, the trial demonstrated a vaccine efficacy of only 50% in children aged 5 – 17 months and only 30% efficacy in infants (Theander and Lusingu, 2015). While RTS,S validates the development of malaria vaccines, an ideal vaccine candidate would need to have a higher efficacy than what is currently achieved.

1.3.2.2 Chemotherapies

In antimalarial drug discovery, there are specific requirements for the types of molecules (target candidate profiles (TCPs)) that will ultimately lead to medicines (target product profiles (TPPs), Table 1) (Burrows *et al.*, 2017). The TCPs and TPPs are strategic tools to provide guidance during drug discovery and development of ideal medicines.

Table 1: An overview of target candidate profiles (TCPs) required for molecules that are subsequently developed into therapies with the requisite target product profile (TPPs) Adapted from (Burrows *et al.*, 2017).

Profile	Intended use
TPP-1	Treatment of acute uncomplicated malaria in children/adults. Combination of two or more molecules with TCP-1, TCP-5 for reducing transmission and TCP-3 for relapse prevention
TPP-2	Chemoprotection: given to subjects migrating into areas of high endemicity, or during epidemics. Combination of TCP-4, potentially with TCP-1 for emerging infections
TCP-1	Molecules that clear asexual stages
TCP-2	Profile retired
TCP-3	Molecules with activity against hypnozoites (mainly <i>P. vivax</i>)
TCP-4	Molecules with activity against hepatic schizonts
TCP-5	Molecules that block transmission (targeting gametocyte stages)
TCP-6	Molecules that block transmission by targeting the insect vector

TCP-1 focuses on the clearance of asexual stages, therefore, reducing the parasite burden and ultimately relieving the symptoms of malaria (Burrows *et al.*, 2017). Previously used antimalarials that comply with this profile include the quinoline-related compounds, antifolates and artemisinin derivatives (Delves *et al.*, 2012). Of these, artemisinin-based combination therapies (ACTs), where quick-acting artemisinin or one of its derivatives (e.g. artesunate, artemether, dihydroartemisinin) are combined with longer-lasting partner drugs such as mefloquine, amodiaquine or lumefantrine, are currently recommended by the WHO as the first-line treatment for *P. falciparum* malaria (World Health Organisation, 2017).

TCP-5 focuses on targeting gametocyte stages to prevent the transmission from the human host to the mosquito vector (Burrows *et al.*, 2017). Transmission blocking requires killing stage V gametocytes or rendering them non-functional and not able to form gametes. However, the biology of gametocyte development is not fully understood, making it difficult to develop transmission-blocking antimalarial compounds. Primaquine is the only licenced drug that is active against stage V gametocytes, leading to reduced gametocyte carriage (Butterworth *et al.*, 2013). However, the clinical evidence of this reduced gametocyte carriage translating to reducing transmission dynamics is not established (Rodrigo *et al.*, 2016). Furthermore, side effects are observed with the use of primaquine, such as haemolytic anaemia (Bolchoz *et al.*, 2001) and methaemoglobin formation (Anders *et al.*, 1988), especially in patients with glucose-6-phosphate dehydrogenase deficiency (Carson *et al.*, 1956). Several other drugs, such as tafenoquine, methylene blue and the endoperoxides OZ439 and OZ277, with activity against gametocytes, are currently in clinical development (Butterworth *et al.*, 2013).

The ideal medicine is captured in TPP-1, which is described by a combination of TCP-1 (treatment of asexual stages), TCP-3 (antihypnozoite activity) and TCP-5 (transmission-blocking activity) (Table 1). For *P. falciparum*, the ideal medicine will only include TCP-1 and TCP-5 activities since TCP-3 focuses on targeting the dormant liver stages of *P. vivax* and *P. ovale* infections (Burrows *et al.*, 2017).

Parasite resistance has emerged against quinolones (Foley and Tilley, 1997), antifolates (Gregson and Plowe, 2005) and artemisinin (Noedl *et al.*, 2010), even when used in combination therapies (Saifi *et al.*, 2013). Therefore, to comply with TCP-1 and TCP-5 to generate medicines as described by TPP-1, there is a need for the continuous development of new antimalarial compounds targeting novel biological activities in the parasite, in both asexual and gametocyte stages. It is thus particularly important for ongoing functional studies of *P. falciparum* parasites to highlight potential novel drug targets that have important biological roles in the asexual and gametocyte stages.

1.4 Metabolite exchange and membrane transport proteins (MTPs) as drug targets

Proteins that are essential for survival, and specific to the disease-causing organism, are ideal drug targets as these ensure efficiency, while maintaining selectivity. One group of proteins that are absolutely essential for survival is membrane transport proteins (MTPs) since only a few molecules such as uncharged non-polar compounds can cross the phospholipid bilayer via simple diffusion (Kirk and Lehane, 2014). As the exchange of most metabolites across the phospholipid bilayer is mediated by MTPs, these proteins play important physiological roles in all cells, including metabolite uptake (import) for metabolism, removal (export) of waste products from metabolic

pathways, as well as the exchange of metabolites between organelles and maintenance of the electrochemical gradient (Kenthirapalan *et al.*, 2016).

MTPs can be divided into three classes of integral membrane proteins embedded by multiple transmembrane domains (TMDs): (i) Channels, (ii) ATP-powered pumps and (iii) Transporters (Staines *et al.*, 2010; Lodish *et al.*, 2016). Channels transport water molecules, specific ions or hydrophilic small molecules across membranes down the concentration gradient without the requirement of energy (Fig. 3 A) (Lodish *et al.*, 2016). These channels are formed by a hydrophilic tube, which can consist of α -helices and/or β -sheets across the membrane, through which the water molecules or ions move (Catterall, 1995; Hiller and Wagner, 2009; MacKinnon, 1995). Channels can be classified as either non-gated or gated channels. Non-gated channels are open most of the time, and gated channels open only in response to specific chemical or electrical signals. In both instances, channels remain selective for the type of molecule being transported (Lodish *et al.*, 2016). ATP-powered pumps are responsible for active transport, where ions or small molecules are transported against the concentration gradient, which requires energy that is coupled to the hydrolysis of ATP (Fig. 3 B) (Lodish *et al.*, 2016). Transporters, also known as carriers, mediate the transport of molecules across the membrane that is based on highly specific substrate-binding induced conformational changes of the transporter. Transporters consist of three different groups that include uniporters, antiporters and symporters (Fig. 3 C, D and E) (Lodish *et al.*, 2016). Uniporters transport a single molecule down its concentration gradient with no energy requirement. Antiporters and symporters couple the movement of one type of molecule against its concentration gradient with the transport of another molecule down its concentration gradient (same direction – symporter, different direction – antiporter) (Lodish *et al.*, 2016).

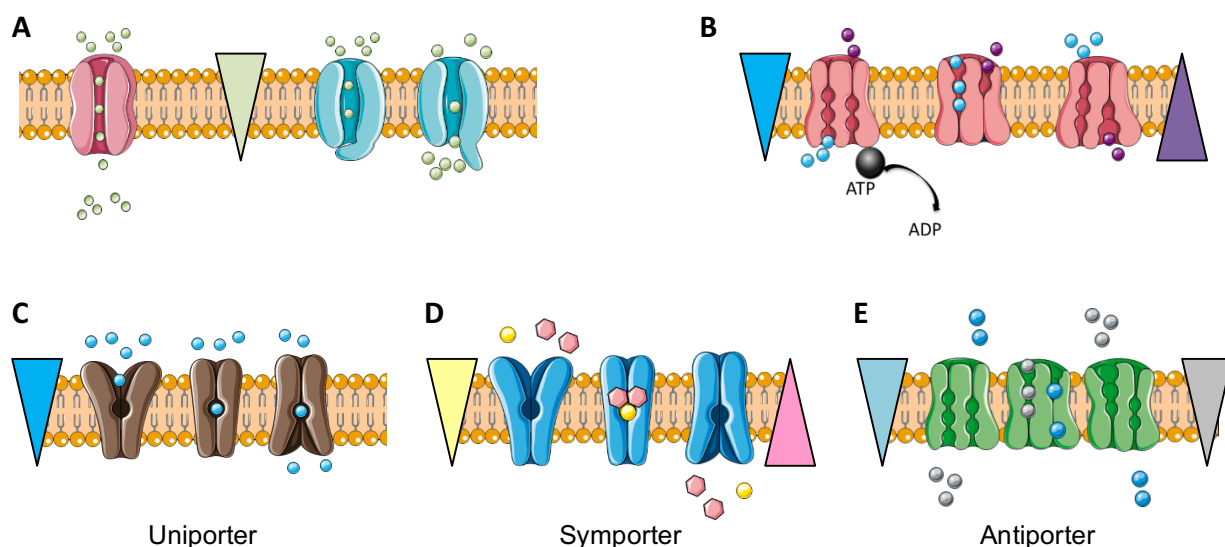


Figure 3: Classes of integral membrane proteins. The triangles represent the direction of the concentration gradient. (A) Channels mediate the transport of water molecules, ions or small molecules across the membrane down the concentration gradient. (B) ATP-powered pumps mediate the transport of molecules against the concentration gradient due to ATP hydrolysis. Transporters mediate the transport of molecules across the membrane due to a conformational change of the transporter protein. Transporters

consist of three different groups: (C) uniporters, (D) symporters and (E) antiporters (Lodish *et al.*, 2016). This work “Classes of integral membrane proteins” was compiled using graphic components of “Creative Commons Receptors and Channels” by Servier, used under CC BY 3.0.

In *P. falciparum* parasites, MTPs are promising drug targets as MTPs ensure survival in the host cell by mediating the uptake of essential metabolites and removal of waste products across multiple membranes. These MTPs are also used by antimalarial compounds to either reach their target site (Basore *et al.*, 2015) or are directly targeted to kill the parasite (Desai *et al.*, 2016). Furthermore, *P. falciparum* MTPs can also be involved in antimalarial drug resistance. Chloroquine resistance is enabled by the export of chloroquine from the acidic digestive vacuole through the activity of a mutated *P. falciparum* chloroquine-resistant transporter (PfCRT) (Martin and Kirk, 2004). In addition to chloroquine resistance, the mutated PfCRT also increases parasite susceptibility to other antimalarial drugs such as artemisinin and mefloquine (Sidhu *et al.*, 2002; Sanchez *et al.*, 2010). The mutated *P. falciparum* P-glycoprotein homologue 1 (PfPgh1, also known as the *P. falciparum* multidrug resistance protein 1 – PfMDR1) also confers resistance to chloroquine, mefloquine, quinine and halofantrine (Reed *et al.*, 2000). Other MTPs, including the *P. falciparum* Na⁺/H⁺ exchanger (PfNHE) (Ferdig *et al.*, 2004) and the *P. falciparum* multidrug resistance-associated protein 1 (PfMRP1) (Raj *et al.*, 2009) decrease parasite drug sensitivity. A number of other candidate transporter proteins showed altered expression in drug-resistant and/or drug-treated parasites (Gunasekera *et al.*, 2003; Jiang *et al.*, 2008). However, only a small portion of the *P. falciparum* genome (2 - 3%) is annotated as MTPs (Ren *et al.*, 2007), which implies that the parasite tends to not have multiple MTPs for the transport of the same metabolites (Martin *et al.*, 2005). Therefore, compounds targeting a single MTP that transports an essential metabolite required for parasite survival may be highly effective, as the parasite is then unlikely to have alternative MTPs for the same metabolite. Currently, there are new potent antimalarial drugs including the spiroindolones and dihydroisoquinolones under clinical evaluation, which are known to target the *P. falciparum* Ca²⁺ transporting P-ATPase (PfATP4), resulting in severe disturbance of the Na⁺ homeostasis in the parasite (Rottmann *et al.*, 2010; Spillman *et al.*, 2013b; Jiménez-Díaz *et al.*, 2014). There is also antimalarial compounds targeting MTPs that are being explored in various other species (Meier *et al.*, 2018). Accordingly, MTPs are validated drug targets, as these rank among the top five protein classes that are molecular targets of FDA approved drugs, making up 20% of the currently druggable protein families (Overington *et al.*, 2006).

Since it is clear that MTPs are promising novel drug targets in *P. falciparum* parasites, it is imperative that the presence and absence of MTPs in asexual and gametocyte stages should be investigated to ultimately generate medicines that comply with TCP-1 and TCP-5 (Table 1).

1.5 MTPs in *P. falciparum* intraerythrocytic parasites

In *P. falciparum* parasites, MTPs mediate the exchange of specific metabolites, metabolic waste and inorganic ions that are required for the growth and development of these parasites, across membranes enclosing different cell compartments (Kirk and Lehane, 2014). Although biochemical studies have identified the uptake of a wide range of solutes across these membranes, there are still relatively few cases where the MTP involved has been identified. This knowledge gap was addressed by previous bioinformatic analyses that investigated the genome of *P. falciparum* parasites to identify all MTPs encoded by *P. falciparum* parasites (Martin *et al.*, 2009; Martin *et al.*, 2005). These 136 identified *P. falciparum*-encoded MTPs, termed the predicted “permeome” included candidate transporters for a range of metabolites (sugars, amino acids, nucleosides and vitamins), a number of ion channels as well as MTPs predicted to be involved in maintaining ion homeostasis of the parasite (Martin *et al.*, 2005).

These identified *P. falciparum*-encoded MTPs are still part of the overall membrane transport processes of the parasite that also include endogenous erythrocyte MTPs. The following sections contain a brief overview of the membrane transport processes in asexual and gametocyte stages, with specific focus on the expression of the permeome (parasite-encoded MTPs) across the different membranes as these MTPs are specific to the parasite and would therefore, be promising novel drug targets.

1.5.1 Membrane transport processes in the asexual stages

Asexual parasites are separated from the extracellular environment by the erythrocyte plasma membrane (EPM), a parasitophorous vacuolar membrane (PVM) and the parasite plasma membrane (PPM) (Kirk, 2001). The parasite also contains different organelles that include an acidic digestive vacuole and a smaller acidocalcisome, both confined by single membranes, a single mitochondrion confined by double membranes, and a vestigial plastid, the apicoplast, confined by four membranes (Köhler *et al.*, 1997; Van Dooren *et al.*, 2006; Kirk, 2001; Martin *et al.*, 2009; Kirk and Lehane, 2014).

The membrane transport processes in the asexual stages thus include the use of both endogenous erythrocyte and parasite-encoded MTPs on the EPM; modification of erythrocyte permeability through the induction of new permeation pathways (NPP) as well as a variety of parasite-encoded MTPs across the PPM.

1.5.1.1 Transport across the EPM

After the *P. falciparum* parasite infected the erythrocyte, some endogenous erythrocyte MTPs remain active (Supplementary Table 1) (Kirk and Lehane, 2014; Kirk, 2001), while other endogenous transporters' characteristics are altered. For example, erythrocytes infected with

P. falciparum parasites show increased activity of the Na⁺/K⁺ pump (Staines *et al.*, 2001) and a significant increase in the maximum velocity (V_{max}) for the saturable component of tryptophan uptake (Ginsburg and Krugliak, 1983). Different endogenous erythrocyte transporters are also activated after *P. falciparum* infection, which include a chloride channel 2 (ClC-2) anion selective channel (Huber *et al.*, 2004) and a glutamate transporter (Winterberg *et al.*, 2012).

Additionally, an increase in the permeability of the EPM to low-molecular-mass solutes required for macromolecular synthesis, including amino acids, peptides, nucleosides and various organic and inorganic ions is observed. This increase in permeability is attributed to parasite-induced NPP (Ginsburg *et al.*, 1985; Kirk *et al.*, 1994). The NPP display anion channel properties (Krugliak and Ginsburg, 2006) with anion substrate preferences (Supplementary Table 1) (Kirk *et al.*, 1994). However, the number and identity of the channels still remain unclear. One candidate for NPP is the plasmoidal surface anion channel (PSAC) that correlates with reduced metabolite uptake with the addition of a PSAC inhibitor (Pillai *et al.*, 2012). Another study reported that cytoadherence-linked asexual gene 3 (*clag3*) proteins are responsible for the activity of the PSAC (Nguiragool *et al.*, 2011) although the exact mechanism for channel activity has not been established.

Parasite-encoded MTPs are also predicted to be present on the EPM (Table 2), which include a copper P-ATPase transporter (PF3D7_0904900) (Rasoloson *et al.*, 2004), a K⁺ ion channel (PfK1, PF3D7_1227200) (Waller *et al.*, 2008) and a multi-subunit V-type H⁺-ATPase transporter (Marchesini *et al.*, 2005).

Table 2: The predicted *P. falciparum*-encoded MTPs across the EPM in asexual parasites. The localisation of the parasite-encoded MTPs to the EPM has been determined using antibodies, and the metabolites of these MTPs are also summarised below.

Parasite-encoded MTPs on EPM				
Transporter	Gene ID	Metabolite	Function	Reference
K ⁺ ion channel (PfK1)	PF3D7_1227200	K ⁺	Effect maintenance of the membrane potential and electrochemical gradient across the erythrocyte plasma membrane	(Waller <i>et al.</i> , 2008)
Copper P – ATPase	PF3D7_0904900	Reduced copper	Export copper to reduce its toxicity	(Rasoloson <i>et al.</i> , 2004)
V - H ⁺ - ATPase	PF3D7_0519200 PF3D7_0806800 PF3D7_1354400 PF3D7_1464700 PF3D7_1140100 PF3D7_0406100 PF3D7_0106100 PF3D7_1311900 PF3D7_1323200 PF3D7_1341900 PF3D7_1306600 PF3D7_0934500	H ⁺	Regulate intracellular pH and plasma membrane potential	(Marchesini <i>et al.</i> , 2005)

1.5.1.2 Transport across the PVM

The PVM enclosing the intracellular parasite is formed at the time of invasion and expands as the parasite matures from ring to trophozoite to schizont stages. The transport mechanisms of PVM include a 140-pS channel (Desai *et al.*, 1993; Desai and Rosenberg, 1997), postulated to be a parasite exported protein 2 (EXP2) that forms the membrane-associated component of the *Plasmodium* translocon of exported proteins (PTEX) complex (de Koning-Ward *et al.*, 2009). This PVM channel is open more than 98% of the time at the resting potential of the PVM, thus indicating that the PVM acts as a molecular sieve (Desai and Rosenberg, 1997), which is highly permeable to small solutes, including both anions and cations, lysine, glucuronate, and can readily transport amino acids and monosaccharides (Supplementary Table 1) (Desai *et al.*, 1993; Desai and Rosenberg, 1997; Kirk, 2001).

1.5.1.3 Transport across the PPM

The PPM has a large inward negative membrane potential (Allen and Kirk, 2004b), which plays an important role in the transport of a range of metabolites. This membrane contains only parasite-encoded MTPs that mediate the import and export of metabolites (Martin *et al.*, 2009).

The transport across the PPM for key metabolites such as glucose (hexose transporter) (Saliba *et al.*, 2004), nucleosides and nucleobases (nucleoside transporters) (Downie *et al.*, 2006; Downie *et al.*, 2008) and amino acids (amino acid transporters) (Martin and Kirk, 2007; Cobbold *et al.*, 2011), is fast and equilibrative. However, for other metabolites such as the essential vitamin pantothenate (Saliba and Kirk, 2001) or ion P_i (Saliba *et al.*, 2006), uptake is slower and coupled to the transport of either H^+ (pantothenate) or Na^+ (P_i). The predicted parasite-encoded MTPs across the PPM is summarised in Table 3.

Table 3: The predicted *P. falciparum*-encoded MTPs across the PPM in asexual parasites. The predicted localisation of the parasite-encoded MTPs to the PPM has been determined using antibodies and the metabolites of these MTPs were also included.

Parasite-encoded MTPs on PPM				
Transporter	Gene ID	Metabolite	Function	Reference
Hexose transporter (uniporter) (PfHT)	PF3D7_0204700	Glucose	The primary route of glucose uptake into parasites	(Woodrow <i>et al.</i> , 1999; Krishna <i>et al.</i> , 2000)
Aquaglyceroporin	PF3D7_1132800	Water, Glycerol, Urea, Methylglyoxal and Ammonia	The primary route of entry for glycerol. Use glycerol for lipid backbone.	(Beitz <i>et al.</i> , 2004; Pavlovic-Djuranovic <i>et al.</i> , 2006; Zeuthen <i>et al.</i> , 2006; Beitz, 2005)
H ⁺ / lactate co-transporter (symporter) (monocarboxylate transporter)	PF3D7_0926400 PF3D7_0210300	Lactate export	Remove lactate to maintain the cell's integrity and metabolic viability	(Elliott <i>et al.</i> , 2001; Cranmer <i>et al.</i> , 1995; Kanaani and Ginsburg, 1991)
Formate – nitrite transporter (PFNT)	PF3D7_0316600	Formate and Lactate export	Remove lactate to maintain the cell's integrity and metabolic viability	(Marchetti <i>et al.</i> , 2015; Wu <i>et al.</i> , 2015)
Nucleoside/nucleobase transporters (specifically PfNT1)	PF3D7_1347200	Nucleoside and Nucleobase	Provide parasite with purines	(Quashie <i>et al.</i> , 2010; Rager <i>et al.</i> , 2001)
ATP/ADP co-transporters (antiporters)	PF3D7_1004800 PF3D7_1037300	ATP and ADP	Mediate net uptake of ATP into parasite/supply ATP to host cell	(Kanaani and Ginsburg, 1989)
Ile/Leu co-transporter (antiporter) (amino acid transporters)	PF3D7_0629500 PF3D7_1208400 PF3D7_1231400	Isoleucine and Leucine	Required for growth and multiplication of the parasite	(Martin and Kirk, 2007)
Methionine transporter (amino acid transporters)	PF3D7_0209600 PF3D7_0515500 PF3D7_1132500	Methionine (equilibrate across PPM with properties matching isoleucine uptake)	Essential for normal parasite growth	(Cobbold <i>et al.</i> , 2011)
Multidrug resistance-associated proteins (PfMRP1 and PfMRP2) - ATPase	PF3D7_0112200 PF3D7_1229100	Glutathione export	Aid in redox defence	(Raj <i>et al.</i> , 2009; Barrand <i>et al.</i> , 2012; Klokouzas <i>et al.</i> , 2004; Kavishe <i>et al.</i> , 2009)
ABC transporter B family member 5	PF3D7_1339900	Glutathione export	Aid in redox defence	(Kavishe <i>et al.</i> , 2009)
H ⁺ / pantothenic acid co-transporter (symporter)	PF3D7_0206200	H ⁺ and Pantothenic acid	Requirement for an external source of the coenzyme A precursor pantothenic acid	(Saliba and Kirk, 2001; Augagneur <i>et al.</i> , 2013)
Folate transporters (uniporters)	PF3D7_0828600 PF3D7_1116500	Folate, Pteridine and 4-aminobenzoic acid	Essential cofactors for DNA synthesis	(Salcedo-Sora <i>et al.</i> , 2011)
H ⁺ / Na ⁺ exchanger (antiporter) (PfNHE)	PF3D7_1303500	H ⁺ and Na ⁺	Parasite maintains cytosolic [Na ⁺]	(Spillman <i>et al.</i> , 2013b; Spillman <i>et al.</i> , 2013a; Martin <i>et al.</i> , 2009)
Na ⁺ -dependent phosphate transporter (PfPiT) (symporter)	PF3D7_1340900	2Na ⁺ H ₂ PO ₄ ⁻ (monovalent form of P _i ion)	Requires a source of P _i to sustain normal growth rate	(Saliba <i>et al.</i> , 2006)
Cation ATPase (PfATP4)	PF3D7_1211900	Ca ²⁺ / Na ⁺	Required for parasite growth (however, recently PfATP4 functions as a Na ⁺ pump)	(Krishna <i>et al.</i> , 2001; Spillman <i>et al.</i> , 2013b; Dyer <i>et al.</i> , 1996)
Copper P-ATPase	PF3D7_0904900	Reduced copper	Export copper to reduce its toxicity	(Rasoloson <i>et al.</i> , 2004)
V-type H ⁺ -ATPase	PF3D7_0519200 PF3D7_0806800 PF3D7_1354400 PF3D7_1464700 PF3D7_1140100 PF3D7_0406100 PF3D7_0106100 PF3D7_1311900 PF3D7_1323200 PF3D7_1341900 PF3D7_1306600 PF3D7_0934500	H ⁺	Regulate intracellular pH and plasma membrane potential	(Marchesini <i>et al.</i> , 2005)
K ⁺ ion channels (PfK1 and PfK2)	PF3D7_1227200 PF3D7_1465500	K ⁺	Effect maintenance of the membrane potential and electrochemical gradient across the erythrocyte plasma membrane	(Waller <i>et al.</i> , 2008)
Inorganic anion exchanger (PFSulP)	PF3D7_1471200	HCO ₃ ⁻ /Cl ⁻	Aid in the import and export of anions	(Henry <i>et al.</i> , 2007)
V-type K ⁺ -independent H ⁺ -translocating inorganic pyrophosphatase (PfVPP1 and 2)	PF3D7_1456800 PF3D7_1235200	H ⁺	Establish transmembrane H ⁺ gradients through the hydrolysis of inorganic pyrophosphate (PP _i)	(McIntosh <i>et al.</i> , 2001; Luo <i>et al.</i> , 1999)
Zinc transporters	PF3D7_0715900 PF3D7_0609100	Zn ²⁺	-	(Ginsburg, 2006)
CorA-like Mg ²⁺ transporter s (PfMIT1, 2 and 3)	PF3D7_1120300 PF3D7_1304200 PF3D7_1427600	Mg ²⁺	Required for parasite growth	(Mauroid <i>et al.</i> , 1989)
Copper transporters	PF3D7_1439000 PF3D7_1421900	Cu ²⁺	Require copper that is a co-factor for metabolically important cellular enzymes, such as cytochrome-c oxidase	(Choveaux <i>et al.</i> , 2012)

1.5.1.4 Transport across membranes enclosing organelles

There is limited knowledge available about the transport of metabolites across membranes enclosing different organelles in intraerythrocytic parasites. The acidic digestive vacuole, where the digestion of the host cell haemoglobin takes place, is surrounded by a single membrane. Parasite-encoded MTPs present on the digestive vacuole membrane include a multi-subunit V-type H⁺ ATPase (Hayashi *et al.*, 2000), *P. falciparum* V-type H⁺-translocating pyrophosphatase (PfVP1, PF3D7_1456800) (Luo *et al.*, 1999), a Ca²⁺ pump (PfATP4, PF3D7_1211900) (Biagini *et al.*, 2003), multidrug resistance protein 2 (PfMDR2, PF3D7_1447900) (Zalis *et al.*, 1993), lipid/H⁺ symporter (PF3D7_0107500) and an iron transporter (PF3D7_1223700) (Martin *et al.*, 2009).

The parasite-encoded MTPs localised to the parasite's apicoplast membranes, include a triose phosphate transporter (PFTPT, PF3D7_0508300) (Lim *et al.*, 2016), a phosphoenolpyruvate translocator (PfPPT, PF3D7_0530200) (Mullin *et al.*, 2006), a cation-transporting ATPase (PF3D7_0516100) (Krishna *et al.*, 1993) together with an ABC transporter (PF3D7_0302600) and a drug/metabolite transporter (PF3D7_0716900) (Sayers *et al.*, 2018).

The acidic digestive vacuole and the apicoplast are the target sites of several antimalarial compounds (Kirk and Lehane, 2014). The MTPs present also play an important role in the occurrence of antimalarial drug resistance and influence parasite drug sensitivity. These parasite-encoded MTPs include the PfCRT (PF3D7_0709000) (Martin and Kirk, 2004; Kuhn *et al.*, 2010), PfPgh1/PfMDR1 (PF3D7_0523000) (Cowman *et al.*, 1991) and the PfMRP1 (PF3D7_0112200) (Raj *et al.*, 2009).

An acidocalcisome is an acidic electron-dense organelle, rich in polyphosphate, calcium and other cations (Marchesini *et al.*, 2000; Miranda *et al.*, 2008). Acidocalcisomes are the largest Ca²⁺ store in *Toxoplasma gondii* and have been found to also occur in *P. falciparum* parasites, especially during the merozoite stages (Miranda *et al.*, 2008) confirming the regulation of [Ca²⁺] in the parasite. Hence, parasite-encoded MTPs localised to the acidocalcisome membrane include a multi-subunit V-type H⁺ ATPase (Hayashi *et al.*, 2000) to establish a proton gradient and the PfATP4 (PF3D7_1211900) for the exchange of Ca²⁺ (Dyer *et al.*, 1996).

Additionally, the parasite-encoded MTPs localised to the inner mitochondrial membrane include the multi-subunit ATP synthase complex (Nina *et al.*, 2011), ATP/ADP transporters (PF3D7_1004800 and PF3D7_1037300) (Hatin *et al.*, 1992), a mitochondrial phosphate carrier protein (PF3D7_1202200) (Van Dooren *et al.*, 2006), a cation/H⁺ antiporter (PF3D7_0603500) (Rotmann *et al.*, 2010) and a dicarboxylate/tricarboxylate carrier (PfDTC, PF3D7_0823900) (Van Dooren *et al.*, 2006).

1.5.2 Membrane transport processes in the gametocyte stages

Given the importance of *P. falciparum* membrane transport processes, it is surprising that there is limited information available about these processes, including the expression of the permeome in the gametocyte stages of the parasite. The membrane transport processes in the gametocyte stages may be more complicated in comparison to the asexual stages since from stage II gametocytes onwards, an additional membrane, apart from the EPM, PVM and PPM, is observed. This additional membrane is an inner membrane complex (IMC) (Dearnley *et al.*, 2012) that develops under the gametocyte PPM (Fig. 4). The transport across the IMC in gametocytes may be due to regular pores, such as those described in *P. gallinaceum* ookinete IMC (Raibaud *et al.*, 2001). However, the transport across the IMC still needs to be determined in *P. falciparum* parasites.

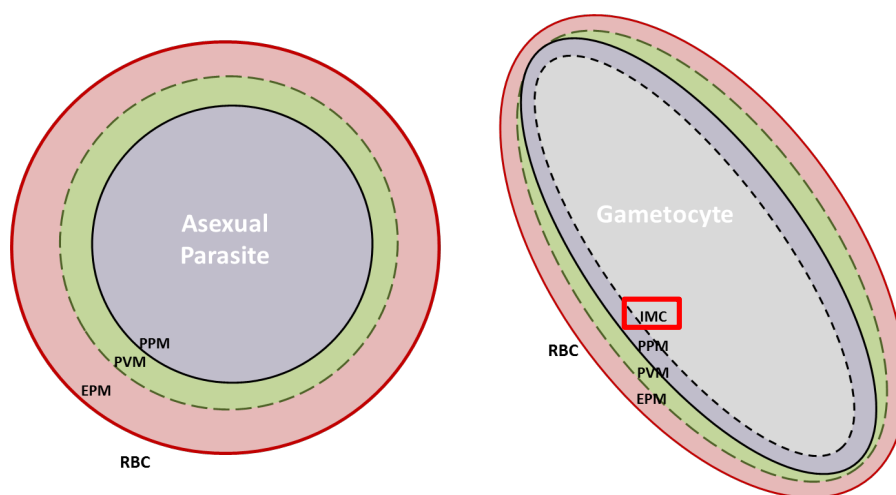


Figure 4: Morphological differences between asexual and gametocyte stages. The asexual stages contain three membranes including the EPM, PVM and PPM. However, from stage II gametocytes, an IMC is generated and indicated in the red box.

When investigating the expression of the *P. falciparum* permeome in the gametocyte stages, only a few parasite-encoded MTPs have been identified to date, with unknown subcellular localisation preventing localisation to the EPM, PVM, PPM or IMC. Direct evidence of parasite-encoded MTPs essential to gametocyte development is limited to two reports. Recently, a cationic amino acid transporter (novel putative transporter, NPT) was identified in *P. berghei* (PbNPT1), based on its homology to a selective arginine transporter from *T. gondii* (TgNPT1) (Rajendran *et al.*, 2017). PbNPT1 is essential for gametocyte stage production in *P. berghei* (the murine malaria parasite) (Boisson *et al.*, 2011) and was found to localise predominantly to the PPM in asexual parasites, with a more diffuse localisation in gametocyte stages (Boisson *et al.*, 2011). This may suggest that the *P. falciparum* NPT1 ortholog (PfNPT1, PF3D7_0104800) is also essential for gametocyte stage production in *P. falciparum* parasites. Additionally, a putative *P. falciparum* ABC transporter (PF3D7_1426500) was reported to play an essential role in both lipid metabolism and gametocyte development as it has higher expression in the gametocyte stages than in the asexual stages (Tran *et al.*, 2014). While the exact MTPs expressed in gametocytes as opposed to asexual parasites are unknown, it is expected that the different metabolic requirements of the asexual and

gametocyte stages must be supported by the presence of different parasite-encoded MTPs between and within the asexual and gametocyte stages.

1.6 Metabolic differences between and within asexual and gametocyte stages

As *P. falciparum* parasites develop through the different life cycle stages, they are exposed to different environments, ranging from both vertebrate and invertebrate hosts as well as different biological compartments and cell types in each instance. These parasites, therefore, have to adjust to these environmental changes by developing different metabolic adaptations (Bouvier *et al.*, 2004; Talman *et al.*, 2004), which include strategy-specific metabolic differences between the asexual (proliferation) and gametocyte (differentiation) stages, as well as stage-specific (i.e. ring - schizont stages; stage I – V gametocytes) differences within each strategy.

1.6.1 Strategy-specific metabolic differences between asexual and gametocyte stages

Strategy-specific metabolic differences are observed between asexual and gametocyte stages. The asexual stages are highly proliferative due to the rapid intracellular cell growth, multiplication and re-invasion that is repeated every 48 h asexual cycle (Bannister and Mitchell, 2003). Hence, there is a heavy dependence on the exchange of metabolites required for the rapid proliferation of these stages. The metabolites required by this proliferative stage for macromolecular synthesis and growth are either obtained by the uptake of these metabolites from the extracellular environment or are biosynthesised from the pool of available metabolites (Olszewski *et al.*, 2009; Olszewski and Llinás, 2011). In contrast to the asexual stages, the non-proliferative gametocyte stages only require limited metabolite exchange to sustain differentiation that ultimately allows for the transmission to the mosquito vector (MacRae *et al.*, 2013; Daily *et al.*, 2007; White *et al.*, 1983). Stage-specific metabolic differences are also observed within both the proliferation strategy, followed by asexual parasites during the development from the ring stages to multinucleated schizont stages, as well as to a lesser extent during the differentiation strategy observed in gametocyte stages. Here, amino acid metabolism, carbohydrate metabolism, DNA synthesis and lipid metabolism, illustrative of the stage-specific metabolic requirements in the asexual and gametocyte stages, are discussed.

1.6.1.1 Stage-specific metabolite exchange in the asexual stages

In asexual parasites, the ring stages develop into metabolically active trophozoite and ultimately schizont stages, each with specific active metabolic pathways and metabolite exchange requirements (Bozdech *et al.*, 2003; Bannister and Mitchell, 2003). The ring stages are seen as relatively inactive, however, as they undergo a morphological transformation in which they fold onto themselves, these stages internalise haemoglobin (Elliott *et al.*, 2008). Haemoglobin is then transferred to the parasite's acidic digestion vacuole, where it is degraded, generating free amino

acids as well as a haem derivative, which is converted to haemozoin crystals that can be observed as the parasite grows (Francis *et al.*, 1997). The parasite also degrades haemoglobin (Liu *et al.*, 2006) in order to maintain an osmotic balance in the host erythrocyte (Lew *et al.*, 2004) and ensures there is enough space for parasite growth (Krugliak *et al.*, 2002; Allen and Kirk, 2004a).

Haemoglobin degradation generates 19 of the naturally occurring amino acids, but lacks isoleucine, which is taken up from the extracellular environment (Martin and Kirk, 2007). However, the parasite only uses up to about 16% of the free amino acids generated from haemoglobin (Krugliak *et al.*, 2002), resulting in the exporting of the rest of the available amino acids. The parasite also takes up amino acids from the extracellular environment to incorporate them into proteins (Ginsburg *et al.*, 1985; Kirk *et al.*, 1994; Divo *et al.*, 1985; Sherman, 1977; Elford *et al.*, 1985). This uptake and release of amino acids, which is mediated by amino acid transporters, may already start in the ring stages (Lamour *et al.*, 2014). Previous biochemical studies have identified the uptake of a few amino acids (Martin and Kirk, 2007; Cobbold *et al.*, 2011; Ginsburg and Krugliak, 1983; Winterberg *et al.*, 2012). However, the specific amino acid transporters responsible for a specific amino acid have not been identified. Expression pattern analyses of six *P. falciparum* amino acid transporters during the asexual stages showed that only one (MAL6P1.133/PF3D7_0629500) was expressed in the ring stages, with peak expression at 24 h post merozoite invasion (hpi, trophozoite stage) (Martin *et al.*, 2005), whereas the other five amino acid transporters only showed peak expression between 24 – 40 hpi (trophozoite and schizont stages) (Martin *et al.*, 2005), suggesting that amino acid import for protein synthesis and export following haemoglobin digestion may start in the ring stages, but peak during the trophozoite stages.

As the parasite enters the metabolically active maturation phase during trophozoite stage development, the parasite becomes highly reliant on glucose metabolism (Sana *et al.*, 2013) as the 12 known glycolysis enzymes reach maximal expression in the trophozoite stages (Bozdech *et al.*, 2003). The glucose consumption rate of a parasite-infected erythrocyte increases up to a 100-fold, when compared to uninfected erythrocytes (Roth, 1989). The primary route of glucose uptake is through the *P. falciparum* hexose transporter (PfHT, PFB0210c/PF3D7_0204700), which showed peak transcript expression between 24 – 40 hpi (trophozoite stages) (Martin *et al.*, 2005), therefore, correlating with the high levels of glucose required by the trophozoite/schizont stages. Most of the glucose consumed passes through anaerobic glycolysis (Embden-Meyerhof pathway) and is metabolised to lactic acid (Roth *et al.*, 1988; Jensen *et al.*, 1983; Zolg *et al.*, 1984). Lactic acid needs to be exported from the parasite cytosol as it decreases the intracellular pH resulting in osmotic instability and also interferes with the oxidation of glycolytic nicotinamide adenine dinucleotide (NADH) to NAD⁺ (Kanaani and Ginsburg, 1991). Lactic acid is transported out of the cell across the PPM via a monocarboxylate transporter (PFI1295c/PF3D7_0924400) (Elliott *et al.*, 2001; Wu *et al.*, 2015), which also showed peak transcript expression between 28 – 42 hpi (trophozoite stages) (Martin *et al.*, 2005). Comparatively less than 7% of internalised glucose is

additionally metabolised in the mitochondrion through an active tricarboxylic acid (TCA) cycle (MacRae *et al.*, 2013; Cobbold and McConville, 2014; Bozdech *et al.*, 2003), which can also use glutamine as a carbon source (Lamour *et al.*, 2014; MacRae *et al.*, 2013; Cobbold *et al.*, 2013; Jacot *et al.*, 2016). Glutamine can also be taken up through an amino acid transporter, which may be one of the six *P. falciparum* amino acid transporters that showed peak transcript expression between 24 – 42 hpi in the asexual stages (Martin *et al.*, 2005), correlating with the requirement of the TCA cycle in the trophozoite/schizont stages (Bozdech *et al.*, 2003). The metabolic strategy of the trophozoite stages therefore, includes glycolysis that is coupled with a TCA cycle to generate adenosine triphosphate (ATP) and glycolytic intermediates that are essential for rapid biomass generation for schizogony (Sana *et al.*, 2013).

In the mature trophozoite stages, schizogony is initiated as deoxyribonucleic acid (DNA) content is replicated and results in the development of multinucleated schizont stages, each containing 6 – 32 daughter merozoites (Wipasa *et al.*, 2002). Hence, the use of purines and pyrimidines in the asexual stages is required for the rapid rate of DNA synthesis. *P. falciparum* parasites have retained the capacity for *de novo* synthesis of pyrimidines and do not have active pathways for the uptake of pyrimidines from the host due to small concentrations of pyrimidines present in the host erythrocyte (Cassera *et al.*, 2011). In contrast to pyrimidines, *P. falciparum* parasites salvage host purines for synthesis of DNA as the host erythrocytes contain millimolar concentrations of ATP in equilibrium with ADP and AMP (Cassera *et al.*, 2011). Hence, the parasites do not retain *de novo* purine synthetic pathways (De Koning *et al.*, 2005; Cassera *et al.*, 2011). Therefore, the uptake of purine nucleosides and nucleobases can be mediated by four parasite-encoded nucleoside transporters (PfNT1 - PF3D7_1347200, PfNT2 - PF3D7_0824400, PfNT3 - PF3D7_1469400 and PfNT4 - PF3D7_0103200), which showed peak transcript expression between 24 – 42 hpi (schizont stages), supporting the uptake of purines for the synthesis of DNA in the trophozoite/schizont stages.

The multinucleated schizont stages subsequently undergo cytokinesis, thereby enclosing each new daughter parasite with a plasma membrane (Ben Mamoun *et al.*, 2010; Gulati *et al.*, 2015; Palacpac *et al.*, 2004). Thus, membrane biogenesis is driven by the uptake of precursors such as fatty acids, serine, ethanolamine and choline as they are the major building blocks used by the parasite in the synthesis of its structural and regulatory phospholipids (such as phosphatidylcholine and phosphatidylethanolamine) (Ben Mamoun *et al.*, 2010). *P. falciparum* parasites have the ability to generate some fatty acids *de novo* in the apicoplast (Lim and McFadden, 2010) as the parasite expresses all the enzymes for the synthesis of fatty acids (Gardner *et al.*, 2002). However, most fatty acids are scavenged from the host serum (Mi-Ichi *et al.*, 2006). The specific MTPs involved in the uptake of the phospholipid precursors are yet to be identified (Kirk and Saliba, 2007; Ben Mamoun *et al.*, 2010). However, as membrane biogenesis peaks in the trophozoite stages (Pessi

et al., 2004), it is expected that the uptake of the precursors and the synthesis of the phospholipids is required in the trophozoite/schizont stages.

1.6.1.2 Stage-specific metabolite exchange in the gametocyte stages

Despite entering non-proliferative gametocyte stages, different metabolic pathways (and thus metabolite exchange) become active as the parasite differentiates from stage I to stage V gametocytes. For example, in the early gametocyte stages, haemoglobin degradation is present, resulting in the abundance of free amino acids (Rajendran *et al.*, 2017; Krugliak *et al.*, 2002; Liu *et al.*, 2006), which can either be used or exported (Krugliak *et al.*, 2002). Additionally, as protein synthesis occurs in the gametocyte stages (Florens *et al.*, 2002), there is also a requirement for amino acid uptake in these stages. Thus, the import of amino acids for protein synthesis and export following haemoglobin digestion in the gametocyte stages suggests the requirement of amino acid transporters that may mediate these processes.

Also during the early gametocyte stages, previous studies showed increased levels of glucose consumption (Lamour *et al.*, 2014; MacRae *et al.*, 2013), which may indicate the requirement of glycolysis. However, the pathway for glucose uptake in the gametocyte stages has only been predicted in *P. berghei* (Slavic *et al.*, 2011) to pass through the *P. berghei* hexose transporter (PbHT). It is therefore, suggested that *P. falciparum* gametocyte stages will also use the PfHT for the uptake of glucose required in the early gametocyte stages.

Together with glycolysis, early gametocyte stages showed increased levels of TCA catabolism of pyruvate in comparison to the asexual stages (Lamour *et al.*, 2014; MacRae *et al.*, 2013). This metabolic switch to TCA catabolism in the mitochondrion may be due to the fact that the gametocyte stages are in the metabolite-deprived bone marrow. Therefore, there is reduced availability of glutamine and glucose in gametocyte stages, which requires a more efficient method of ATP synthesis (MacRae *et al.*, 2013) that is essential for the progression in the mosquito (Jacot *et al.*, 2016). TCA catabolism requires the transport of pyruvate to the mitochondrion, as pyruvate is broken down to produce acetyl-CoA, leading to a decrease in the release of glycolytic end-products (lactic acid, pyruvate, alanine and glycerol) (MacRae *et al.*, 2013; Lamour *et al.*, 2014). The increased production of acetyl-CoA, which is specifically linked to stage III gametocyte glucose metabolism (MacRae *et al.*, 2013), can then either be further metabolised through the TCA cycle (Jacot *et al.*, 2016) or transported out of the mitochondrion, using the acetyl-CoA transporter (PfACT, PF3D7_1036800) for further pyruvate metabolism or histone acetylation (Van Dooren *et al.*, 2006; Ralph *et al.*, 2004). Thus, the transport of pyruvate and acetyl-CoA suggests the requirement of MTPs that may mediate these processes in the gametocyte stages.

Additionally to the TCA cycle, in stage I gametocytes, DNA is synthesised to twice the haploid amount, which then stays constant through to stage V gametocytes (Janse *et al.*, 1988). DNA synthesis is thus supported by the requirement of purines and pyrimidines in the early gametocyte stages. *P. falciparum* parasites salvage host purines such as hypoxanthine, which is the key precursor for all purine synthesis (Cassera *et al.*, 2011). Therefore, DNA synthesis is supported by the uptake of hypoxanthine in gametocyte stages (Raabe *et al.*, 2009), which may be mediated by the four parasite-encoded nucleoside transporters (PfNT1 - PF3D7_1347200, PfNT2 - PF3D7_0824400, PfNT3 - PF3D7_1469400 and PfNT4 - PF3D7_0103200).

During the gametocyte stages, the parasites are preparing for the transition from the human host to the mosquito vector and, therefore, sequester phospholipids obtained from the human host, which are less readily available in the mosquito vector (Tran *et al.*, 2014; van Schaijk *et al.*, 2014), suggesting that the gametocyte stages either synthesise or take up the precursors of phospholipids required for membrane biogenesis. In the gametocyte stages, five of the six enzymes required for an active Type II fatty acid biosynthesis pathway are upregulated (Young *et al.*, 2005), correlating with the *de novo* synthesis of fatty acids, which is a precursor that is part of the building blocks used by the parasite in the synthesis of phospholipids (Ben Mamoun *et al.*, 2010). In addition, a putative ABC transporter was identified predominantly in the gametocyte stages and reported to play an essential role in neutral lipid transport (Tran *et al.*, 2014), which is also required for membrane biogenesis, confirming that the gametocyte stages can also take up lipids that may only be required in the mosquito vector.

Although direct evidence for MTPs, associated with transport of metabolites required for these upregulated metabolic processes, is still lacking, the enhanced activity of amino acid transport, carbohydrate metabolism, specifically the increased dependence on the TCA cycle, DNA synthesis and lipid metabolism, implies some mechanism of metabolite transport to be present in gametocyte stages.

Here, it is hypothesised that the different metabolic requirements of the asexual and gametocyte stages must be supported by the differential expression of the permeome between and within the asexual and gametocyte stages. While a great deal is known about the expression of the permeome in the asexual stages, limited information is available about the presence of parasite-encoded MTPs in the gametocyte stages. Therefore, to get a comprehensive overview of the strategy- and/or stage-specific expression of the *in silico* predicted permeome, this study evaluated the mRNA expression of the entire complement of *P. falciparum*-encoded MTPs in both the asexual and gametocyte stages. Ultimately, by identifying parasite-encoded MTPs essential in both asexual and gametocyte stages of the *P. falciparum* parasites, it is envisioned that new drug targets will be identified that may be used in malaria elimination and eradication strategies.

1.7 Hypothesis

The permeome is differentially expressed in the asexual and gametocyte stages of *P. falciparum* parasites.

1.8 Aim

To identify and biochemically evaluate strategy- and stage-specific differential expression of the permeome in both asexual and gametocyte stages of *P. falciparum* parasites.

1.9 Objectives

The following objectives were evaluated:

1. *In silico* evaluation and characterisation of the permeome of *P. falciparum* parasites.
2. Investigation of the strategy- and stage-specific mRNA expression of the permeome between and within the asexual and gametocyte stage *P. falciparum* parasites.
3. Isotopic confirmation of selected activities from the permeome in *P. falciparum* asexual parasites.

1.10 Outputs

Research findings generated in this study were presented at the following conferences:

Naude, M.; van Biljon, R.; Birkholtz, L.M., and Niemand, J. Membrane transport in the sexual, transmissible stages of *Plasmodium falciparum*. Poster presentation, 2nd South African Malaria Research Conference Pretoria (MOMR), South Africa (August 2016).

Naude, M.; van Biljon, R.; Birkholtz, L.M., and Niemand, J. Membrane transport in the sexual, transmissible stages of *Plasmodium falciparum*. Poster presentation, University of Pretoria Postgraduate Biochemistry Symposium, University of Pretoria, South Africa, (October 2016).

van Biljon, R.A., Naude, M., Birkholtz, L., and Niemand, J. Dynamic evaluation of metabolite transport in the intraerythrocytic lifecycle stages of *Plasmodium falciparum* parasites. Poster presentation, BioMalPar XIII: Biology and Pathology of the Malaria Parasite, Heidelberg, Germany (May 2017).

Naude, M.; van Biljon, R.; Birkholtz, L.M., and Niemand, J. Dynamic bioinformatics and isotopic evaluation of the permeome of intraerythrocytic *Plasmodium falciparum* parasites. Oral presentation, University of Pretoria Postgraduate Biochemistry Symposium, University of Pretoria, South Africa, (September 2017). Received best MSc Biochemistry oral presentation award.

Naude, M.; van Biljon, R.; Birkholtz, L.M., and Niemand, J. Dynamic bioinformatics and isotopic evaluation of the permeome of intraerythrocytic *Plasmodium falciparum* parasites. Poster presentation, 3rd South African Malaria Research Conference Pretoria (MOMR), South Africa (November 2017).

Chapter 2: Materials and Methods

All experiments were carried out in the Malaria Parasite Molecular Laboratory (M²PL) under the supervision of Dr Niemand and Prof Birkholtz. The laboratory has a certified P2 facility, in which *P. falciparum* parasites were cultivated for this study. Ethical clearance for the use of human blood and parasite culturing was obtained from the University of Pretoria, Faculty of Natural and Agricultural Sciences Ethics Committee (EC120821 - 077). The M²PL also has a certified Type-C Radioisotope laboratory (Authority 0031/7/16/0699), which was used for the radioisotope uptake experiments in this study.

2.1 *In silico* analyses of the permeome of *P. falciparum* parasites

For the *in silico* analyses that included the identification and characterisation of the current permeome encoded by the *P. falciparum* parasite, the strategy that was followed is illustrated in Fig. 5.

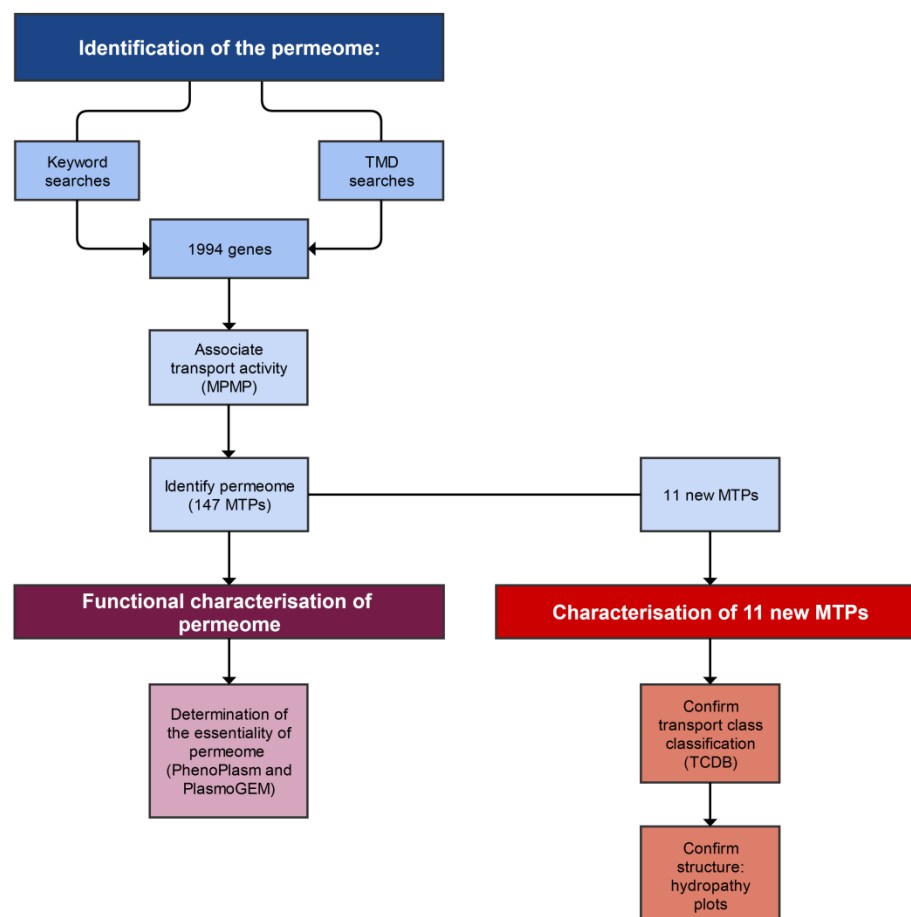


Figure 5: The workflow that was followed for the identification and characterisation of the current permeome encoded by the *P. falciparum* genome. For the identification of the current permeome, the previous permeome (Martin *et al.*, 2005; Martin *et al.*, 2009) was improved on by using the revised annotation of the *P. falciparum* genome (PlasmogEM version 28) to identify genes encoding MTPs, using keyword searches as well as searching for proteins with TMDs ranging from 2 – 30 domains. The genes were then associated with their metabolic functions (Malaria Parasite Metabolic Pathways, MPMP) to predict if they have transport activity and therefore, identify the updated permeome. Eleven new MTP genes were identified in addition to the original 136 MTP genes (previous permeome) (Martin *et al.*, 2005; Martin *et al.*,

2009). The 11 newly identified MTPs were characterised based on the classification into integral membrane protein classes (compared to other organisms, TCDB: Transport Classification Database) and structure prediction (hydrophobicity, ProtScale server - Kyte-Doolittle hydrophobicity scale). Additionally, the current permeome (147 MTP genes) were investigated for the essentiality in the asexual and gametocyte stages (PlasmoGEM and PhenoPlasm).

2.1.1 Identification of the current permeome encoded by *P. falciparum* parasites

A previous study investigated the permeome of *P. falciparum* parasites and identified 136 genes encoding MTPs, specifically investigating MTPs with seven or more TMDs (Martin *et al.*, 2005). However, due to the subsequent revision of genome data, comparative genomics and proteomics data that improved the existing annotation of the *P. falciparum* genome, the possibility of identifying more parasite-encoded MTPs that may previously been overlooked was investigated in this study, using keyword searches as well as TMD searches (including MTPs with less than seven TMDs) from the *Plasmodium* genome database (PlasmoDB) (Aurrecoechea *et al.*, 2008). First, the Gene Text search tool was used to search for keywords, including “ATPase”, “carrier”, “permease”, “transport”, “channel”, “ATP synthase”, “pump”, “porin”, “symporter”, “antiporter”, “porter”, “diffusion” and “translocator” (<http://plasmodb.org/plasmo/>, Accessed March 2016) and resulted in the identification of 1362 genes.

Second, the TMD-based search tool (TMHMM algorithm) was used for the identification of genes encoding proteins with TMDs ranging from 2 – 30 domains (<http://plasmodb.org>, Accessed May 2016). TMHMM is a membrane protein topology prediction method, based on a hidden Markov model (HMM). The TMHMM predicts TMDs, based on the probability of amino acids characteristics belonging to one of three states: (i) inside loops, (ii) transmembrane region or (iii) outside loops (Sonnhammer *et al.*, 1998). This model can discriminate between soluble and membrane proteins with both specificity and sensitivity (Sonnhammer *et al.*, 1998; Krogh *et al.*, 2001). The TMD search identified 889 genes that were combined with the results from the keyword searches, which resulted in a total of 1996 putative MTP genes (225 genes were present in both keyword and TMD searches).

In order to determine if transport activity can be associated with the 1996 putative MTP genes, their empirical metabolic functions were searched for using the Malaria Parasite Metabolic Pathways (MPMP) database (<http://mpmp.huji.ac.il/>, Accessed September 2016). MPMP is a *Plasmodium*-specific metabolic database, where genomic, transcriptomic and proteomic data, as well as published biochemical data is correlated to biological processes (Ginsburg, 2006). The Kyoto Encyclopedia of Genes and Genomes (KEGG) and Gene Ontology (GO) databases were not used due to the predictive annotation of the genes (Kanehisa and Goto, 2000; Gene Ontology Consortium, 2014). Transport activity was defined as the description of the gene as either channel, transport, transporter, transporting, antiporter, symporter or porin in the function description. From the metabolic function association, only 147 genes were associated with transport activity. These

147 genes were therefore classified as the current predicted permeome (referred to as the permeome), consisting of 136 previously identified MTP genes (Martin *et al.*, 2005; Martin *et al.*, 2009) and 11 newly identified MTP genes encoded by *P. falciparum*.

2.1.2 Characterisation of the 11 newly identified MTPs

These 11 newly identified MTPs were further characterised on 1) the classification into integral membrane protein classes based on the sequence homology to other organism proteins and 2) structure predictions, using hydropathy plots.

For the classification of the 11 new MTPs into integral membrane protein classes, the protein sequences of these 11 MTPs were queried against protein sequences of other organisms, using the BLASTP algorithm (Basic Local Alignment Search Tool Protein, where the protein sequence is queried against a protein database) and a BLOSUM62 matrix of the Transport Classification Database (TCDB) (<http://www.tcdb.org/>, Accessed September 2016) (Saier *et al.*, 2016) to (i) determine the sequence similarity to MTPs of other organisms as well as (ii) determine whether these proteins belong to known integral membrane protein classes.

Additionally, the predicted structures of the 11 newly identified MTPs were investigated, using hydropathy plots. Hydropathy plots allowed for the visualisation of the hydrophobicity of the protein sequence and therefore, identified membrane-spanning regions, which can resemble typical MTP profiles. The hydropathy plots were generated by the Kyte-Doolittle hydrophobicity scale (Kyte and Doolittle, 1982) of the ProtScale server (window size of 9) (<https://web.expasy.org/protscale/>, Accessed November 2016). A Kyte-Doolittle hydrophobicity scale defines the relative hydrophobicity of amino acid residues, based on the measurement of how the amino acid R group interacts with water (Kyte and Doolittle, 1982). The calculations are dependent on the free energy of transfer ($\Delta G_{\text{trans}}^{\circ}$) of the solute amino acid between water and a hydrophobic phase. A negative $\Delta G_{\text{trans}}^{\circ}$ indicates a strong preference of the R group to water (hydrophilic), whereas a positive value indicates the opposite (hydrophobic) (Ciborowski and Silberring, 2016). Hence, positive peaks corresponded to predicted TMDs.

2.1.3 The functional characterisation of the permeome

Genome modification approaches have resulted in experimental phenotypic data indicating whether a gene is essential within a specific stage of *P. falciparum* or *P. berghei*. The essentiality of the 147 MTP genes during the intraerythrocytic developmental stages were investigated, using both PlasmogEM (<http://plasmogem.sanger.ac.uk/>, Accessed December 2016) (Schwach *et al.*, 2015; Bushell *et al.*, 2017) and PhenoPlasm (<http://phenoplasm.org/>, Accessed December 2016) (Sanderson and Rayner, 2017) databases. The PlasmogEM database consists of the asexual stage phenotypic data of > 2 500 *P. berghei* genes that have been generated from gene knock-out

mutants in female Balb/c mice, expressed as relative growth rates (Schwach *et al.*, 2015). To correlate the essential *P. berghei* genes to the *P. falciparum*-encoded MTP genes, the *P. berghei* orthologs of the *P. falciparum* MTP genes were obtained from PlasmoDB (version 29) and investigated using the PlasmoGEM database. The PhenoPlasm database is a collection of phenotypic data from attempts to knock-out, including both *P. berghei* and *P. falciparum* genes. Therefore, both *P. falciparum*-encoded MTP genes and the *P. berghei* orthologs of the *P. falciparum*-encoded MTP genes (also obtained from PlasmoDB version 29) were investigated in PhenoPlasm. Genes that are refractory to knock-out were characterised as essential genes.

2.2 Analyses of strategy- and stage-specific expression of the permeome

To investigate the strategy- and stage-specific expression of the *in silico* predicted permeome, the expression profiles of mRNA transcripts identified during previous DNA microarray analyses across both asexual and gametocyte stages were analysed. For the asexual stages, data from a global transcriptome of a complete 48 h cycle (expression value at each h) of *P. falciparum* parasites (strain 3D7), using DNA microarray, were obtained from the authors (Painter *et al.*, 2017). This transcript dataset has subsequently been released on PlasmoDB version 33. For the gametocyte stages, data were obtained from a previous global transcriptome of the complete gametocytogenesis of *P. falciparum* parasites, generated in a PhD study of Riëtte van Biljon, University of Pretoria, 2018. The transcriptome spans daily samples over 13 days, which included gametocyte commitment and development. Transcript expression profiles were provided as $\log_2(\text{Cy5}/\text{Cy3})$ expression values (log of the ratio between sample and reference, in a reference pool microarray design) at each time point. Expression values >0 indicated relative increased transcript expression, while expression values <0 indicated relative decreased transcript expression. Both expression datasets were filtered for the set of 147 MTP genes, which were subsequently analysed separately for strategy- and stage-specific expression.

The asexual and gametocyte transcript expression datasets of the permeome were assessed on the identification of clusters of MTPs with similar transcript expression profiles, using K-means clustering. For K-means clustering, centroids are placed in the results to define similar expression profiles (connect data points to its centroid) (Hartigan and Wong, 1979). Euclidean distance (squared) was used to assign data points to its closest centroid, resulting in clusters with similar expression profiles. For K-means clustering, the optimum number of centroids (clusters) that represent similar expression profiles for the asexual or gametocyte expression were determined using elbow plots. Elbow plots were generated from the asexual and gametocyte permeome expression datasets, respectively using RStudio (version 1.0.44) (Bholowalia and Kumar, 2014) by measuring the sum of squared error (SSE; distance between each transcript expression of the cluster) for each number of clusters (Tibshirani *et al.*, 2001; Cho *et al.*, 2004). With increasing cluster number, the SSE will decrease due to smaller distortion. The optimum number of clusters

was chosen where the SSE started to plateau (seen as the “elbow effect” in the graph). The determined optimum number of clusters was used for K-means clustering, using Euclidean distance. K-means clustering and heatmap visualisation were done, using the Multiple experiment viewer (MeV, version 4.9) (Saeed *et al.*, 2003).

2.3 Experimental analysis of metabolite uptake in *P. falciparum* asexual parasites

2.3.1 Erythrocyte collection and storage

Human blood (O⁺, A⁺ or B⁺) was collected in a blood bag containing citrate phosphate adenine anticoagulant (Adcock Ingram, RSA) and the erythrocytes (RBCs) were washed three times with phosphate buffered saline (1 x PBS, 137 mM NaCl, 2.7 mM KCl, 10 mM phosphate, pH 7.2) to remove serum and the buffy coat, as leukocytes could compromise the parasites in culture (Celada *et al.*, 1983; Brown and Smalley, 1981). Packed RBCs were subsequently resuspended in incomplete malaria culture media (Roswell Park Memorial Institute medium 1640 (RPMI), supplemented with 23.81 mM sodium hydrocarbonate (NaHCO₃), 25 mM HEPES (4-(2-hydroxyethyl)-1-piperazineethanesulfonic acid), 0.2% (w/v) D-glucose, 0.2 mM hypoxanthine (Sigma-Aldrich, Germany) and 0.024 mg/ml gentamycin (HyClone Laboratories Inc.)) to a final haematocrit of 50% and kept at 4°C until use.

2.3.2 Asexual parasite cultivation

P. falciparum asexual (strain NF54) parasites (infected erythrocytes, iRBCs) were maintained in sterile *in vitro* conditions at 5% haematocrit and ~5% parasitaemia in complete malaria culture media (incomplete media supplemented with 2.5 g/l Albumax II) under a nitrogen gas mixture of 5% O₂, 5% CO₂ and 90% N₂ (Afrox, South Africa), followed by incubation at 37°C with agitation at 60 rpm in a shaking incubator (Ratek, Australia) to maintain a high single cell infection rate and mimic *in vivo* growth conditions (Allen and Kirk, 2004b). Spent media was replaced daily and the parasitaemia monitored with Giemsa (1:6 Giemsa’s azur eosin methylene blue solution, VWR Chemicals Prolabo, in water) stained thin blood smears and light microscopy (1000x magnification, Zeiss Microscope, Japan). The parasitaemia was expressed as the number of iRBCs relative to the uninfected RBCs, as counted in approximately 10 fields of 100 RBCs each.

The ring stages were synchronised with D-sorbitol (Sigma-Aldrich, Germany) for iso-osmotic lysis of trophozoite and schizont stages (Lambros and Vanderberg, 1979), resulting in a homogeneous ring stage population. Parasite cultures (5% haematocrit) were pelleted by centrifugation (Boeco, Germany) at 3500g for 5 min, resuspended in three times pellet volume of 5% (w/v) sorbitol solution and incubated for 15 min at 37°C. The sorbitol and lysed parasites were removed by three washes of complete malaria culture media. The remaining ring stages were transferred back into culture and maintained as described above.

2.3.3 Isotopic evaluation of the permeome in *P. falciparum* parasites

For the evaluation of glucose uptake into *P. falciparum* asexual stages, [¹⁴C]-2-deoxyglucose (2DG, 55 mCi/mmol, PerkinElmer) was used. 2DG is taken up by glucose transporters and metabolised to 2DG-6-phosphate (2DG6P). The 2DG6P, however, cannot be further metabolised with phosphoglucose isomerase and therefore 2DG can be used as a direct indication of the uptake and not metabolism of glucose by the parasite. For the evaluation of amino acid uptake into *P. falciparum* asexual stages, [¹⁴C]-leucine (318 mCi/mmol, AEC Amersham), [¹⁴C]-lysine (56 mCi/mmol, ARC), [¹⁴C]-glutamic acid (282 mCi/mmol, PerkinElmer) and [¹⁴C]-aspartic acid (0.1 mCi/ml) were used.

2.3.3.1 Buffered solutions

Different HEPES buffered saline solutions (125 mM NaCl, 5 mM KCl, 25 mM HEPES and 1 mM MgCl₂, pH 7.1), supplemented with different glucose concentrations, were used for the uptake experiments: solution A (20 mM Glucose) and solution B (5 mM Glucose).

2.3.3.2 Parasite cultivation and preparation

The uptake experiments were done with either uninfected RBCs (O⁺, A⁺ or B⁺) or enriched mature *P. falciparum* (NF54 strain) trophozoite (30 - 36 hpi) iRBCs. Trophozoite iRBCs were enriched to high parasitaemia, based on the magnetic properties of the trophozoite stage parasite. As the haemoglobin is metabolised in the iRBCs as a food source (Miller *et al.*, 2002), an iron-containing haem moiety (Fitch *et al.*, 1983) is obtained. The parasite eludes the toxicity of the haem by chemically altering it into a haemozoin crystal in the food vacuole (Francis *et al.*, 1997). The iron in the haemozoin has an oxidative state, which differs from the one in haem (Fitch and Kanjanangulpan, 1987) and develops a paramagnetic property.

Mature trophozoite iRBCs (*P. falciparum* cultures at 5% haematocrit and 10 - 20% parasitaemia) were enriched to ≥90% parasitaemia, using a CS column (Miltenyi Biotec, USA) (Teng *et al.*, 2009; Trang *et al.*, 2004). The *P. falciparum* cultures were loaded onto the plastic-coated ferromagnetic fibres of the CS column in the VarioMacs (Miltenyi Biotec, Australia) separation unit's magnetic field. Uninfected RBCs was washed away using 5 column volumes (25 ml) of the appropriate solution as required for each study. The CS column was removed from the magnetic field and the *P. falciparum* trophozoite iRBCs eluted.

In experiments, where the iRBCs were compared to the uninfected RBCs, uninfected RBCs were incubated in parallel with the iRBC cultures under identical conditions for at least 48 h prior to the experiment. In order to ensure that the iRBCs and uninfected RBCs were comparable, the uninfected RBCs were run through the CS column and collected.

The uninfected RBCs and iRBCs were washed 3 times with the appropriate solution as required for each study prior to the initiation of the experiment and resuspended to a final concentration of between $5 \times 10^7 - 1 \times 10^8$ cells/ml, using an improved Neubauer cell counting chamber. The cells were subsequently recovered in the appropriate solution for 10 min at 37°C before subsequent experimentation.

2.3.3.3 Uptake measurements in uninfected RBCs and trophozoite iRBCs

Uptake of [^{14}C]-2DG, [^{14}C]-leucine, [^{14}C]-lysine, [^{14}C]-glutamic acid and [^{14}C]-aspartic acid, respectively, into uninfected RBCs and mature trophozoite iRBCs was investigated as described previously (Kirk and Horner, 1995; Kirk *et al.*, 1996). The uptake of [^{14}C]-2DG over time was initiated by the addition of [^{14}C]-2DG (0.1 $\mu\text{Ci/ml}$ final concentration) to the cell suspension ($5 \times 10^7 - 1 \times 10^8$ cells/ml in solution B). For the uptake reactions at fixed time periods (30 min or 2 h) [^{14}C]-2DG or [^{14}C]-amino acids (final concentration 1 $\mu\text{Ci/ml}$) was added in a 1:1 ratio to the cell suspensions (final concentration $5 \times 10^7 - 1 \times 10^8$ cells/ml in solution A).

All uptake experiments were performed at 37°C. At the specific time points, triplicate volumes (200 μl each) were transferred to microcentrifuge tubes containing 300 μl of dibutyl phthalate oil (density 1.04 g/ml) to terminate the reactions by centrifuging the cells through the oil (17 000g for 1 min). A 10 μl sample of the upper aqueous phase was transferred to a scintillation vial to determine the extracellular concentration of the radiolabelled metabolite. The amount of radiolabel trapped in the extracellular space of the cell pellet was estimated by taking replicate samples as quickly as possible after combining the cells and radiolabelled metabolite, and immediately centrifuging these through an oil layer as described above. The aqueous phase was aspirated, and the dibutyl phthalate oil layer rinsed three times with water to remove residual radioactivity. The remaining cell pellet was lysed with 0.1% (v/v) Triton X-100 (0.5 ml) and the proteins were precipitated with 5% (w/v) trichloroacetic acid (0.5 ml). The samples were centrifuged at 17 000g for 10 min to clear the cellular debris before transferring the supernatant to scintillation vials. To the scintillation vials, 2 ml of scintillation liquid (Ultima Gold, PerkinElmer, RSA) was added. The radioactivity present in the supernatant was measured using a β -scintillation counter (Tri-Carb 2800TR Liquid Scintillation Analyser, PerkinElmer, RSA).

2.3.3.4 Data analysis

The uptake of radiolabelled metabolites was represented as a distribution ratio, i.e. the concentration of radiolabelled metabolite inside the cell relative to the concentration of the metabolite in the extracellular solution (extracellular concentration of radiolabelled metabolite). The concentration of radiolabelled metabolite inside the cells was calculated from the amount of radiolabel in the cell pellet by first subtracting the radioactivity trapped in the extracellular space and adhering to the cell surface. This background measurement was subtracted from the data to

obtain a measurement of the amount of [¹⁴C]-2DG, -leucine, -lysine, -glutamic acid and -aspartic acid imported into the cells comprising the cell pellet. This was divided by the number of the cells in the pellet and by the intracellular water volume to yield an estimation of the intracellular concentration. The intracellular water volume was taken as 86 fl for uninfected RBCs (Hanssen *et al.*, 2012) and 75 fl for *P. falciparum* trophozoite iRBCs (Saliba *et al.*, 1998). Unless otherwise specified, the data are presented as the means from at least three independent experiments with the standard error of the mean (S.E.) indicated. Statistical significance was determined either with paired t-tests or with two-way ANOVA, using GraphPad Prism (version 5.00) program.

Chapter 3: Results

3.1 *In silico* evaluation and characterisation of the permeome encoded by *P. falciparum* parasites

3.1.1 Identification of the permeome

To investigate the strategy- and stage-specific expression of MTPs, a current, updated permeome is needed. While a previous study investigated the permeome of *P. falciparum* parasites, specifically focusing on MTPs with seven or more TMDs (Martin *et al.*, 2005), the genome has subsequently been re-annotated as more information became available. Here, the current permeome encoded by the *P. falciparum* genome was identified by using the revised annotation of the genome to search for keywords and for putative MTPs encoding 2 - 30 TMDs (Table 4). These searches were performed using PlasmoDB (version 28).

Table 4: Putative MTP genes identified with keyword searches and a TMD (2-30 domains) search, using the TMHMM algorithm. Both analyses were performed using PlasmoDB version 28.

Keyword searches		TMD search	
PlasmoDB Searches	Nr of Genes Identified	PlasmoDB Searches	Nr of Genes Identified
Keywords		Nr of TMDs	
ATPase	90	2	341
Carrier	39	3	144
Permease	1	4	105
Transport	388	5	56
Channel	21	6	42
ATP synthase	790	7	44
Pump	4	8	32
Porin	2	9	23
Symporter	10	10	26
Antiporter	10	11	29
Porter	1	12	24
Diffusion	1	13	6
Translocator	5	14-22	17
Total	1362	Total	889

The keyword search included transport-related keywords (as listed in Table 4) and resulted in the identification of 1362 genes (Table 4), including 135/136 (99%) of the MTP genes previously identified with the exception of one previously identified MTP gene (PF3D7_0613300 - Rhoptry protein). From the TMD search, 889 genes were identified with TMDs ranging between 2 – 30 domains (Table 4). This search included 115 MTP genes of the previously identified permeome (85% of the 136 previously identified MTP genes). Therefore, by combining the genes obtained from the keyword searches and the TMD search, a complete working list of 1994 putative MTP genes encoded by *P. falciparum* were obtained, which included all 136 previously identified MTP genes. Interestingly, after combining the results from the keyword and TMD searches, it was observed that the keyword search results also identified genes with less than two TMDs, which correlate to non-membrane spanning domains of multi-subunit MTPs. For example, ATP-binding

cassette (ABC) transporters contain not only two membrane-spanning domains (each containing multiple TMDs), but also two cytosolic ATP-binding domains that couple ATP hydrolysis to solute movement (Lodish *et al.*, 2013) as well as F-ATPases that contain multi-subunits, of which the cytosolic domain (F1) consists of five subunits with no TMDs and the membrane-spanning domain (F0) that consists of subunits with TMDs (Lodish *et al.*, 2000). These identified genes included genes such as the V-ATPase subunit H (PF3D7_1306600; 0 TMDs), and the F-ATPase alpha subunit, F1 complex (PF3D7_0217100; 0 TMDs).

To determine if the 1994 putative MTP genes have been associated with transport activity, their empirical metabolic functions were searched, using the MPMP database (<http://mpmp.huji.ac.il/>). MPMP determined, if the putative MTP genes either have a (i) transport activity defined as the description of the gene as either channel, transport, transporter, transporting, antiporter, symporter or porin in the function description or (ii) non transport activity (surface proteins, Rab proteins, secreted ookinete protein, kinases and genes with no identified pathway).

A total of 150 genes (8% of 1994 putative MTP genes) were classified as predicted MTP genes, based on the predicted transport function/activity from MPMP. However, three genes that were initially predicted as having transport activity were shown to not be part of the actual transporter complex and are therefore, not required for the transporter to function. Specifically, the gene encoding the nuclear transport factor 2 protein (NTF2, PF3D7_1412300) that mediates nuclear import (Ribbeck *et al.*, 1998) by facilitating in the cargo-receptor complex dissociation at the nuclear pore complex (Black *et al.*, 2001), but is not directly part of the actual nuclear pore (Bayliss *et al.*, 2002; Tuteja and Mehta, 2010). Similarly, the gene encoding the transportin protein (PF3D7_0627700; importin β) associates with the nuclear pore complex (NPC), but is not the actual transporter (Xu *et al.*, 2002; Bayliss *et al.*, 2002). Lastly, one of the ABC transporters (PF3D7_0810200) belongs to the ABC1 family, which is unrelated to ABC transporters (Bousquet *et al.*, 1991). Therefore, these genes (NTF2, importin β and ABC1 transporter) were removed from the list of predicted MTPs, resulting in a current, updated list of 147 MTP genes encoded by *P. falciparum* parasites (referred to as the permeome) that included all 136 previously identified MTP genes (Martin *et al.*, 2005; Martin *et al.*, 2009) and 11 newly identified MTP genes. These 11 new MTPs that were identified in this study included mitochondrial pyruvate carrier proteins (pyruvate:H⁺ symporters), Arsenical pump-driving ATPase, ATP synthase subunit c, magnesium transporters, ABC transporters, a zinc transporter and a nucleoporin (Table 5).

Table 5: Overview of the current *P. falciparum*-encoded permeome. A total of 147 MTP genes were identified, which consisted of 136 previously identified MTP genes (Martin *et al.*, 2005; Martin *et al.*, 2009) and 11 newly identified MTP genes.

***P. falciparum* encoded permeome**

Gene ID	Nr of TMDs	Function	Gene ID	Nr of TMDs	Function
Previously identified MTPs					
PF3D7_0204700	12	PfHT	PF3D7_0811100	4	Mitochondrial carrier protein
PF3D7_0919500	11	Sugar transporter	PF3D7_0905200	0	Mitochondrial carrier protein
PF3D7_0916000	11	Sugar transporter	PF3D7_1202200	1	Mitochondrial phosphate carrier protein
PF3D7_0529200	12	Sugar transporter	PF3D7_1223800	0	Mitochondrial carrier protein
PF3D7_1218400	10	Triose or hexose phosphate translocator	PF3D7_1241600	4	Mitochondrial carrier protein
PF3D7_0508300	9	PfTPT	PF3D7_1368700	2	Mitochondrial carrier protein
PF3D7_0530200	7	PfPPT	PF3D7_1147700	0	Mitochondrial ATP synthase delta subunit
PF3D7_0210300	12	Monocarboxylate transporter	PF3D7_0217100	0	ATP synthase F1, alpha subunit
PF3D7_0926400	11	Monocarboxylate transporter	PF3D7_1235700	0	Mitochondrial ATP synthase subunit beta
PF3D7_0823900	1	PfDTC	PF3D7_1310000	0	Mitochondrial ATP synthase delta subunit
PF3D7_0316600	6	PfFNT	PF3D7_1311300	0	Mitochondrial ATP synthase subunit gamma
PF3D7_1036800	10	PfACT	PF3D7_0715500	0	Mitochondrial ATP synthase F1, epsilon subunit
PF3D7_0206200	11	Pantothenate transporter	PF3D7_0519200	4	V-type proton ATPase proteolipid subunit
PF3D7_0828600	12	Folate transporter 1	PF3D7_0806800	6	Vacuolar proton translocating ATPase subunit A
PF3D7_1116500	11	Folate transporter 2	PF3D7_1354400	4	V-type proton ATPase proteolipid subunit
PF3D7_0629500	9	Amino acid transporter	PF3D7_1464700	0	ATP synthase (C/AC39) subunit
PF3D7_1208400	10	Amino acid transporter	PF3D7_1140100	0	V-type proton ATPase subunit F
PF3D7_1231400	9	Amino acid transporter	PF3D7_0406100	0	V-type proton ATPase subunit B
PF3D7_0209600	13	Amino acid transporter	PF3D7_0106100	0	V-type proton ATPase subunit C
PF3D7_0515500	14	Amino acid transporter	PF3D7_1311900	0	V-type proton ATPase catalytic subunit A
PF3D7_1132500	15	Amino acid transporter	PF3D7_1323200	0	V-type proton ATPase subunit G
PF3D7_0104800	12	PfNPT1	PF3D7_1341900	0	V-type proton ATPase subunit D
PF3D7_1227200	8	PfK1	PF3D7_1306600	0	V-type proton ATPase subunit H
PF3D7_1465500	7	PfK2	PF3D7_0934500	0	V-type proton ATPase subunit E
PF3D7_1132800	6	Aquaglyceroporin	PF3D7_1348800	9	E1-E2 ATPase
PF3D7_1107900	5	Mechanosensitive ion channel	PF3D7_0319700	13	ABC transporter
PF3D7_1432100	0	Voltage-dependent anion-selective channel protein	PF3D7_0302600	6	ABC transporter B family member 4
PF3D7_1203400	12	Transporter	PF3D7_1145500	6	ABC transporter B family member 3
PF3D7_0104700	12	Transporter	PF3D7_1209900	5	ABC transporter B family member 7
PF3D7_0312500	12	Transporter	PF3D7_1339900	4	ABC transporter B family member 5
PF3D7_0914700	11	Transporter	PF3D7_1352100	5	ABC transporter B family member 6
PF3D7_1129900	12	Transporter	PF3D7_1426500	6	ABC transporter G family member 2
PF3D7_0908800	4	Transporter	PF3D7_0523000	11	PfMDR1
PF3D7_1347200	9	PfNT1	PF3D7_1447900	10	PfMDR2
PF3D7_0824400	10	PfNT2	PF3D7_0112200	11	PfMRP1
PF3D7_1469400	11	PfNT3	PF3D7_1229100	11	PfMRP2
PF3D7_0103200	11	PfNT4	PF3D7_0709000	10	PfCRT

Gene ID	Nr of TMDs	Function	Gene ID	Nr of TMDs	Function
PF3D7_0603500	11	Cation/H ⁺ antiporter	PF3D7_1104800	9	Metabolite/drug transporter
PF3D7_1340900	10	PfPiT	PF3D7_1428200	12	Metabolite/drug transporter
PF3D7_1303500	14	PfNHE	PF3D7_1440800	12	Metabolite/drug transporter
PF3D7_1471200	11	PfSulP	PF3D7_0516500	10	Metabolite/drug transporter
PF3D7_0212800	11	Organic solutes/Na ⁺ or H ⁺ antiporter	PF3D7_0716900	9	Drug metabolite transporter
PF3D7_0523800	11	Divalent cation (metal) :H ⁺ symporter	PF3D7_0715800	9	Drug metabolite transporter
PF3D7_0614300	12	Organic anion transporter	PF3D7_1004800	5	ADP/ATP carrier protein
PF3D7_0609100	8	Zn ²⁺ or Fe ²⁺ permease	PF3D7_1037300	3	ADP/ATP transporter on adenylate translocase
PF3D7_0715900	6	Zinc transporter	PF3D7_1404600	4	Adenylyl cyclase alpha
PF3D7_1223700	5	Fe ²⁺ transporter	PF3D7_1138400	19	Guanylyl cyclase
PF3D7_1120300	2	PfMIT1	PF3D7_1360500	21	Guanylyl cyclase beta
PF3D7_1304200	2	PfMIT2	PF3D7_0212000	7	GDP-fructose:GMP antiporter
PF3D7_1427600	2	PfMIT3	PF3D7_0505300	9	UDP-N-acetyl glucosamine:UMP antiporter
PF3D7_1421900	4	Copper transporter	PF3D7_1113300	8	UDP-galactose transporter
PF3D7_1439000	2	Copper transporter	PF3D7_0515700	10	Glideosome-associated protein 40
PF3D7_0904900	7	Copper-transporting ATPase	PF3D7_0522600	8	Inner membrane complex protein
PF3D7_0504000	12	Cation transporting P-ATPase 3	PF3D7_0613300	11	Rhoptry protein
PF3D7_0516100	10	Cation-transporting ATPase 1	PF3D7_0824700	10	Lipase maturation factor
PF3D7_0727800	12	Cation transporting ATPase	PF3D7_1022200	12	Unknown function/metabolite/vitamin transporter
PF3D7_0106300	8	Calcium-transporting ATPase 6	PF3D7_1436100	5	Unknown function
PF3D7_1211900	8	PfATP4	PF3D7_0216800	14	Unknown function
PF3D7_0319000	10	P-type ATPase 7	PF3D7_0924500	14	Unknown function
PF3D7_1219600	10	Aminophospholipid-transporting P-ATPase 2	PF3D7_0614900	11	Unknown function
PF3D7_1223400	10	Phospholipid-transporting ATPase	PF3D7_0806200	9	Unknown function
PF3D7_1468600	10	Aminophospholipid transporter	PF3D7_1250200	9	Unknown function
PF3D7_0107500	12	Lipid/sterol:H ⁺ symporter	PF3D7_1332100	11	Unknown function
PF3D7_1456800	16	PfVFP1	PF3D7_0305300	11	Unknown function
PF3D7_1235200	16	PfVFP2	PF3D7_0315700	12	Unknown function
PF3D7_0108400	5	Mitochondrial carrier protein	PF3D7_0530500	13	Unknown function
PF3D7_0108800	0	Mitochondrial carrier family, unknown function	PF3D7_0628400	7	Unknown function
PF3D7_0407500	3	Mitochondrial carrier protein	PF3D7_1135300	8	Unknown function
Newly identified MTPs					
PF3D7_1470400	0	Pyruvate:H ⁺ Symporter	PF3D7_0827700	9	Magnesium transporter
PF3D7_1340800	1	Pyruvate:H ⁺ Symporter	PF3D7_0306700	2	Magnesium transporter
PF3D7_0905100	4	Nucleoporin	PF3D7_0415000	0	Arsenical pump-driving ATPase
PF3D7_1368200	0	ABC transporter E family member 1	PF3D7_0705900	2	ATP synthase subunit c
PF3D7_1121700	0	ABC transporter GCN20	PF3D7_1022300	7	Zinc transporter
PF3D7_0813700	0	ABC transporter			

3.1.2 Characterisation of the 11 newly identified MTPs

These 11 newly identified MTPs were subsequently characterised to identify the integral membrane protein class each MTP belongs to, as well as confirm the predicted structures, similar to what was previously done for the other MTPs (Martin *et al.*, 2005).

3.1.2.1 Classification of the 11 newly identified MTPs into integral membrane protein classes

First, the 11 newly identified MTP sequences were queried against proteins from other organisms (BLASTP) to classify them into specific integral membrane protein classes (Channels, ATP-powered pumps, Transporters or Other transporters) using the TCDB (<http://www.tcdb.org/>, Fig. 6, Supplementary Table 2) (Saier *et al.*, 2016). This database uses functional and phylogenetic information to classify MTPs, using the International Union of Biochemistry and Molecular Biology (IUBMB) approved Transporter Classification System (Busch and Saier, 2003). These data were combined with the integral membrane protein classification of the 136 previously identified MTPs (Martin *et al.*, 2005; Martin *et al.*, 2009) to obtain an overview of the integral membrane protein classes encoded by *P. falciparum* parasites.

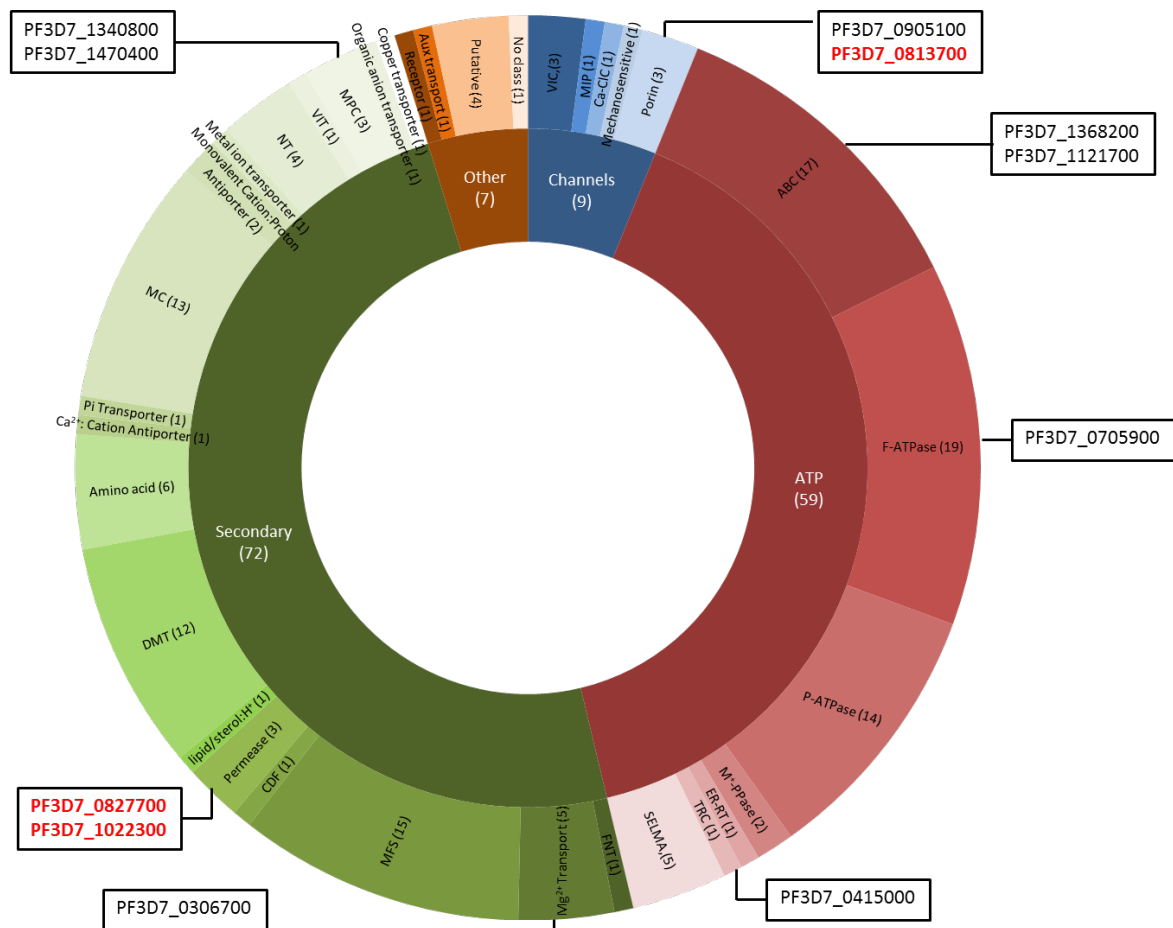


Figure 6: Classification of the *P. falciparum*-encoded permeome into specific integral membrane protein classes. The permeome was classified as either Channels, ATP-powered pumps, Transporters or Other transporters (inner ring) with the corresponding number of MTPs in each class (indicated in brackets). Within each class, the MTPs were further classified into specific integral membrane protein families (outer ring) according to the IUBMB approved Transporter Classification System (Busch and Saier, 2003). The size of each segment correlates to the number of MTPs (indicated in brackets) allocated to the segment. The 11 newly identified MTPs are shown in black boxes. The red gene IDs are the proteins that were classified into the indicated classes, which did not correlate with their annotations obtained from PlasmoDB. Abbreviations: Ion channels: Voltage-gated Ion channel Superfamily (VIC); The Major Intrinsic Protein family (MIP); The Calcium-Dependent Chloride Channel (Ca-ClC) Family; Small Conductance Mechanosensitive Ion Channel Family; Porins: The Human Coronavirus 229E Viroporin Family; Mitochondrial and Plastid Porin Family, and the Nuclear Pore Complex Family (NPC); ATP dependent transporters: ABC: The ATP-binding Cassette Superfamily; F/-ATPase: The H⁺- or Na⁺-translocating F-type, V-type and A-type ATPase Superfamily; P-ATPase: The P-type ATPase Superfamily; M⁺-PPase: The H⁺, Na⁺-translocating Pyrophosphatase Family; The endoplasmic Reticular Retrotranslocon (ER-RT) Family; TRC: The TMS Recognition/Insertion Complex Family; The Symbiont-specific ERAD-like Machinery (SELMA) Family; Transporters: The Formate-Nitrite Transporter Family (FNT); Major Facilitator Superfamily (MFS); Cation Diffusion Facilitator Family (CDF); Permease: Zinc (Zn²⁺)-iron (Fe²⁺) Permease Family; The NIPA Mg²⁺ Uptake Permease (NIPA) Family and the Sulfate Pemease (SulP) Family; Lipid/sterol H⁺: Resistance-Nodulation-Cell Division Superfamily; The Drug/Metabolite Transporter Superfamily (DMT); Amino acid: Amino acid/Auxin Permease Family and the Neurotransmitter: Na⁺ Symporter Family, Ca²⁺: Cation Antiporter Family; The Mitochondrial Carrier Family (MC); the Monovalent Cation: Proton Antiporter-1 (CPA1) Family; Metal Ion Transporter Family; The Nucleoside Transporter Family (NT); The Vacuolar Iron Transporter (VIT) Family; The Mitochondrial Pyruvate Carrier Family (MPC); Other: Receptor: The Outer Membrane Receptor Family, Putative: The Putative Heme Handling Protein Family and Aux transport: The SLC and TCST-Associated Component (STAC-A) Family.

The 11 MTPs were classified into the specific integral membrane protein classes of the proteins from other organisms to which the MTPs showed the highest sequence similarities to (TCDB). Of the 11 MTP sequences queried against proteins from other organism, eight showed similar MTP annotations between *P. falciparum* (PlasmoDB) and other organisms (Fig. 6 black gene IDs), while the other three MTPs showed similarities to different MTP annotations in other organisms (different MTP annotation between *P. falciparum* and other organisms) (Fig. 6 red gene IDs), resulting in classifying these three MTPs into integral membrane protein classes, which did not correlate with their annotations obtained from PlasmoDB. For example, PlasmoDB annotated PF3D7_0813700 as an ABC transporter, but showed similarity to *Bacillus thuringiensis* Vegetative Insecticidal Protein-3 (TCDB), which resulted in classifying PF3D7_0813700 as a Channel (Fig. 6) and not as an ATP-powered pump.

Nevertheless, all 11 MTPs belonged to known integral membrane protein families. Some are new additions to the Zinc (Zn^{2+})-iron (Fe^{2+}) Permease family (Permease – Fig. 6), the NIPA Mg^{2+} Uptake Permease (NIPA) family (Permease – Fig. 6), the Mitochondrial Pyruvate Carrier (MPC) family (MPC – Fig. 6), the *Bacillus thuringiensis* Vegetative Insecticidal Protein-3 (Vip3) family (Porin – Fig. 6), the Nuclear Pore Complex (NPC) family (Porin – Fig. 6), the Membrane Mg^{2+} Transporter (MMgT) family (Mg^{2+} transporters – Fig. 6), the ATP-binding Cassette (ABC) superfamily (ABC – Fig. 6) and the H^+ - or Na^+ -translocating F-type, V-type and A-type ATPase (F-ATPase) superfamily (F-ATPase – Fig. 6). One MTP was classified into an integral membrane protein family that was not previously identified in *P. falciparum*, the TMS Recognition/Insertion Complex (TRC) family (TRC – Fig. 6, Supplementary Table 2). This classification of the 11 newly identified MTPs was subsequently combined with the integral membrane protein classification of the 136 previously identified MTPs (Martin *et al.*, 2005; Martin *et al.*, 2009), which showed that the permeome (147 MTPs) consists of 6% Channels (9/147 MTPs), 40% ATP-powered pumps (59/147 MTPs), 49% Transporters (72/147 MTPs) and 5% Other transporters (7/147 MTPs) (Fig. 6). In summary, the 11 newly identified MTPs were characterised on integral membrane protein classification as all 11 belonged to known integral membrane protein families. These 11 newly identified MTPs were subsequently interrogated on their predicted structure, using hydropathy plots, to determine, if the 11 MTPs conform to the typical MTP profile.

3.1.2.2 Hydrophobicity of the 11 newly identified MTPs

MTPs have typical hydropathy profiles, which include regularity of spacing and a single large extracellular domain in the middle of the protein (Martin *et al.*, 2005). Here, the hydropathy profiles of the 11 newly identified MTPs were investigated, based on the hydrophobicity of entire protein sequences (read through successive windows, Fig. 7).

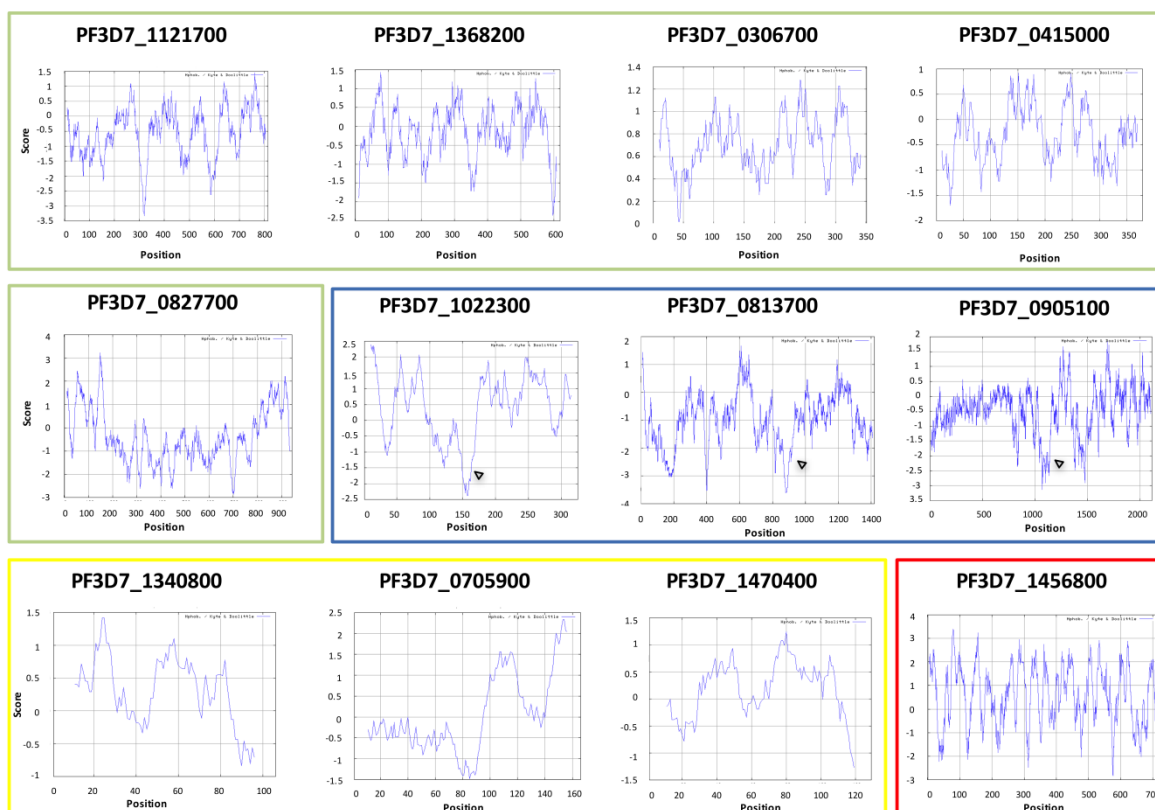


Figure 7: Comparison of hydropathy plots of the 11 new MTPs to a typical MTP hydropathy plot generated using ProtScale – Kyte & Doolittle hydropathy input. The PfVP1 with a typical MTP hydropathy plot is shown in the red block. The hydropathy plots of the 11 newly identified MTPs (in the green, blue and yellow blocks) were compared to the typical MTP hydropathy plot. Green blocks indicate regularly spaced hydropathy profiles; the blue block indicates hydropathy profiles with single large extracellular domains (indicated with arrows); and the yellow block indicates hydropathy profiles with neither regular spacing nor a single large extracellular domain.

The hydropathy plot of the PfVP1 (PF3D7_1456800; Fig. 7 – red box) shows 15 peaks (peaks with positive scores) in the hydrophobicity index, corresponding to 15 predicted TMDs, which is a characteristic of pyrophosphatases (McIntosh and Vaidya, 2002). The hydropathy plots of the proteins encoded by PF3D7_1121700, PF3D7_1368200, PF3D7_0306700, PF3D7_0415000 and PF3D7_0827700 had regular spacing (Fig. 7 – green blocks) and therefore these proteins resembled those of typical MTPs (Martin *et al.*, 2005). By contrast, the hydropathy profiles of the MTPs indicated in the blue block (PF3D7_1022300, PF3D7_0813700 and PF3D7_0905100, Fig. 7) were not regularly spaced; however, a single large extracellular domain in the middle of the protein was observed, which is characteristic of a MTP (Martin *et al.*, 2005). The hydropathy profiles of PF3D7_1340800, PF3D7_0705900 and PF3D7_1470400 (Fig. 7 – yellow block) did not resemble typical MTPs since no regular spacing between the predicted TMDs were observed and several large extracellular domains were indicated. However, two of these MTPs are subunits of the mitochondrial pyruvate carrier, which has been described in yeast (Bricker *et al.*, 2012; Herzig *et al.*, 2012; Oppenheim *et al.*, 2014). The other protein is the ATP synthase subunit *c*, which is the main transmembrane subunit (Nina *et al.*, 2011). Therefore, even when these proteins did not

show typical MTP hydropathy plots, they cannot be excluded as MTPs as they are essential subunits of either the whole mitochondrial pyruvate carrier or ATP synthase transporters and are required to perform the function of these transporters.

In summary, the structure predictions of the 11 newly identified MTPs indicated that most of these MTPs conform to the typical MTP profile. However, the position of the protein should be considered as some MTPs contain multiple subunits, of which some may be cytosolic domains with no TMDs and will not conform to the typical MTP profile. The structure of the 11 newly identified MTPs were therefore characterised based on the hydrophobicity of these proteins.

3.1.3 Identification of MTPs essential for *P. falciparum* intraerythrocytic parasites

One way to determine which *P. falciparum*-encoded MTPs may be viable drug targets is to indicate whether the gene is essential or dispensable for life cycle progression. Genes that are refractory to knock-out were characterised as essential, whereas dispensable genes are disruptable by knock-out, which either influence parasite growth or have no effect on parasite growth. The essentiality of the permeome (147 MTP genes) was investigated to observe whether these genes show strategy and/or stage importance in the *P. falciparum* intraerythrocytic parasites, using PlasmoGEM and PhenoPlasm databases (<http://plasmogem.sanger.ac.uk/> and <http://phenoplasm.org/>).

Thirty six MTP genes were classified as essential by both PlasmoGEM and PhenoPlasm, with an additional 14 MTP genes identified as essential by PhenoPlasm alone. Therefore, a total of 50 MTP genes were classified as essential (34% of the permeome, 45% of MTPs tested – no phenotype data in PhenoPlasm and PlasmoGEM for 35 MTP genes, Fig. 8 – red), of which most were identified from *P. berghei* orthologs whereas only ~16% (8 of 50 essential genes) of the essential MTP genes were tested in *P. falciparum*. Gene disruptions were possible for dispensable MTP genes (62 genes, 42% of the permeome dispensable, 55% of MTPs tested, Fig. 8 – green) and there were MTP genes with no phenotypic investigations as yet (35 genes, 24% of the permeome, Fig. 8 – blue). The essential and dispensable MTP genes in each integral membrane protein class are provided in Supplementary Table 3.

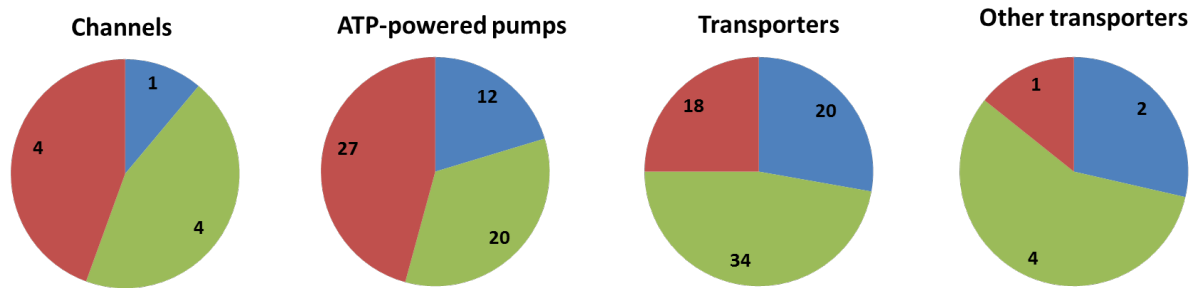


Figure 8: The phenotype distribution of each MTP gene in the specific integral membrane protein classes. Essential, dispensable and genes with no phenotype data are indicated in red, green and blue, respectively. The number of MTP genes for each phenotype is included. The phenotypes are from the combination of PhenoPlasm and PlasmogEM.

It was observed that ~50% of the Channels (4 of 9 MTP genes) and ATP-powered pumps (27 of 59 MTP genes) are essential, while 25% of the Transporters (18 of 72 MTP genes) and 14% of the Other transporters (1 of 7 MTP genes) are essential. As the Channels and ATP-powered pumps have the most essential MTP genes, these classes may have less alternative MTPs for the gaining and utilisation of energy and the generation of ion gradients across membranes, and therefore, may be good drug targets. The essential Channels identified in this study correlated with a previous study that identified MTP genes required for the acquisition and distribution of energy and the generation of ion gradients across membranes, as essential for the *Plasmodium* parasite (Bushell *et al.*, 2017).

By contrast, ~50% of the Channels (4 of 9 MTP genes), 34% of the ATP-powered pumps (20 of 59 MTP genes), 47% of the Transporters (34 of 73 MTP genes) and 57% of the Other transporters class (4 of 7 MTP genes) were dispensable with a reduction in either asexual or gametocytes growth (Supplementary Table 3).

For the investigation of the permeome's strategy-specificity between the asexual and gametocyte stages, the MTP genes that affected the asexual or gametocyte stages were investigated. Of the 112 MTP genes tested (50 essential MTP genes and 62 dispensable MTP genes), nine had affected both asexual and gametocyte stages, 33 affected asexual stages with no effect on the gametocytes, while three MTP genes showed a reduction in gametocyte growth with no effect on the asexual stages (Supplementary Table 3). These results suggest that certain MTPs may thus be either TCP-1 or TCP-5 targets (Burrows *et al.*, 2017), allowing for specific targeting of either asexual or gametocyte stages.

Not all MTP genes have been tested for essentiality in asexual or gametocyte stages. Furthermore, no phenotype data are available for specifically the ring, trophozoite, schizont stages and stage I - V gametocytes; hence, no stage-specific essentiality can be determined. In the absence of complete datasets that tested essentiality of all 147 MTP genes throughout intraerythrocytic

development, strategy- and stage-specific expression of the permeome in *P. falciparum* will be investigated as an indication of where in the intraerythrocytic stages each MTP is required.

3.2 The strategy- and stage-specific expression of the permeome

The strategy- and stage-specific mRNA expression of the entire complement of *in silico* predicted *P. falciparum*-encoded MTPs were evaluated during both asexual and gametocyte stages of *P. falciparum* parasites, using K-means clustering. K-means clustering enabled the identification of clusters of MTPs with similar transcript expression profiles in the asexual or gametocyte stages, respectively.

For K-means clustering, the optimum number of centroids (clusters) was determined, using elbow plots (Fig. 9). Elbow plots were generated using RStudio (version 1.0.44) (Bholowalia and Kumar, 2014) from the asexual and gametocyte MTP expression datasets, respectively. The expression profiles represented as \log_2 (Cy5/Cy3) expression values were obtained for the asexual (hourly sampling across the 48 h asexual cycle) (Painter *et al.*, 2017) and gametocyte stages (daily sampling for 13 days) (unpublished data, PhD study: Riëtte van Biljon), which were filtered for the 147 MTPs. Since there were no expression values available for the MTP PF3D7_0628400 in either the asexual or gametocyte datasets, subsequent analyses were performed for 146 MTPs.

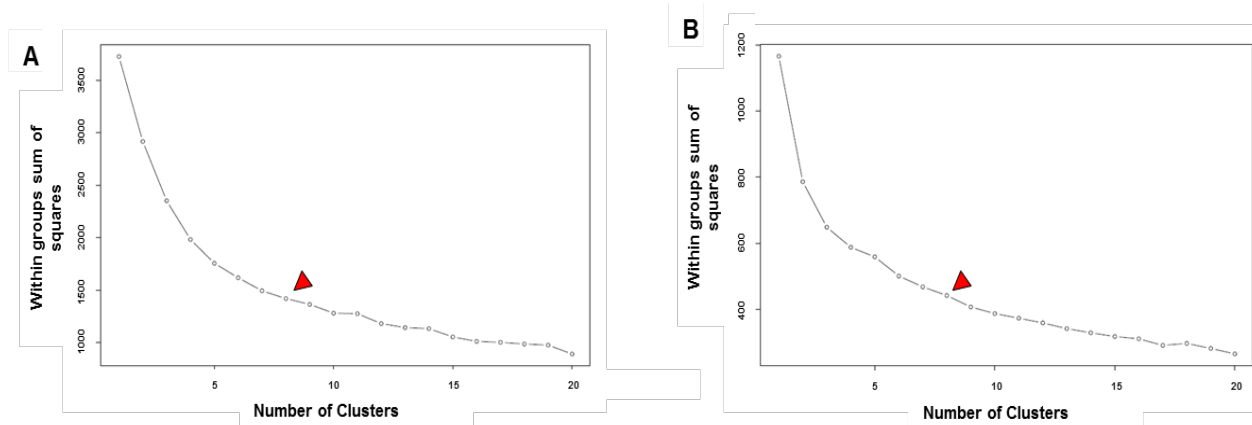


Figure 9: Determination of the optimum number of transcript expression clusters, using elbow plots. Elbow plots were generated, using the transcriptome data of the predicted MTPs in the (A) asexual and (B) gametocyte stages. The optimum number of clusters is indicated by the red triangles.

From the elbow plot analysis for both asexual and gametocyte stages, the elbow was observed between 5 and 10 clusters. Within this range of clusters, the smallest difference of SSE (distance between each transcript expression of the cluster) was observed between clusters 8 and 9 for both asexual and gametocyte stages. Therefore, 8 clusters were chosen for K-means clustering ($K = 8$) as within these clusters, a small distortion between the transcript expression profiles will be maintained (Fig. 9 red triangles).

3.2.1 Strategy-specific expression of the permeome

The mRNA expression profiles of the 146 MTP genes, represented as \log_2 (Cy5/Cy3), were K-means clustered ($K = 8$) in the asexual and gametocyte stages, respectively and were visually represented using a heatmap for the asexual (Fig. 10) and for the gametocyte stages (Fig. 11). The MTP mRNA expression profiles in each cluster were evaluated, using the average peak expression relative to the 48 h asexual stages (Fig. 10) or the 13 days sampled during gametocytogenesis (Fig. 11). The average peak expression of each cluster enabled the identification of MTP genes that showed increased transcript expression in specific developmental stages of the asexual and gametocyte stages. The percentage of the permeome with increased transcript expression in each cluster was also evaluated to determine the number of MTP genes that showed increased transcript expression during each of the specific intraerythrocytic developmental stages.

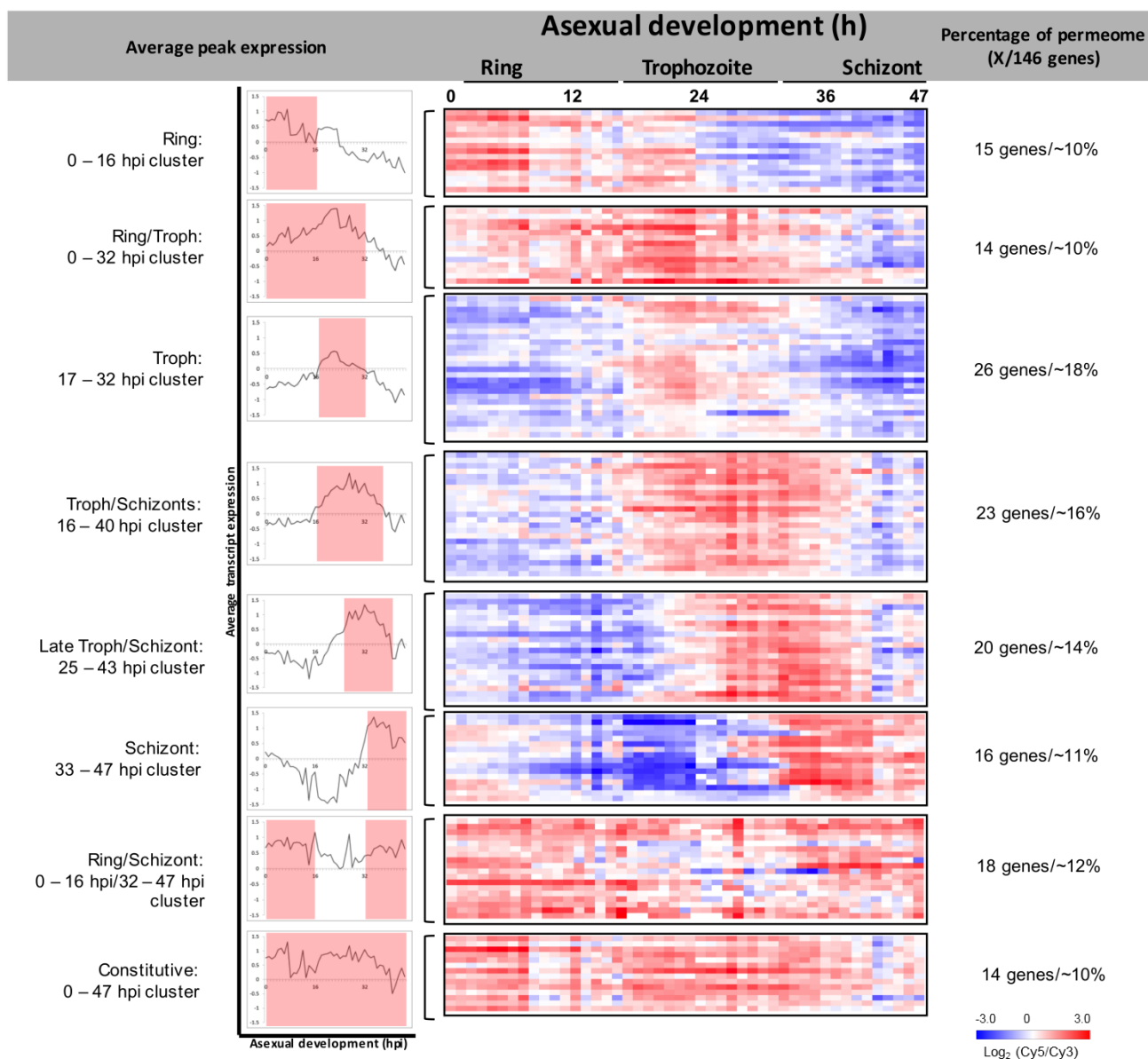


Figure 10: Transcript expression profiles of the MTP genes in *P. falciparum* asexual stages. Based on elbow plot analysis, $K = 8$ clusters were selected for K-means clustering, using Euclidean distance for asexual stages (Painter *et al.*, 2017). Transcript expression profiles of the MTP genes is given as \log_2 (Cy5/Cy3) expression values over time courses (hpi). Each horizontal line represents a single MTP (total

= 146 MTPs). Asexual stages were sampled hourly for 48 h. Blue represents decreased transcript expression, while red represents increased transcript expression. Colour intensity is directly proportional to the level of expression. The average peak expression graph for each cluster is indicated with asexual development time (0 – 48 hpi) on the x - axis and average expression values (1.5 to -1.5) of the specific cluster on the y - axis. Ring stages observed at 0 – 16 hpi, trophozoite stages observed at 17 – 32 hpi and schizont stages observed at 33 – 47 hpi. Constitutive expression observed at 0 – 47 hpi (average increased expression during 0 – 47 hpi).

The entire complement of MTP genes (146 MTPs) had increased transcript expression at some point during asexual development, supporting the heavy dependence on the exchange of metabolites in asexual stages (Olszewski *et al.*, 2009; Olszewski and Llinás, 2011). A phase-like distribution, following K-means clustering (Fig. 10), showed peak MTP transcript expression during the different developmental asexual stages as observed from the average peak expression for each cluster. It was observed that MTP transcript expression was time- and stage-dependent with increases from the ring (42%) to trophozoite (66%) stages, and with a subsequent decrease in the number of MTP genes expressed during the schizont (62%) stages. A subset of genes (10%) exhibited constitutive increased transcript expression during asexual development.

By contrast, during gametocytogenesis, there was a general decrease in the transcript expression of MTP genes, with only 39% of the MTP genes (57/146 MTPs) showing increased transcript expression, suggesting a reduced range of MTPs active in the gametocyte stages, indicative of the more quiescent metabolism of gametocytes in comparison to asexual parasites (Shute, 1960; Sinden and Smalley, 1979; Delves *et al.*, 2013). Here, K-means clustering also enabled the identification of clusters of MTP genes with increased/decreased transcript expression profiles during the different developmental stages of gametocytogenesis (Fig. 11). Peaks in MTP transcript expression were seen during stage I, stage III-IV and stage V gametocytes with 18% (27/146 MTPs) of the entire permeome constitutively expressed during all the developmental stages of gametocytogenesis (Fig. 11).

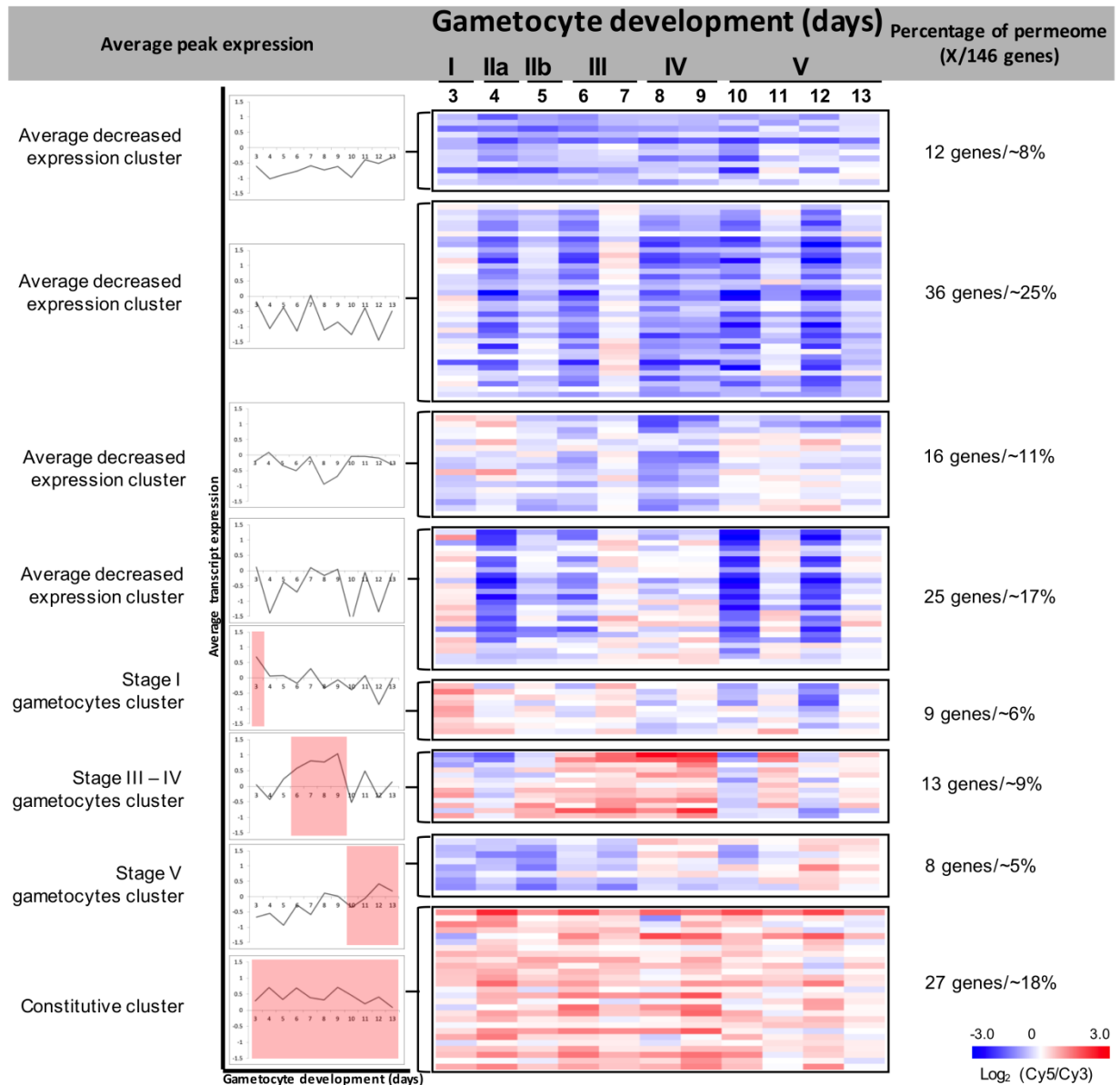


Figure 11: Transcript expression profiles of the MTP genes in *P. falciparum* gametocyte stages. Based on elbow plot analysis, K = 8 clusters were selected for K-means clustering using Euclidean distance for gametocyte stages (Riëtte van Biljon). Transcript expression profiles of the MTP genes is given as $\log_2(\text{Cy5}/\text{Cy3})$ expression values over time courses (days). Each horizontal line represents a single MTP (total = 146 MTPs). Gametocyte stages were sampled daily for 13 days, but expression values from day 3 – 13 were shown representing the five stages of gametocytogenesis. Blue represents decreased transcript expression, while red represents increased transcript expression. Colour intensity is directly proportional to the level of expression. The average peak expression graph for each cluster is indicated with gametocyte time development (days) on the x - axis and average expression values (1.5 to -1.5) of the specific cluster on the y - axis. Stage I gametocytes are observed at day 3, stage II observed at day 4 – 5, stage III observed at day 6 – 7, stage IV observed at day 8 – 9 and stage V gametocytes observed at day 10 – 13. Constitutive expression observed at day 3 - 13 (average increased expression during day 3 - 13).

Interestingly, more MTP genes were constitutively expressed in gametocytes (18%) in comparison to the asexual stages (10%). Unexpectedly, only ~1.5% of the permeome (2 MTP genes), including adenylyl cyclase alpha and a conserved *Plasmodium* membrane protein with unknown function, showed increased transcript expression throughout both asexual and gametocyte development (Fig. 12), further suggesting that MTPs may be separately targeted as either TCP-1 or TCP-5.

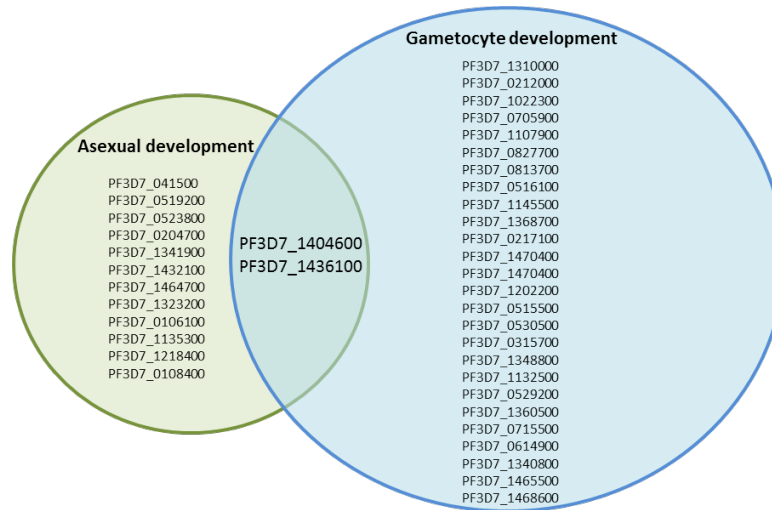


Figure 12: Constitutively expressed MTP genes in both asexual (green) and gametocyte (blue) stages. Common constitutively expressed MTP genes are shown in the overlap.

In conclusion, the whole complement of parasite-encoded MTP genes showed increased transcript expression during the asexual stages, whereas in the gametocyte stages, less than half of the predicted MTP genes showed increased transcript expression, suggesting the strategy-specific expression of the MTPs in *P. falciparum* parasites. Subsequently, the stage-specific expression of the MTP genes was investigated.

3.2.2 Stage-specific expression of the permeome

As stated in the introduction, there are stage-specific metabolic processes that occur in the ring, trophozoite and schizont stages and in stage I – V gametocytes, which are hypothesised to be supported by the stage-specific expression of MTPs. This was investigated by looking at the transcript expression profiles of MTPs that could be involved in amino acid transport (haemoglobin degradation and protein synthesis), carbohydrate metabolism (glycolysis and TCA cycle), DNA synthesis and lipid metabolism.

3.2.2.1 Investigation of the stage-specific MTP expression profiles during the asexual stages

The stage-specific expression profiles of the six parasite-encoded amino acid transporters in the permeome that may mediate the uptake and release of amino acids were investigated (Fig. 13).

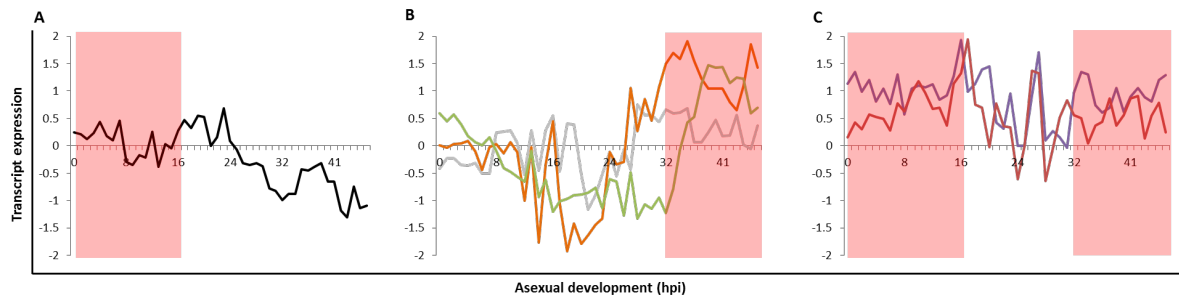


Figure 13: Stage-specific transcript expression profiles of six amino acid transporter genes throughout the asexual stages, clustered using Euclidian distance in similar profiles of transcript expression. The clusters are shown with shaded blocks. (A) 0 – 16 hpi expression cluster (PF3D7_0629500 – black), (B) 32 – 47 hpi expression cluster (PF3D7_0209600 – orange, PF3D7_1208400 – grey and PF3D7_1231400 – green) and (C) 0 – 16 hpi and 32 – 47 hpi expression cluster (PF3D7_0515500 – purple and PF3D7_1132500 – red). The transcript expression profiles of the MTP genes is given as $\log_2(\text{Cy5/Cy3})$ expression values (y - axis) at each time point in the 48 h time course of asexual development (x - axis). Ring stages observed at 0 – 16 hpi, trophozoite stages observed at 17 – 32 hpi and schizont stages observed at 33 – 47 hpi.

Amino acid transporter genes associated to clusters, which showed average transcript expression between 0 – 16 hpi and 32 – 47 hpi (Fig. 13 – expression clusters that were obtained from Fig. 10). The PF3D7_0629500 gene showed increased transcript expression during 0 – 16 hpi (ring stages), with peak expression at 23 hpi (early trophozoite stages, Fig. 13 A). PF3D7_1208400, PF3D7_0209600 and PF3D7_1231400 genes showed increased transcript expression between 32 – 47 hpi (schizont stages), with peak expression at 28 hpi (late trophozoite stages, Fig. 13 B), 35 hpi and 39 hpi (schizont stages, Fig. 13 B), respectively. By contrast, PF3D7_1132500 and PF3D7_0515500 genes had similar transcript expression profiles, with increased expression between 0 -16 hpi (ring stages) and peak expression at 16 and 17 hpi, respectively (Fig. 13 C), after which the expression decreased and increased again between 32 – 47 hpi (schizont stages). These data indicate stage-specific expression of amino acid transporter genes, as different amino acid transporters were expressed at either ring and trophozoite or trophozoite and schizont stages. However, two amino acid transporters were expressed throughout the asexual stages. Therefore, at any given point during the asexual stages, there is an amino acid transporter gene expressed.

For carbohydrate metabolism, glycolysis requires the import of sugars such as glucose that may be mediated by four sugar transporters (PF3D7_0919500, PF3D7_0529200, PF3D7_0204700 – PfHT and PF3D7_0916000). The PF3D7_0529200 gene (Fig. 14 A) showed increased transcript expression between 0 – 32 hpi (ring and trophozoite stages), with a peak expression at 17 hpi (early trophozoite stages), while the other two sugar transporter genes (PF3D7_0919500 – Fig. 14 C – light blue and PF3D7_0916000 – Fig. 14 D) showed increased transcript expression in the later asexual stages (late trophozoite/schizont stages), with corresponding peak expression at 27 hpi for PF3D7_0919500 and at 38 hpi for PF3D7_0916000. The PfHT transcript was constitutively expressed during the asexual stages, but showed peak expression at 21 hpi (trophozoite stages – Fig. 14 F) and continued in the schizont stages. This data indicates stage-specific expression of

sugar transporter genes as during the asexual stages, different sugar transporters were expressed in each stage. However, the PfHT gene did not show stage-specific expression.

Glucose is metabolised to either lactic acid or pyruvate during glycolysis (Roth *et al.*, 1988; Jensen *et al.*, 1983; Zolg *et al.*, 1984), of which lactic acid is exported from the parasite cytosol (Kanaani and Ginsburg, 1991). Pyruvate can be further metabolised through the TCA cycle as *P. falciparum* asexual stages also use the TCA cycle for ATP production, although to a lesser extent than anaerobic glycolysis (MacRae *et al.*, 2013; Cobbold and McConville, 2014; Lamour *et al.*, 2014). The two monocarboxylate transporters that export lactic acid to the host RBC were expressed during the trophozoite stages with peak transcript expression at 27 hpi (PF3D7_0210300 – Fig. 14 B – red) and during the late trophozoite/schizont stages, with peak transcript expression at 32 hpi (PF3D7_0926400, Fig. 14 C – light green). By contrast, the two pyruvate:H⁺ symporters that are required to transport pyruvate to the mitochondrion for the TCA cycle showed increased transcript expression in the ring and schizont stages, with peak expression at 27 hpi (trophozoite stages, Fig. 14 E). The PfPPT (PF3D7_0530200, Fig. 14 C – dark green) that can also transport pyruvate to the mitochondrion was expressed between 25 – 43 hpi, with peak transcript expression at 28 hpi (trophozoite stages).

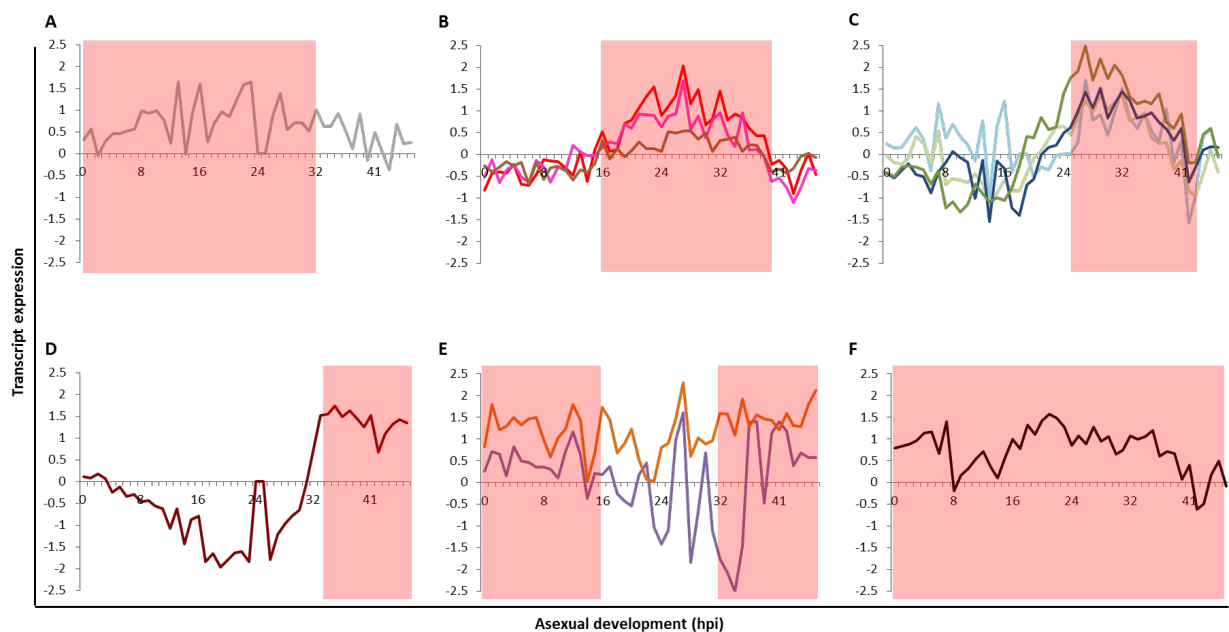


Figure 14: Stage-specific transcript expression profiles of MTP genes involved in carbohydrate metabolism (glycolysis and TCA cycle) throughout the asexual stages, clustered using Euclidian distance in similar patterns of transcript expression. The clusters are shown with shaded blocks. (A) 0 – 32 hpi expression cluster (PF3D7_0529200 – sugar transporter - grey), (B) 16 – 40 hpi expression cluster (PF3D7_0210300 – monocarboxylate transporter – red, PF3D7_0823900 - PfDTC – pink and PF3D7_1368700 - mitochondrial carrier protein – brown), (C) 25 – 43 hpi (PF3D7_0919500 – sugar transporter – light blue, PF3D7_1036800 - PfACT – dark blue, PF3D7_0926400 – monocarboxylate transporter – light green and PF3D7_0530200 – PfPPT – dark green), (D) 33 – 47 hpi expression cluster (PF3D7_0916000 – sugar transporter – dark red), (E) 0 -16 hpi and 32 – 47 hpi expression cluster (two pyruvate:H⁺ symporters: PF3D7_1470400 – orange and PF3D7_1340800 – purple) and (F) 0 - 47 hpi expression cluster (PF3D7_0204700 – PfHT – black). The transcript expression profiles of the MTP genes is given as log₂(Cy5/Cy3) expression values (y – axis) at each time point in the 48 h time course of asexual development (x - axis). Ring stages observed at 0 – 16 hpi, trophozoite stages at 17 – 32 hpi and schizont stages at 33 – 47 hpi. Constitutive expression observed at 0 – 47 hpi.

Pyruvate is broken down to produce acetyl-CoA in the mitochondrion that can either be further metabolised in the TCA cycle or be transported out of the mitochondrion. For the production of acetyl-CoA, the PfDTC (PF3D7_0823900, Fig 14 B – pink) that mediates the oxoglutarate–malate exchange across the inner mitochondrial membrane (Nozawa *et al.*, 2011) for CoA biosynthesis was expressed between 16 – 40 hpi. Likewise, the mitochondrial carrier protein (PF3D7_1368700, Fig 14 B – brown) that transports CoA across the mitochondrion, for the production of Acetyl-CoA (Cobbold *et al.*, 2013) was also expressed between 16 – 40 hpi. Acetyl-CoA can then be transported out of the mitochondrion, using the PfACT (PF3D7_1036800, Fig. 14 C – dark blue), which was expressed between 25 – 43 hpi, with peak transcript expression at 29 hpi (trophozoite stages). The transcript expression profiles of the MTP genes involved in the export of lactate and pyruvate, specifically PfPPT, and which is also involved in the TCA cycle, showed stage-specific expression during the trophozoite and schizont stages, whereas the two pyruvate: H⁺ symporters did not show stage-specific expression during the asexual stages.

P. falciparum parasites salvage host purine for DNA synthesis (De Koning *et al.*, 2005; Cassera *et al.*, 2011) that may be mediated by the four PfNT genes (PfNT1 - PF3D7_1347200, PfNT2 - PF3D7_0824400, PfNT3 - PF3D7_1469400 and PfNT4 - PF3D7_0103200, Fig. 15), which showed increased transcript expression between 0 – 32 hpi (ring and trophozoite stages). PfNT3 and 4 transcripts already showed increased expression between 0 – 16 hpi (ring stages, Fig 15 A), after which peak transcript expression was observed at 20 hpi (PF3D7_0103200, Fig. 15 A - grey) and 23 hpi (PF3D7_1469400, Fig. 15 A - black). Similar peak transcript expression was observed in the trophozoite stages for PfNT1 at 22 hpi (PF3D7_1347200, Fig. 15 B – green) and for PfNT2 at 21 hpi (PF3D7_0824400, Fig. 15 B – orange). These transcript expression profiles show stage-specific expression of the PfNT genes in the ring and trophozoite stages, correlating with the requirement of DNA synthesis in the trophozoite stages prior to the development into multinucleated schizont stages (Bozdech *et al.*, 2003).

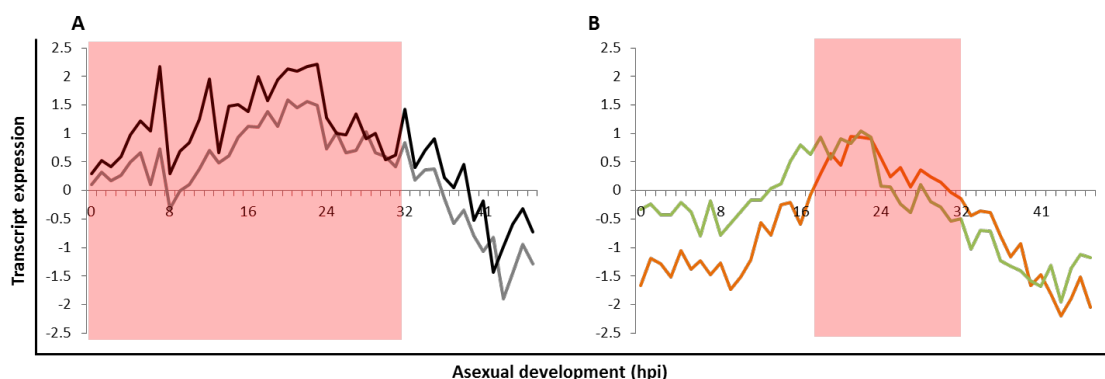


Figure 15: Stage-specific transcript expression profiles of four PfNT genes throughout the asexual stage, clustered using Euclidian distance in similar patterns of transcript expression. The clusters are shown with shaded blocks. (A) 0 – 32 hpi expression cluster (PF3D7_1469400 - PfNT3 – black and PF3D7_0103200 - PfNT4 – grey) and (B) 17 – 32 hpi expression cluster (PF3D7_1347200 – PfNT1 – green and PF3D7_0824400 – PfNT2 – orange). The transcript expression profiles of the MTP genes is given as $\log_2(\text{Cy5}/\text{Cy3})$ expression values (y – axis) at each time point in the 48 h time course of asexual

development (x – axis). Ring stages observed at 0 – 16 hpi, trophozoite stages at 17 – 32 hpi and schizont stages at 33 – 47 hpi.

The multinucleated schizont stages subsequently undergo cytokinesis, thereby enclosing each new daughter parasite with a plasma membrane (Ben Mamoun *et al.*, 2010; Gulati *et al.*, 2015; Palacpac *et al.*, 2004). Membrane biogenesis, which is at the peak during the trophozoite stages (Pessi *et al.*, 2004) is thus driven by the uptake of precursors such as fatty acids, serine, ethanolamine and choline as they are the major building blocks used by the parasite in the synthesis of its structural and regulatory phospholipids (Ben Mamoun *et al.*, 2010). The specific MTPs involved in the uptake of the phospholipid precursors are yet to be identified (Kirk and Saliba, 2007; Ben Mamoun *et al.*, 2010). However, the *P. falciparum* genome encodes certain lipid-related MTPs that may be used for the uptake of these precursors and were therefore, investigated for stage-specific expression (Fig. 16).

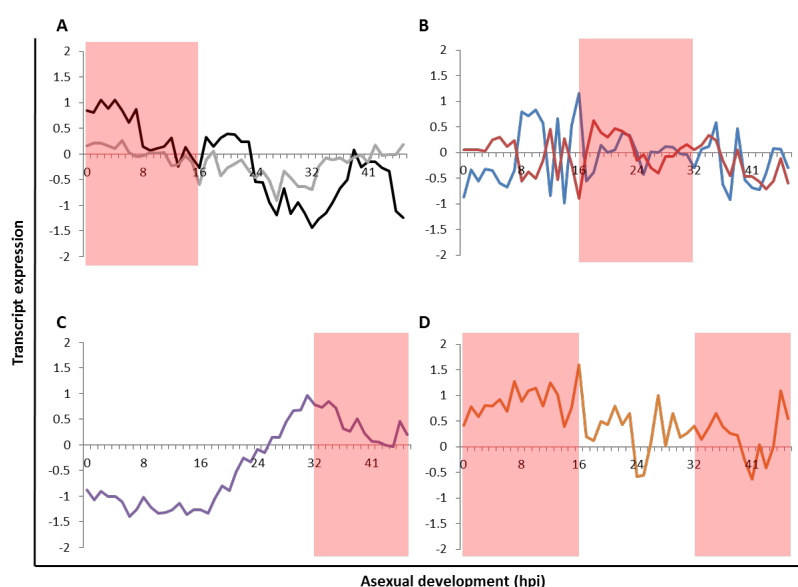


Figure 16: Stage-specific transcript expression profiles throughout the asexual stages of lipid-related MTP genes, clustered using Euclidian distance in similar patterns of transcript expression. The clusters are shown with shaded blocks. (A) 0 – 16 hpi expression cluster (PF3D7_0107500 – lipid/sterol:H⁺ symporter – black and PF3D7_1223400 – phospholipid-transporting ATPase – grey), (B) 16 – 32 hpi expression cluster (PF3D7_1219600 - aminophospholipid-transporting ATPase – red and PF3D7_1468600 - aminophospholipid transporter – blue), (C) 32 – 47 hpi expression cluster (PF3D7_0319000 – phospholipid-translocating ATPase – purple) and (D) 0 -16 hpi and 32 – 47 hpi expression cluster (PF3D7_1426500 - ABC transporter – orange). The transcript expression profiles of the MTP genes is given as log₂(Cy5/Cy3) expression values (y - axis) at each time point in the 48 h time course of asexual development (x – axis). Ring stages observed at 0 – 16 hpi, trophozoite stages observed at 17 – 32 hpi and schizont stages observed at 33 – 47 hpi.

In the ring stages, a lipid/sterol:H⁺ symporter showed peak transcript expression at 3 hpi (PF3D7_0107500, Fig. 16 A – black), and a phospholipid-transporting ATPase showed peak transcript expression at 5 hpi (PF3D7_1223400, Fig. 16 A – grey). Two aminophospholipid transporters showed increased transcript expression during the ring stages, with peak expression in the ring/early trophozoite stages at 16 hpi (PF3D7_1468600, Fig. 16 B – blue) and at 18 hpi (PF3D7_1219600, Fig. 16 B – red) after which the expression decreased during the subsequent

stages. A phospholipid-translocating ATPase showed peak transcript expression at 31 hpi (PF3D7_0319000 late trophozoite stages, Fig. 16 C), after which the transcript decreased steadily through the schizont stages. An ABC transporter that has recently been shown to play a role in the accumulation of neutral lipids (Tran *et al.*, 2014) showed increased transcript expression during the ring stages, with peak expression at 16 hpi, after which the expression decreased during the trophozoite stages and increased again during the schizont stages (Fig. 16 D). This data indicates stage-specific expression of lipid-related MTPs as different lipid-related MTP genes were expressed specifically during the ring, late trophozoite and schizont stages.

3.2.2.2 Investigation of the stage-specific MTP expression profiles during the gametocyte stages

The stage-specific expression of the amino acid transporters that may mediate the import of amino acids for protein synthesis (Florens *et al.*, 2002) and export, following haemoglobin digestion (Rajendran *et al.*, 2017; Krugliak *et al.*, 2002; Liu *et al.*, 2006) during the early gametocyte stages was investigated (Fig. 17).

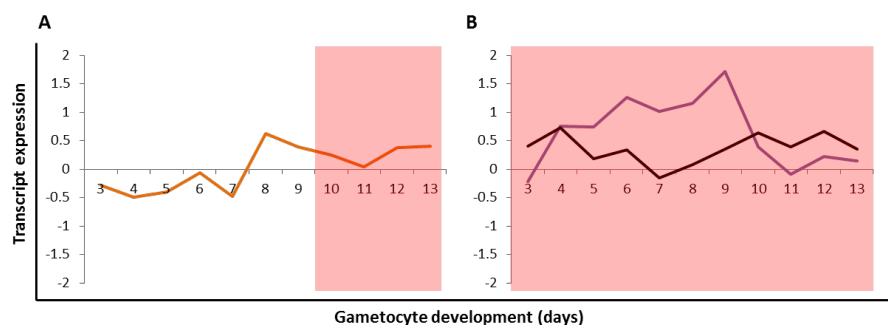


Figure 17: Stage-specific transcript expression profiles of six amino acid transporter genes throughout the gametocyte stages, clustered using Euclidian distance in similar patterns of transcript expression. The clusters are shown with shaded blocks. (A) Stage V gametocytes expression cluster (PF3D7_1231400 – orange) and (B) stage I – V gametocytes expression cluster (PF3D7_0515500 – purple and PF3D7_1132500 – black). The transcript expression profiles of the MTP genes is given as $\log_2(\text{Cy5}/\text{Cy3})$ expression values (y – axis) at each time point in the 13 day time course of gametocyte development (x – axis). Stage I gametocytes are observed at day 3, stage II observed at day 4 – 5, stage III observed at day 6 – 7, stage IV observed at day 8 – 9 and stage V gametocytes observed at day 10 – 13. Constitutive expression observed at day 3 – 13 (average increased expression).

From the expression profiles of the parasite-encoded amino acid transporters, it was observed that one amino acid transporter gene (PF3D7_1231400, Fig. 17 A) showed specific transcript expression for the late gametocyte stages, with a peak in transcript expression on day 8 (stage IV gametocytes). Two amino acid transporter genes associated with a cluster that showed increased transcript expression during all gametocyte stages (Fig. 17 B), with one (PF3D7_1132500, Fig. 17 B – black) showing increased transcript expression on day 3 and 4 (stage I and II gametocytes), after which the expression decreased, but peak transcript expression was observed during day 10 – 13 (stage V gametocytes). The other amino acid transporter gene (PF3D7_0515500, Fig. 17 B - purple) showed transcript expression from day 4 (stage II gametocytes) onwards and only reached

peak expression on day 9 (stage IV gametocytes), after which the expression decreased rapidly. The other three amino acid transporter genes (PF3D7_0629500, PF3D7_0209600 and PF3D7_1208400) had decreased expression throughout gametocytogenesis. This data indicates stage-specific expression of the amino acid transporters because at any point during the gametocyte stages, the three amino acid transporter genes showed increased expression in stage I – II, II – IV and IV – V.

In previous studies, increased levels of glucose consumption was observed in the gametocyte stages, together with increased levels of TCA catabolism of pyruvate, suggesting the requirement of carbohydrate metabolism during the gametocyte stages (Lamour *et al.*, 2014; MacRae *et al.*, 2013). The stage-specific expression of MTP genes involved in glycolysis and the TCA cycle were investigated during the gametocyte stages (Fig. 18).

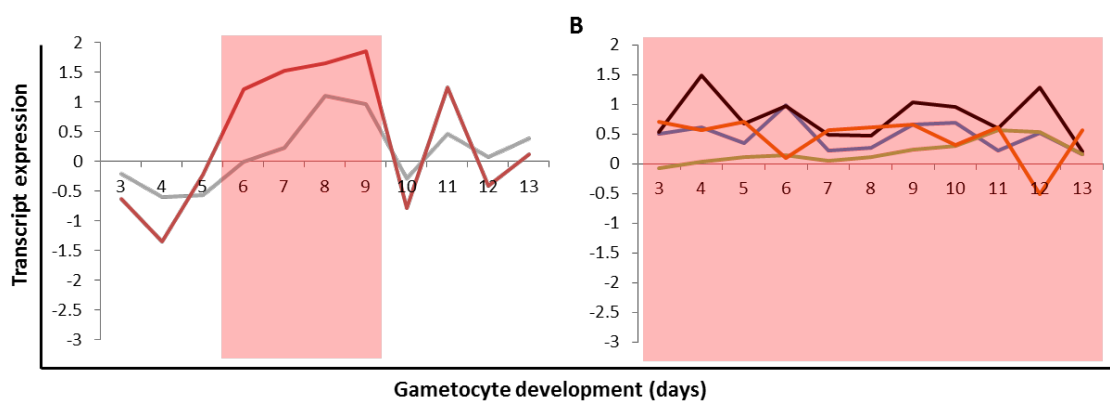


Figure 18: Stage-specific transcript expression profiles throughout the gametocyte stages of MTP genes involved in carbohydrate metabolism, clustered using Euclidian distance in similar patterns of transcript expression. The clusters are shown with shaded blocks. (A) Stage III – IV gametocytes expression cluster (PF3D7_0926400 – monocarboxylate transporter – red and PF3D7_0916000 – sugar transporter – grey) and (B) stage I – V gametocytes expression cluster (PF3D7_1470400 – pyruvate:H⁺ symporter – black, PF3D7_1340800 – pyruvate:H⁺ symporter – blue, PF3D7_0529200 – sugar transporter – green and PF3D7_1368700 – mitochondrial carrier protein – orange). The transcript expression profiles of the MTP genes is given as log₂(Cy5/Cy3) expression values (y – axis) at each time point in the 13 day time course of gametocyte development (x – axis). Stage I gametocytes are observed at day 3, stage II observed at day 4 – 5, stage III observed at day 6 – 7, stage IV observed at day 8 – 9 and stage V gametocytes observed at day 10 – 13. Constitutive expression observed at day 3 – 13 (average increased expression).

Of the four sugar transporters encoded by *P. falciparum* parasites, two had increased transcript expression during the gametocyte stages, specifically during stage III – IV gametocytes (PF3D7_0916000, Fig. 18 A – grey), with peak expression on day 8 (stage IV gametocytes) and also during stage I – V gametocytes (PF3D7_0529200, Fig. 18 B – green), with peak expression on day 11 (stage V gametocytes). By contrast, the PfHT gene (PF3D7_0204700) and the other sugar transporter gene (PF3D7_0919500) showed decreased expression throughout gametocytogenesis. When investigating the MTPs that export the end-metabolites obtained from glycolysis, only one monocarboxylate transporter gene showed increased transcript expression during stage III – IV gametocytes with peak expression on day 9 (PF3D7_0926400, Fig. 18 A –

red, stage IV gametocytes), whereas the other monocarboxylate transporter gene showed decreased expression during the gametocyte stages (PF3D7_0210300).

Interestingly, both pyruvate:H⁺ symporters that transport pyruvate to the mitochondrion for the TCA cycle were expressed throughout all the gametocyte stages with peak transcript expression on day 4 (PF3D7_1470400, Fig. 18 B – black, stage II gametocytes) and on day 6 (PF3D7_1340800, Fig. 18 B – blue, stage III gametocytes). However, the PfPPT (PF3D7_0530200) that can also transport pyruvate to the mitochondrion showed decreased transcript expression during the gametocyte stages. Unexpectedly, PfDTC and PfACT genes also showed decreased transcript expression throughout gametocytogenesis, whereas the mitochondrial carrier protein (PF3D7_1368700, Fig. 18 B – orange) was present throughout all the gametocyte stages with peak transcript expression on day 9 (stage IV gametocytes). These transcript expression profiles of MTPs involved in carbohydrate metabolism, indicated stage-specific expression of two sugar transporter genes and a monocarboxylate transporter gene in the late gametocyte stages, whereas the two pyruvate:H⁺ symporters and the mitochondrial carrier protein did not show stage-specific expression as these were expressed throughout the gametocyte stages.

In stage I gametocytes, DNA is synthesised to twice the haploid amount, which then stays constant through to stage V gametocytes (Janse *et al.*, 1988). This implies that hypoxanthine must be taken up in gametocyte stages (Raabe *et al.*, 2009) as the *P. falciparum* parasite is unable to synthesize purines *de novo*. The uptake of hypoxanthine may be mediated by four PfNTs, which were investigated for stage-specific expression (Fig. 19).

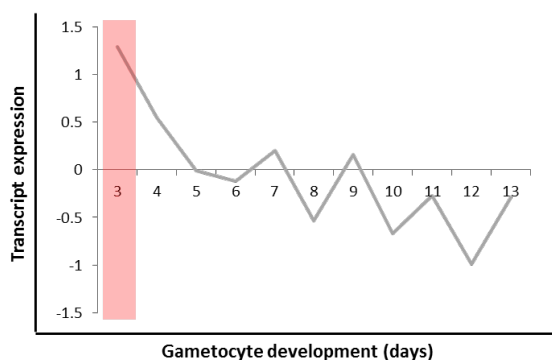


Figure 19: Stage-specific transcript expression profile of a nucleoside transporter gene throughout the gametocyte stages, clustered using Euclidian distance in similar patterns of transcript expression. The clusters are shown with shaded blocks. Stage I gametocytes expression cluster (PF3D7_1469400 – PfNT 3 – grey). The transcript expression profile of the MTP gene is given as $\log_2(\text{Cy5}/\text{Cy3})$ expression values (y – axis) at each time point in the 13 day time course of gametocyte development (x – axis). Stage I gametocytes observed at day 3, stage II observed at day 4 – 5, stage III observed at day 6 – 7, stage IV observed at day 8 – 9 and stage V gametocytes observed at day 10 – 13.

From the expression profiles, a single nucleoside transporter gene, PfNT3 (PF3D7_1469400, Fig. 19) was expressed on day 3 (stage I gametocytes) only, whereas the other three PfNTs (PF3D7_1347200 - PfNT1, PF3D7_0824400 – PfNT2 and PF3D7_0103200 - PfNT4) all had

decreased expression during the gametocyte stages, which indicate the stage-specific expression of PfNT3, correlating to the requirement of DNA synthesis in stage I gametocytes.

During gametocyte stages, phospholipids are sequestered as they are less readily available in the mosquito vector (Tran *et al.*, 2014; van Schaijk *et al.*, 2014). Therefore, the gametocyte stages can either synthesise or take up the precursors of phospholipids required for membrane biogenesis. Here, lipid-related MTPs may be used for the uptake and were investigated for stage-specific expression (Fig. 20).

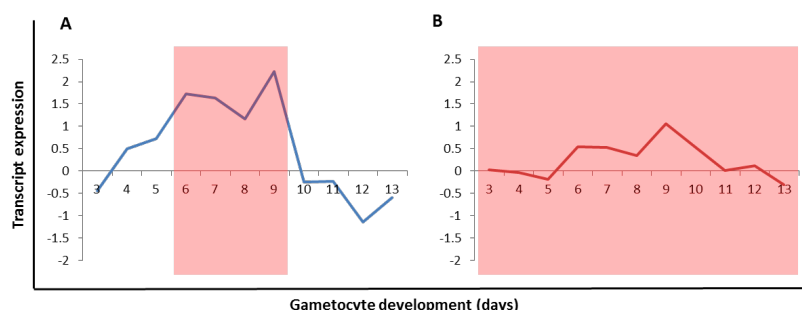


Figure 20: Stage-specific transcript expression profiles throughout the gametocyte stages of lipid-related MTP genes, clustered using Euclidian distance in similar patterns of transcript expression. The clusters are shown with shaded blocks. (A) Stage III – IV gametocytes expression cluster (PF3D7_1426500 - ABC transporter – blue) and (B) stage I – V gametocytes expression cluster (PF3D7_1468600 - aminophospholipid transporter – red). The transcript expression profiles of the MTP genes is given as log₂(Cy5/Cy3) expression values (y – axis) at each time point in the 13 day time course of gametocyte development (x – axis). Stage I gametocytes observed at day 3, stage II observed at day 4 – 5, stage III observed at day 6 – 7, stage IV observed at day 8 – 9 and stage V gametocytes observed at day 10 – 13. Constitutive expression observed at day 3 – 13 (average increased expression).

Interestingly, only two lipid-related MTP genes showed increased transcript expression during the gametocyte stages. An ABC transporter gene (PF3D7_1426500, Fig. 20 A – blue) showed transcript expression during stage III – IV gametocyte stages, with peak expression on day 9 (stage IV gametocytes), after which the expression decreased rapidly. A similar expression profile was observed for the aminophospholipid transporter gene (PF3D7_1468600, Fig. 20 B – red) that showed increased transcript expression during stage III – IV gametocytes, with peak expression also on day 9 (stage IV gametocytes). The other four lipid-related MTP genes showed decreased transcript expression levels during gametocyte development (PF3D7_0319000, PF3D7_1223400, PF3D7_1219600 and PF3D7_0107500). This data indicates the stage-specific expression of two lipid-related MTP genes specifically to stage III – IV gametocytes.

3.2.2.3 Stage-specific expression of MTPs involved in ion regulation during asexual and gametocyte stages

While investigating MTP stage-specific expression during the asexual and gametocyte stages, it was observed that the permeome consists of 12% MTPs predicted to be involved in transporting ions. These MTPs may be involved in ion regulation during these stages, although it is not known,

if these have stage-specific expression. Therefore, the stage-specific expression of the MTPs that transport either K^+ , Na^+ , Ca^{2+} , Mg^{2+} or Zn^{2+}/Fe^{2+} were specifically investigated in the asexual (Fig. 21) and gametocyte stages (Fig. 22).

As the *P. falciparum* parasite invades the erythrocyte, it induces an increase in the permeability of the EPM to monovalent ions and this has consequences for the ionic composition of the host erythrocyte cytosol (Kirk, 2015). The ion regulation during the asexual stages is therefore, under tight control to maintain ion gradients as well as for using the membrane ion gradients to energise the movement of solutes in or out of the cell (Kirk, 2001). The stage-specific expression of ion transporting MTPs was investigated during the asexual stages (Fig. 21).

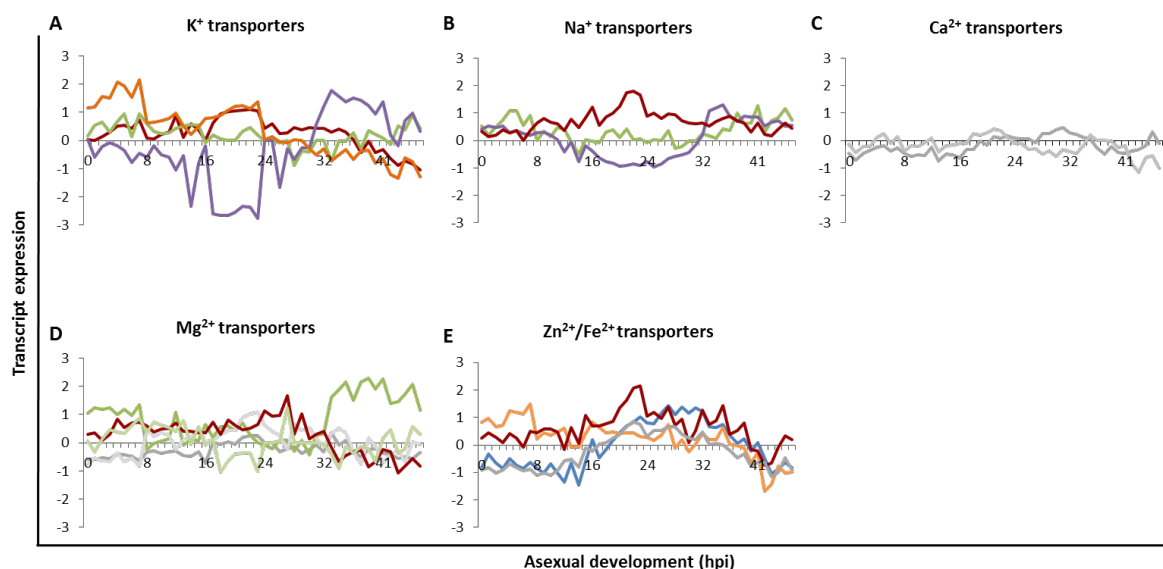


Figure 21: Stage-specific transcript expression profiles throughout the asexual stages of ion transporting MTP genes grouped according to ions. For all graphs, line colour indicates expression clusters MTPs were assigned to: 0 – 16 hpi expression cluster (orange), 0 – 32 hpi expression cluster (dark red), 17 – 32 hpi expression cluster (grey), 16 – 40 hpi expression cluster (blue), 25 – 43 hpi expression cluster (red), 33 – 47 hpi expression cluster (purple), 0 – 16 hpi/32 – 47 hpi expression cluster (green) and 0 – 47 hpi expression cluster (black). (A) K^+ transporters (PF3D7_1235200 – purple, PF3D7_1456800 – orange, PF3D7_1465500 – green and PF3D7_1227200 – dark red), (B) Na^+ transporters (PF3D7_0212800 – dark red, PF3D7_1303500 – purple and PF3D7_1340900 – green), (C) Ca^{2+} transporters (PF3D7_0106300 – grey and PF3D7_1211900 – PfATP4 – grey), (D) Mg^{2+} transporters (PF3D7_1304200 – green, PF3D7_0306700 – dark red, PF3D7_0827700 – light green, PF3D7_1120300 – grey and PF3D7_1427600 – dark grey) and (E) Zn^{2+}/Fe^{2+} transporters (PF3D7_1022300 – dark red, PF3D7_0609100 – orange, PF3D7_0715900 – blue and PF3D7_1223700 – grey). The transcript expression profiles of the MTP genes is given as $\log_2(Cy5/Cy3)$ expression values (y – axis) at each time point in the 48 h time course of asexual development (x – axis). Ring stages observed at 0 – 16 hpi, trophozoite stages observed at 17 – 32 hpi and schizont stages observed at 33 – 47 hpi.

From the transcript expression profiles for K^+ transporters, PfVP1 (PF3D7_1456800, Fig. 21 A – orange) and PfK2 (PF3D7_1465500, Fig. 21 A – green) genes showed peak transcript expression at 7 hpi (ring stages). However, these two MTPs did not associate to the same expression clusters as the PfVP1 transcript expression continued to the trophozoite stages, whereas the PfK2 transcript expression decreased during the trophozoite stages and increased again in the schizont

stages. PfK1 gene (PF3D7_1227200, Fig. 21 A – dark red) was expressed during the ring and trophozoite stages, with peak transcript expression at 22 hpi (trophozoite stages), whereas the PfVP2 gene (PF3D7_1235200, Fig. 21 A – purple) was expressed in the schizont stages, with peak transcript expression at 33 hpi (schizont stages). The transcript expression of the K⁺ transporters showed stage-specific expression as different K⁺ transporter genes were expressed at either ring and trophozoite stages or schizont stages. Therefore, at any given point during the asexual stages, there is a K⁺ transporter gene expressed.

For the Na⁺ transporters, the PfPiT gene (PF3D7_1340900, Fig. 21 B – green) was expressed in the early asexual stages, with decreased expression during the trophozoite stages, followed by peak transcript expression at 41 hpi (schizont stages). The PfNHE gene (PF3D7_1303500, Fig. 21 B – purple) was expressed during the schizont stages, with peak expression in the later stages at 35 hpi (schizont stages), whereas the other Na⁺ or H⁺ antiporter gene (PF3D7_0212800, Fig. 21 B – grey) showed increased transcript expression during the ring and trophozoite stages, and reached peak transcript expression at 22 hpi (trophozoite stages). The expression of these MTP genes also shows stage-specific expression through each asexual stage.

When investigating the Ca²⁺ transporters, it was observed that both calcium-transporting ATPase (PF3D7_0106300, Fig. 21 C – grey) and PfATP4 (PF3D7_1211900, Fig. 21 C – black) genes associated with a cluster that showed increased transcript expression between 17 – 32 hpi (trophozoite stages). However, these transcripts were not expressed as overall decreased transcript expression profiles of these MTPs were observed throughout the asexual stages.

The Mg²⁺ transporter expression profiles included two magnesium transporter genes and three PfMIT genes. The magnesium transporter gene (PF3D7_0306700, Fig. 21 D – dark red) was expressed throughout the ring and trophozoite stages, with peak expression at 27 hpi, after which the transcript decreased steadily. Similar transcript profiles were observed for the magnesium transporter gene (PF3D7_0827700, Fig. 21 D – light green) and for the PfMIT2 gene (PF3D7_1304200, Fig. 21 D – green) that showed increased transcript expression between 0 – 16 hpi (ring stages) with peak expression at 27 hpi (late trophozoite stages) and 39 hpi (schizont stages), respectively. The PfMIT3 (PF3D7_1427600, Fig. 21 D – dark grey) transcript reached a maximum peak expression at 23 hpi (trophozoite stages), whereas the peak transcript expression of PfMIT1 (PF3D7_1120300, Fig. 21 D – grey) occurred in the later stages at 33 hpi (schizont stages). These profiles indicate stage-specific expression as during the asexual stages, Mg²⁺ transporter genes were expressed in each stage.

For the Zn²⁺/Fe²⁺ transporters, the Zn²⁺/Fe²⁺ permease transcript (PF3D7_0609100, Fig. 21 E – orange) peak expression occurred at 7 hpi (ring stages), after which the transcript expression decreased over time. For both the zinc transporter (PF3D7_1022300, Fig. 21 E – dark red) and

iron transporter (PF3D7_1223700, Fig. 21 E – grey), maximum transcript expression was observed at 23 and 22 hpi (trophozoite stages), respectively. By contrast, another zinc transporter gene (PF3D7_0715900, Fig. 21 E – blue) showed peak transcript expression in the later stages at 27 hpi (late trophozoite stages). These expression profiles indicate stage-specific expression of the Zn^{2+}/Fe^{2+} transporter genes specifically to the ring and trophozoite stages.

While no information regarding ion regulation during the gametocyte stages is currently available, it is possible that ion homeostasis is controlled in a similar manner to asexual stage parasites. Therefore, the stage-specific expression of ion transporting MTPs during the gametocyte stages was investigated (Fig. 22).

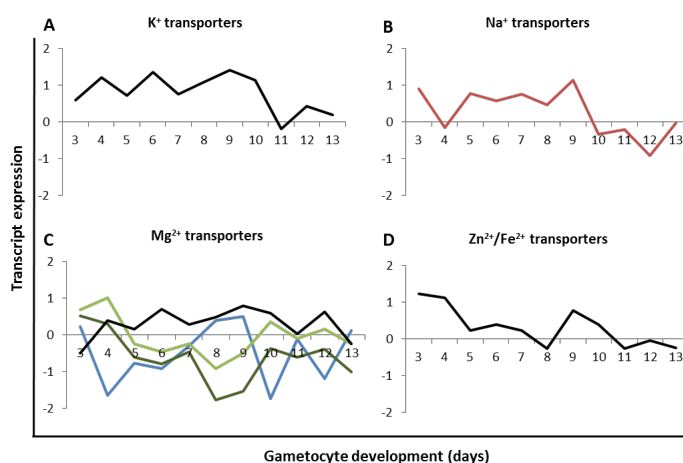


Figure 22: Stage-specific transcript expression profiles throughout the gametocyte stages of MTPs transporting ions grouped according to ions. For all graphs, line colour indicates expression clusters MTPs were assigned to: stage III – IV gametocytes expression cluster (red), stage I – V gametocytes expression cluster (black) and average decreased expression clusters (light green, dark green and blue). (A) K^+ transporter (PF3D7_1465500 – black), (B) Na^+ transporter (PF3D7_0212800 – red), (C) Mg^{2+} transporter (PF3D7_0827700 – black) and (D) Zn^{2+}/Fe^{2+} transporter (PF3D7_1022300 – black). The transcript expression profiles of the MTP genes is given as $\log_2(Cy5/Cy3)$ expression values (y – axis) at each time point in the 13 day time course of gametocyte development (x – axis). Stage I gametocytes observed at day 3, stage II observed at day 4 – 5, stage III observed at day 6 – 7, stage IV observed at day 8 – 9 and stage V gametocytes observed at day 10 – 13.

From the transcript expression profiles for K^+ transporters, the PfK2 (PF3D7_1465500, Fig. 22 A) transcript was the only transcript that showed expression throughout the gametocyte stages, with peak expression on day 9 (stage IV gametocytes), after which the expression decreased between day 10 – 13 (stage V gametocytes). The PfVP2 gene (PF3D7_1235200), PfVP1 gene (PF3D7_1456800) and PfK1 gene (PF3D7_1227200) showed decreased expression during gametocyte development. This data indicates stage-specific expression of the PfK2 gene in stage I – IV gametocytes, suggesting that the gametocyte stages may depend on only one K^+ transporter with no redundancy.

For the Na^+ transporters, the Na^+ or H^+ antiporter (PF3D7_0212800, Fig. 22 B) transcript showed expression from stage I to stage IV gametocytes, with a peak transcript expression on day 9 (stage

IV gametocytes). The PfPiT gene (PF3D7_1340900) and PfNHE gene (PF3D7_1303500) showed decreased transcript expression during gametocyte development. The expression profiles of the Na⁺ transporter genes also showed stage-specific expression of only the one Na⁺ transporter in stage I – IV gametocytes and may also suggest that the gametocyte stages depend on only one Na⁺-related MTP.

When investigating the Ca²⁺ transporters, it was observed that both calcium-transporting ATPase (PF3D7_0106300) and PfATP4 (PF3D7_1211900) genes showed decreased transcript expression throughout the gametocyte stages; therefore, no stage-specific expression was observed and may suggest that the gametocyte stages do not depend on Ca²⁺-related MTPs.

The Mg²⁺ transporter's expression profiles showed that one magnesium transporter (PF3D7_0827700, Fig. 22 C) transcript was observed from stage II to stage V gametocytes, with a peak transcript expression on day 9 (stage IV gametocytes). Three other magnesium transporter genes (PfMIT3 - PF3D7_1427600, PfMIT2 - PF3D7_1304200 and a magnesium transporter - PF3D7_0306700) associated with clusters that showed average decreased expression during gametocytogenesis. However, PfMIT3 showed transcript expression on day 3 (stage I gametocytes), with peak expression on day 4 (stage II gametocytes), after which the expression decreased through day 6 – 9 (stage III and IV gametocytes) and then increased again during day 10 – 13 (stage V gametocytes, Fig. 22 C – light green). The other magnesium transporter gene showed peak transcript expression on day 3 (PF3D7_0306700, Fig. 22 C – dark green, stage I gametocytes). PfMIT2 gene showed transcript expression on day 3 (stage I gametocytes), after which the expression decreased between day 4 – 5 (stage II gametocytes) and then reached a peak expression on day 9 (Fig. 22 C – blue, stage IV gametocytes). Only the PfMIT1 gene (PF3D7_1120300) showed decreased transcript expression during gametocytogenesis. This data indicates stage-specific expression of Mg²⁺-related MTPs, as four different Mg²⁺ MTP genes were expressed during different gametocyte stages.

For the Zn²⁺/Fe²⁺ transporters, the zinc transporter gene (PF3D7_1022300, Fig. 22 D) showed peak transcript expression on day 3 (stage I gametocytes) and steadily decreased between day 4 – 7 (stage III gametocytes), after which the transcript expression increased rapidly at day 9 (stage IV gametocytes) and then decreased steadily again. The other Zn²⁺/Fe²⁺ transporter genes, including a zinc transporter (PF3D7_0715900), iron transporter (PF3D7_1223700) and the Zn²⁺/Fe²⁺ permease (PF3D7_0609100), however, showed decreased transcript expression throughout gametocyte development. This data indicates stage-specific expression of only one zinc transporter gene, specifically in stage I and IV gametocyte stages that may also suggest that the gametocyte stages depend on only one zinc transporter.

In conclusion, stage-specific expression of most of the MTP genes investigated was observed during ring, trophozoite and schizont stages as well as during stage I – V gametocytes, suggesting the presence of these MTPs during specific stages. However, only a few MTP genes such as the PfHT, the two pyruvate: H⁺ symporters and the mitochondrial carrier protein did not show stage-specific expression as these MTP genes were expressed through either all the asexual or gametocyte stages (constitutively expressed), which confirms their importance and involvement in these stages.

Subsequently, isotope uptake assays were performed to measure the uptake of glucose and amino acids into the trophozoite stages to validate the transcript data of the permeome, where sugar and amino acid transporter genes showed increased transcript expression in different asexual stages. The biochemical characterisation of the uptake of metabolites by whole cell gametocyte stages was not done as major challenges exist in the *in vitro* production of gametocytes. Optimised gametocyte production protocols result in ~2 - 3% gametocytaemia (percentage of gametocytes per erythrocyte) (Reader *et al.*, 2015), meaning that to obtain equivalent amounts of parasites, ~5 times more biological starting material is required for gametocyte stages than asexual stages. Therefore, high throughput gametocyte cultivation protocols are of utmost importance for further studies in validating the transcriptome data of the MTP genes in gametocyte stages with isotope uptake assays.

3.3 Functional studies of metabolite uptake in *P. falciparum* parasites

3.3.1 *In vitro* *P. falciparum* asexual parasite cultivation

Intraerythrocytic *P. falciparum* NF54 parasites were cultured for subsequent radioisotope uptake experiments. The parasitaemia was monitored daily by microscopic assessment of thin smear preparation of the asexual cultures (Fig. 23).



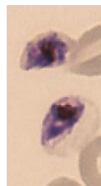
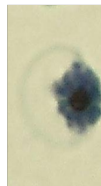
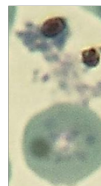
Stage	Ring	Early Trophozoite	Mature Trophozoite	Schizont	Merozoite
Morphology					
~ hpi	10 - 16	17 - 24	25 - 32	33 - 44	48

Figure 23: The microscopic evaluation of the cultivation of different stages of *P. falciparum* asexual parasites. The ring, early and mature trophozoites, schizont and merozoite stages are shown with their respective ages presented in hpi. The morphology images were generated from thin blood smears, fixed with methanol and stained with Giemsa for 5 min. The parasites were viewed and photographed at 1000x magnification.

The development of the *P. falciparum* asexual stages was observed over a time period of 48 h. The ring stages appeared as a thin discoidal ring with a punctate density of nuclear material up until ~16 hpi. The early trophozoite stages appeared approximately ~17 hpi and were characterised by the development of the haemozoin crystal. As the early trophozoite stages progressed to late stage trophozoites, there was an increase in the size of the parasite as well as a decrease in visibility of the host erythrocyte and large haemozoin crystals were observed. The schizont stages were observed at ~38 hpi and were characterised to have multiple nuclei. The merozoites occurred at ~48 hpi, following lysis of the host erythrocyte and the invasion of daughter merozoites into new erythrocytes.

3.3.2 *P. falciparum* intraerythrocytic trophozoite stage enrichment

For the uptake experiments in mature trophozoite iRBCs, the trophozoite iRBCs were firstly purified to $\geq 90\%$ parasitaemia, using magnetic enrichment (Fig. 24) (Fitch and Kanjanangulpan, 1987; Teng *et al.*, 2009; Trang *et al.*, 2004).

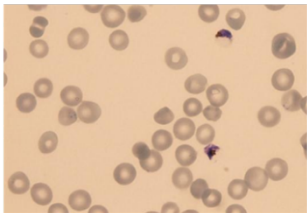
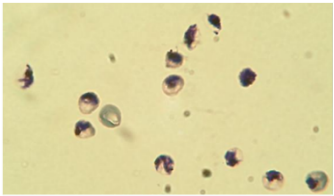
	Before enrichment	After enrichment
Morphology		
~ hpi	34 - 37	34 - 37
Parasitaemia	3%	92%

Figure 24: Microscopic evaluation of the enriched mature trophozoite stages prior and following magnetic enrichment. *P. falciparum* intraerythrocytic parasites (3% parasitaemia, 5% haematocrit) were enriched with CS columns to obtain $\geq 90\%$ parasitaemia. The morphology images were generated from thin blood smears, fixed with methanol and stained with Giemsa for 5 min. The parasites were viewed and photographed at 1000x magnification.

Subsequent to magnetic enrichment, the parasitaemia increased from 3% to $>90\%$, resulting in a parasite population suitable for use in radioisotope uptake assays, without significant signal expected from the presence of uninfected RBCs.

3.3.3 Uptake of 2DG into *P. falciparum* uninfected RBCs and trophozoite iRBCs

For the radioisotope uptake experiments into the trophozoite stage *P. falciparum* parasites, 2DG was used as a proxy for glucose uptake as 2DG is taken up by the glucose transporter and metabolised to 2DG6P. The 2DG6P, however, cannot be further metabolised by phosphoglucose isomerase and thus accumulates in the parasite. The accumulated 2DG6P is therefore, directly proportional to 2DG (or glucose) uptake by asexual stages. For *P. falciparum* asexual parasites,

the IC₅₀ of 2DG was previously determined in the range of 0.7 to 6.2 mM, depending on the concentration of glucose in the media used (van Schalkwyk *et al.*, 2008). Therefore, the uptake of [¹⁴C]-2DG (55 mCi/mmol, PerkinElmer) was done at either 0.1 μCi/ml (1.8 μM) or at 1 μCi/ml (18 μM) (Fig. 25), below the measured IC₅₀, and thus no deleterious effects on parasite viability are expected. A distribution ratio (concentration of radiolabelled metabolite inside the cell/concentration outside of the cell) of 1 indicates that the molecule under investigation equilibrates across the membrane, while a distribution ratio of >1 is indicative of accumulation within the cell. By contrast, a distribution ratio of <1 occurs when the concentration of the metabolite in the extracellular fluid is higher than inside the cell (Kirk *et al.*, 1996).

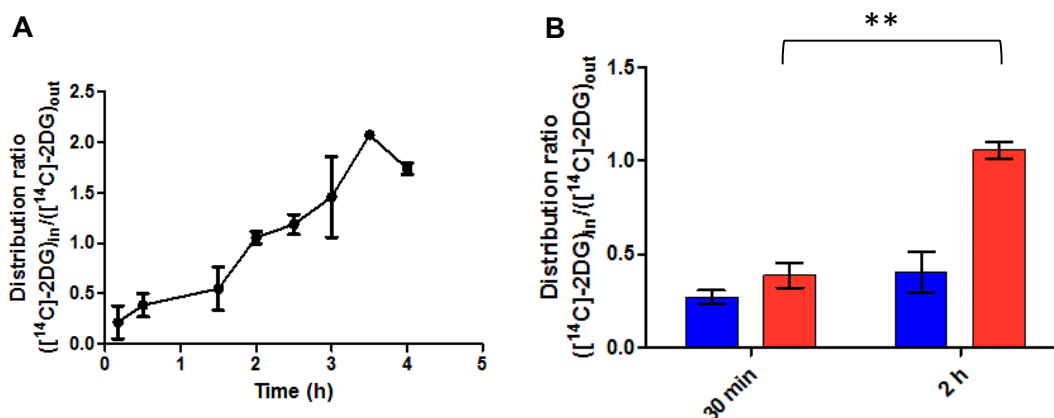


Figure 25: The uptake of [¹⁴C]-2DG into uninfected RBCs and trophozoite iRBCs. (A) The uptake of [¹⁴C]-2DG (0.1 μCi/ml) into trophozoite iRBCs was investigated over a time period of 4 h. The time study was done with 6 x 10⁷ cells/ml in Solution B. The data for the time study were from one independent experiment (n = 1) and error bars indicate SD. (B) The uptake of [¹⁴C]-2DG (1 μCi/ml) into uninfected RBCs (blue) and trophozoite iRBCs (red) were measured, following 30 min and 2 h incubation. The data for the uptake of [¹⁴C]-2DG into uninfected RBCs were averaged from three independent experiments (n = 3), and error bars indicate SEM. The data for the uptake of [¹⁴C]-2DG into trophozoite iRBCs were only from one independent experiment (n = 1 in triplicate), and error bars indicate SD. *P* < 0.01 (**).

The time study of [¹⁴C]-2DG uptake into trophozoite iRBCs (Fig. 25 A) with 6 x 10⁷ cells/ml indicated that there was continuous uptake of [¹⁴C]-2DG into the trophozoite stages. An accumulation of [¹⁴C]-2DG into trophozoite iRBCs was observed from 2 h onwards (distribution ratio > 1), where a peak distribution ratio was observed at 3 h 30 min (2.06 ± 0.02 fmol [¹⁴C]-2DG/10⁷ cells/min). In a previous study, it was observed that with 10⁸ cells/ml, a peak distribution ratio of 4 was observed at 2 h (Kirk *et al.*, 1996), indicating that fewer cells tend to have a longer period preceding accumulation of glucose.

When comparing the uptake of [¹⁴C]-2DG in uninfected RBCs and trophozoite iRBCs (Fig. 25 B), the total uptake of [¹⁴C]-2DG at the end of the 2 h incubation was higher than that seen in the uninfected RBCs (uninfected RBC - 0.41 ± 0.11 fmol [¹⁴C]-2DG/10⁸ cells/min vs iRBC 1.06 ± 0.04 fmol [¹⁴C]-2DG/10⁸ cells/min). However, additional repeats for iRBCs are required in order to determine, if the difference between the uninfected RBCs and iRBCs is statistically significant. The

increased uptake of [¹⁴C]-2DG into iRBCs in comparison to uninfected RBCs is, however, similar to what was previously seen (Kirk *et al.*, 1996). This [¹⁴C]-2DG uptake into the trophozoite stages may be due to any of the four sugar transporter genes, including PfHT, which showed increased transcript expression during the different asexual stages.

3.3.4 Uptake of amino acids into *P. falciparum* uninfected RBCs and trophozoite iRBCs

The uptake of [¹⁴C]-leucine (1 μCi/ml), [¹⁴C]-lysine (1 μCi/ml), [¹⁴C]-glutamic acid (1 μCi/ml) and [¹⁴C]-aspartic acid (1 μCi/ml) into uninfected RBCs and mature trophozoite iRBCs after 30 min at 37°C was compared (Fig. 26).

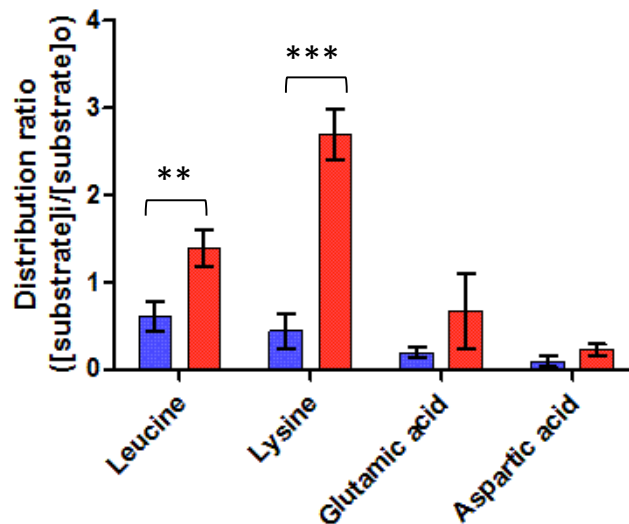


Figure 26: The uptake of 1 μCi/ml [¹⁴C]-leucine, [¹⁴C]-lysine, [¹⁴C]-glutamic acid and [¹⁴C]-aspartic acid into uninfected RBCs (blue) and trophozoite iRBCs (red). The data for the uptake of [¹⁴C]-leucine, [¹⁴C]-glutamic acid and [¹⁴C]-aspartic acid into both uninfected RBCs and trophozoite iRBCs were averaged from two independent experiments (n = 2) and error bars indicate SEM. The data for the uptake of [¹⁴C]-lysine into both uninfected RBCs and trophozoite iRBCs were from only one independent experiments (n = 1 in triplicate), and error bars indicate SD. *P* < 0.01 (**) and *P* < 0.001 (***) (calculated using the t-test).

Consistent with published results, [¹⁴C]-leucine, [¹⁴C]-glutamic acid and [¹⁴C]-aspartic acid were taken up into uninfected RBCs (Fig. 26) (Winter and Christensen, 1964; Winterberg *et al.*, 2012). [¹⁴C]-lysine was also taken up into uninfected RBCs. In the trophozoite iRBCs, the total accumulation of [¹⁴C]-leucine and [¹⁴C]-lysine at the end of the 30 min incubation was significantly higher than that seen in the uninfected RBCs (uninfected RBC – 0.6 ± 0.1 fmol [¹⁴C]-leucine/10⁸ cells/min vs iRBC – 1.39 ± 0.18 fmol [¹⁴C]-leucine/10⁸ cells/min n = 3, *P* < 0.01; uninfected RBC – 0.44 ± 0.19 fmol [¹⁴C]-lysine/10⁸ cells/min vs iRBC – 2.7 ± 0.29 fmol [¹⁴C]-lysine/10⁸ cells/min n = 1, *P* < 0.001). Furthermore, both [¹⁴C]-leucine and [¹⁴C]-lysine accumulated in trophozoite iRBCs, with distribution ratios higher than 1 measured after 30 min. However, additional repeats for [¹⁴C]-lysine uptake into both uninfected RBCs and trophozoite iRBCs are required in order to determine, if this difference is statistically significant between independent experiments.

Neither [^{14}C]-glutamic acid nor [^{14}C]-aspartic acid iRBC distribution ratios after the 30 min incubation were significantly higher than seen in the uninfected RBCs (uninfected RBC – 0.20 ± 0.06 fmol [^{14}C]-glutamic acid/ 10^8 cells/min vs iRBC – 0.7 ± 0.4 fmol [^{14}C]-glutamic acid/ 10^8 cells/min; $n = 2$, $P > 0.05$, uninfected RBC – 0.10 ± 0.06 fmol [^{14}C]-aspartic acid/ 10^8 cells/min vs iRBC – 0.23 ± 0.06 fmol [^{14}C]-aspartic acid/ 10^8 cells/min, $n = 2$, $P > 0.05$). Additional repeats are required for [^{14}C]-glutamic acid uptake to determine, if there may be a statistically significant difference between the uninfected RBCs and trophozoite iRBCs. However, for [^{14}C]-aspartic acid uptake, it was observed that the distribution ratios were similar between uninfected RBCs and trophozoite iRBCs, suggesting that the parasite inside the RBC may not take up aspartic acid more than the uninfected RBC does.

In conclusion, [^{14}C]-leucine and [^{14}C]-lysine were taken up into the trophozoite stages, whereas it cannot be concluded, whether the parasite inside the RBC takes up [^{14}C]-glutamic acid and [^{14}C]-aspartic acid more than the uninfected RBC does, indicating that additional repeats are required for all four amino acids to confirm these results. Further studies are required to determine, which of the six amino acid transporter transcripts that were expressed during the asexual stages (Fig. 10), are responsible for the observed amino acid uptake.

Chapter 4: Discussion

The global implementation of malaria elimination and eradication programmes over the years has resulted in the substantial decrease in the number of malaria-related incidence and mortality rates since 1955 (Nájera *et al.*, 2011; Alonso *et al.*, 2011; World Health Organisation, 2017). A key cornerstone of malaria elimination programmes is the implementation of antimalarial chemotherapies (Bhatt *et al.*, 2015). Moreover, antimalarial chemotherapies targeting *P. falciparum* parasites must target the intraerythrocytic asexual (TCP-1) and gametocyte stages (TCP-5) to alleviate the symptoms of malaria as well as to prevent the transmission from the human host to the mosquito vector (Burrows *et al.*, 2017). However, the increase in resistance against the majority of antimalarial compounds underpins the need for the development of novel antimalarial compounds targeting novel biological activities of the parasites. *P. falciparum*-encoded MTPs are promising novel drug targets as these proteins ensure the survival of the parasite in the host cell by mediating the uptake of essential metabolites and removal of waste products produced from metabolic pathways (Kenthirapalan *et al.*, 2016). It is therefore, imperative that the presence and absence of MTPs in asexual and gametocyte stages be investigated to ultimately generate medicines that comply with TCP-1 and TCP-5. The *P. falciparum*-encoded permeome is well characterised in the asexual stages (Kirk and Lehane, 2014; Martin *et al.*, 2005; Martin *et al.*, 2009). However, limited knowledge is available about the *P. falciparum*-encoded permeome in the gametocyte stages. The different strategy- and stage-specific metabolic requirements of the asexual stages and gametocytes suggest that the parasite-encoded MTPs may be differentially expressed between these stages. An understanding of the strategy- and stage-specific expression of parasite-encoded MTPs between and within the asexual and gametocyte stages enables the identification of the presence of these MTP transcripts during the asexual and gametocyte stages. Furthermore, the identification of the presence of the parasite-encoded MTPs in the asexual and gametocyte stages will aid in identifying new potential drug targets for the development of novel antimalarial compounds that will ultimately contribute to the elimination and eradication of malaria.

This study was aimed at evaluating the strategy- and stage-specific expression of the *in silico* predicted permeome in the asexual and gametocyte stages. In doing so, this is the first study that investigated the stage-specific expression of the entire complement of MTPs in the asexual and gametocyte stages and therefore, identifying the transcript presence of the MTPs in these stages.

Before investigating the strategy- and stage-specific expression of the parasite-encoded MTPs, a current updated permeome was required. This study was successful in identifying the current *in silico* predicted permeome, which consisted of 136 previously identified MTP genes (Martin *et al.*, 2005; Martin *et al.*, 2009) and 11 newly identified MTP genes and included pyruvate:H⁺ symporters, Arsenical pump-driving ATPase, ATP synthase subunit *c*, magnesium transporters, ABC transporters, a zinc transporter and a nucleoporin. The identification of only 11 new MTPs

correlated with a recent study that only identified four new MTPs to the *P. falciparum* permeome (Weiner and Kooij, 2016), of which three correlated with this study. The protein (PF3D7_1033000) that was not identified during this study has an unknown function and also had no TMDs. As this study included MTPs with 0 TMDs, one possible explanation for not identifying this protein as an MTP may be because the protein did not have any annotation to transport and therefore, was not confirmed, based on its predicted function. This signifies the importance of the use of different methods to constantly investigate MTPs as some MTPs may not have been annotated or identified previously and therefore has been overlooked. Other technologies can be investigated such as RNA-sequencing in the search for MTPs that have not been previously identified as well as to improve the existing annotation of the *Plasmodium* genome. RNA-sequencing can (1) detect novel gene transcripts, (2) propose alternative splicing sites that may also identify novel gene transcripts and also (3) improve the recent annotation of genes (Otto *et al.*, 2010). As the existing annotation of the *Plasmodium* genome improves, it is also likely that more MTPs will be annotated as more information will be available about such proteins.

The identification of 147 parasite-encoded MTP genes (136 previously identified with 11 newly identified) allowed for a comprehensive analysis of the entire permeome strategy- and stage-specific expression in the asexual and gametocyte stages. A previous study also investigated the mRNA expression of 34 MTP genes during the asexual stages with only five time points, but with no analyses of the expression during the gametocyte stages (Martin *et al.*, 2005). In this study, the mRNA expression of the entire complement of parasite-encoded MTP genes was investigated throughout the asexual (hourly sampling across the 48 h asexual cycle) and the gametocyte (daily sampling for 13 days) stages, which had never been done before.

Analysis of the permeome revealed a strategy-specific expression between the asexual and gametocyte stages. In the asexual stages, the whole complement of parasite-encoded MTP genes showed increased transcript expression with a phase-like distribution, depicting continuous expression of MTPs during the asexual stages. This correlates with the highly proliferative asexual stages that are dependent on the constant exchange of metabolites required for rapid intracellular cell growth, multiplication and re-invasion that is repeated every 48 h (Bannister and Mitchell, 2003; Olszewski *et al.*, 2009; Olszewski and Llinás, 2011). In contrast, in the gametocyte stages less than half of the MTP genes showed increased transcript expression, which also showed a phase-like distribution during the different gametocyte stages. Such expression indicates a reduced range of MTPs active in the gametocyte stages, suggesting limited metabolite exchange in these stages, but still ensures expression of MTPs during the different gametocyte stages to therefore, maintain the non-proliferative gametocytes for transmission (MacRae *et al.*, 2013; Daily *et al.*, 2007; White *et al.*, 1983). This current data does not support the idea that gametocytes are generally perceived as metabolically quiescent (Shute, 1960; Sinden and Smalley, 1979; Delves *et al.*, 2013). These different expression profiles of the MTP genes in the asexual and gametocyte

stages imply a distinct mode of metabolite exchange in these stages. Such distinct mode of metabolite exchange may suggest that certain MTPs are either TCP-1 or TCP-5 targets (Burrows *et al.*, 2017), allowing for specific targeting of either asexual or gametocyte stages.

Further delineation of the stage-specific expression of MTP genes showed the presence of MTP transcripts that are associated with amino acid transport, carbohydrate metabolism, DNA synthesis, lipid metabolism and ion transport during the specific asexual and gametocyte stages (ring, trophozoite and schizont stages and stage I – V gametocytes). Moreover, the data here show for the first time the presence of specific MTP transcripts during the gametocyte stages.

During the asexual stages, four amino acid transporter genes showed stage-specific expression during either ring and trophozoite or trophozoite and schizont stages (PF3D7_0629500, PF3D7_1208400, PF3D7_0209600 and PF3D7_1231400), whereas the other two amino acid transporter genes (PF3D7_1132500 and PF3D7_0515500) were expressed throughout the asexual stages. Therefore, at any given point during the asexual stages, there is an amino acid transporter transcript expressed which may explain amino acid uptake and release that already start in the ring stages (Lamour *et al.*, 2014) and continue until the schizont stages. The presence of these amino acid transporter transcripts during the different asexual stages suggests that these MTPs fulfil different roles during asexual development (Martin *et al.*, 2005); for example, one amino acid transporter may be responsible for cationic amino acid transport, whereas another may be responsible for anionic amino acid transport. However, the specific metabolites of the amino acid transporters are still unknown and should be investigated as these specificities may help in elucidating the stage during which specific amino acids are transported (Penny *et al.*, 1998). Despite not knowing which amino acid transporters are responsible for specific amino acid substrates, it was observed that [C^{14}]-leucine and [C^{14}]-lysine accumulated in trophozoite iRBCs. The uptake of [C^{14}]-leucine correlated with previous studies (Martin and Kirk, 2007); however, this is the first report of [C^{14}]-lysine uptake into trophozoite iRBCs as this has not been investigated previously. Leucine is a hydrophobic amino acid, whereas lysine is a cationic amino acid, and the uptake of both of these amino acids during the trophozoite stages may therefore, suggest that either one amino acid transporter that was expressed during the asexual stages can transport both of these amino acids or different amino acid transporters that were expressed can transport these amino acids separately. However, further studies are required to determine which of the six amino acid transporter transcripts that were expressed throughout the asexual stages are responsible for the observed amino acid uptake by determining either the substrate specificities of these MTPs or by investigating the protein presence of these MTP transcripts during the asexual stages.

During the gametocyte stages, only three of the six amino acid transporter genes showed stage-specific expression (PF3D7_1231400, PF3D7_1132500 and PF3D7_0515500), which may suggest that the gametocyte stages either require only certain amino acid transporters to ensure

the continuous mediation of amino acid import for protein synthesis/amino acid export following haemoglobin digestion or that the gametocytes require only the import/export of specific amino acids (Rajendran *et al.*, 2017; Krugliak *et al.*, 2002; Liu *et al.*, 2006; Florens *et al.*, 2002). A recent study identified a NPT (TgNPT1 and PbNPT1) as a cationic amino acid transporter, which is essential for gametocyte production (Rajendran *et al.*, 2017). However, in this study, the homologue of the PbNPT1 in *P. falciparum* (PF3D7_0104800) only showed increased transcript expression during the schizont stages of asexual development and decreased transcript expression in the gametocyte stages. One possible explanation for this is that the *P. falciparum* gametocyte stages do not require PfNPT1 for cationic amino acid transport, but may use one of the three amino acid transporters that showed increased transcript expression during gametocyte differentiation for cationic amino acid scavenging. Therefore, further investigations are needed to determine the substrate specificities of these amino acid transporters will help elucidate the specific amino acids that the gametocyte stages require for differentiation.

The MTPs involved in carbohydrate metabolism showed stage-specific expression during the asexual stages. For glycolysis, glucose is taken up through the GLUT1 transporter on the EPM (Kirk and Lehane, 2014), with a minor component via the NPP (Krishna *et al.*, 2000), through the non-selective pore on the PVM (Desai *et al.*, 1993) and then lastly through the PfHT (PF3D7_0204700) (Woodrow *et al.*, 2000; Joet *et al.*, 2003; Cobbold and McConville, 2014) on the PPM (Krishna *et al.*, 2000; Kirk *et al.*, 1996). Here, the PfHT transcript (PF3D7_0204700) was constitutively expressed through the asexual stages, and previous proteomics studies showed the presence of the PfHT protein in the trophozoite and schizont (Florens *et al.*, 2002; Lasonder *et al.*, 2002), confirming that the PfHT protein as the primary route of glucose uptake into the trophozoite stages (Slavic *et al.*, 2010). However, *P. falciparum* encodes three other sugar transporters that were each expressed in different asexual stages (PF3D7_0919500, PF3D7_0529200 and PF3D7_0916000), and from previous proteomics studies, the presence of two sugar transporter proteins was also observed during the trophozoite and merozoite stages (Florens *et al.*, 2002), which may indicate the use of alternative transporters for the uptake of glucose in the asexual stages. However, to confirm that these MTPs can also be used for glucose uptake, the substrate specificities should be investigated by expressing these MTP genes in *Xenopus laevis* oocytes (Penny *et al.*, 1998). The uptake of glucose was subsequently confirmed with functional radioisotope uptake assays that showed [14 C]-2DG accumulation in the trophozoite iRBC, which correlates with the presence of sugar transporter transcripts in the trophozoite stages. During glycolysis, glucose is metabolised to either lactic acid or pyruvate (Roth *et al.*, 1988; Jensen *et al.*, 1983; Zolg *et al.*, 1984). Stage-specific expression of two monocarboxylate transporters (PF3D7_0210300 and PF3D7_0926400) that may mediate lactic acid export was observed in the trophozoite/schizont stages. This can be associated with the increased levels of glycolysis in the trophozoite/schizont stages (Bozdech *et al.*, 2003), resulting in the production of lactic acid that needs to be exported. However, previous proteomic studies only observed protein levels for one of

the monocarboxylate transporter (PF3D7_0926400) during the merozoite stages (Florens *et al.*, 2002), yet it cannot be excluded that the other monocarboxylate transporter can also export lactic acid during the asexual stages, necessitating further investigations of the protein presence of these MTPs. Thus, the presence of these transcripts suggests that the parasite ensures glucose is taken up for glycolysis and that lactic acid that can cause osmotic instability and also interferes with the oxidation of NADH, is exported.

MTPs that may be involved in the TCA cycle showed stage-specific expression specifically in the trophozoite and schizont stages. The PfPPT gene (PF3D7_0530200) showed stage-specific expression specifically to the trophozoite stages, whereas the two pyruvate:H⁺ symporters (PF3D7_1470400 and PF3D7_1340800) were expressed through all the asexual stages, suggesting that the parasite is ensuring that if glucose is metabolised to pyruvate, it is then transported to the mitochondrion for the TCA cycle. However, the protein levels of these MTPs have not been previously identified and should be investigated to confirm the presence of these MTPs that may mediate the transport of pyruvate to the mitochondrion. Pyruvate is broken down for the production of acetyl-CoA that can be further metabolised through the TCA cycle. The MTPs that are involved in the acetyl-CoA production included PfDTC (PF3D7_0823900) that mediate the oxoglutarate–malate exchange across the inner mitochondrial membrane (Nozawa *et al.*, 2011) for CoA biosynthesis, the mitochondrial carrier protein (PF3D7_1368700) that transport CoA across the mitochondrion, which can then be used for the production of Acetyl-CoA (Cobbold *et al.*, 2013) and lastly the PfACT (PF3D7_1036800) that can transport acetyl-CoA out of the mitochondrion for further metabolism. Here, these MTP genes all showed stage-specific expression during the trophozoite and schizont stages, which correlated with the use of the TCA cycle in the trophozoite/schizont stages (Bozdech *et al.*, 2003).

During gametocyte stages, MTPs involved in carbohydrate metabolism also showed stage-specific expression. Here, only two sugar transporter genes were expressed from stage III – V gametocytes (PF3D7_0916000 and PF3D7_0529200), whereas the PfHT gene only showed increased transcript expression in stage I gametocytes, after which the transcript showed decreased expression. The presence of these transcripts correlates with previous studies that showed increased levels of glucose consumption during the gametocyte stages (Lamour *et al.*, 2014; MacRae *et al.*, 2013), which may therefore, indicate the requirement of glycolysis in these stages. However, the presence of only the PfHT protein has been previously observed during the gametocyte stages (Lasonder *et al.*, 2016), implying that as the transcript was expressed in stage I, the transcript was then translated immediately into the protein. The presence of the PfHT protein correlates with a previous study that showed glucose uptake pass through the hexose transporter in *P. berghei* (Slavic *et al.*, 2011). However, since the other sugar transporters proteins have not been measured in the gametocyte stages, it cannot be excluded that these sugar transporters can also be used for glucose uptake in the gametocyte stages.

Interestingly, only one of the monocarboxylate transporter genes (PF3D7_0926400) was expressed during the gametocyte stages, correlating to the decrease in release of glycolytic end-products (lactic acid, pyruvate, alanine and glycerol) (MacRae *et al.*, 2013; Lamour *et al.*, 2014). This associated with the two pyruvate:H⁺ symporters genes (PF3D7_1470400 and PF3D7_1340800) that were expressed through all the gametocyte stages, correlating to the increased levels of TCA catabolism of pyruvate in the gametocyte stages (MacRae *et al.*, 2013; Lamour *et al.*, 2014) as these MTPs will transport pyruvate to the mitochondrion. Unexpectedly, PfPPT, PfDTC and PfACT, which are involved in acetyl-CoA production for the TCA cycle, were not expressed during the gametocyte stages. However, the protein presence of PfDTC has previously been observed in the gametocyte stages (Lasonder *et al.*, 2002; Lasonder *et al.*, 2016). This necessitates the requirement of also investigating the protein levels of these MTPs to confirm their presence during the specific stages. Therefore, it cannot be excluded that these MTPs are present during the gametocyte stages as the transcripts may have been expressed during the commitment stages of gametocytogenesis and then already translated during the gametocyte stages (Bozdech and Ginsburg, 2005), resulting in the observed decreased expression. However, the MTP genes that showed increased transcript expression during the gametocyte stages correlates with the glycolytic flux into pyruvate and acetyl-CoA for the highly active TCA cycle (MacRae *et al.*, 2013; Cobbold and McConville, 2014).

The PfNT genes showed stage-specific expression during the asexual and gametocyte stages. During the asexual stages, stage-specific expression of all four PfNT genes was observed specifically to the ring and trophozoite stages, correlating with the uptake of purines from the host erythrocyte (De Koning *et al.*, 2005; Cassera *et al.*, 2011). This associates with DNA synthesis that is initiated as the parasite develops from the ring to the trophozoite stages (Bozdech *et al.*, 2003), which matures into multinucleated schizont stages (Wipasa *et al.*, 2002). Previous proteomic studies have shown that PfNT4 (PF3D7_0103200) and PfNT2 (PF3D7_0824400) protein levels are present during the trophozoite and schizont stages (Lasonder *et al.*, 2002), confirming the presence of the MTPs transcripts in these stages. During the gametocyte stages, only PfNT3 (PF3D7_1469400) showed stage-specific expression, specifically to stage I gametocytes, which correlates with the uptake of hypoxanthine in gametocyte stages (Raabe *et al.*, 2009) and the inhibition of early gametocyte stages by compounds targeting DNA replication and transcription (Sinden and Smalley, 1979). The expression of only PfNT3 may suggest that the gametocyte stages require only the transport of specific purines for the synthesis of DNA, as in previous studies it was shown that PfNT4 has unique substrate and inhibitor specificity (Frame *et al.*, 2012). Nevertheless, the expression of PfNT3 in stage I gametocytes associated well with DNA synthesis in stage I gametocytes (Janse *et al.*, 1988).

Lipid-related MTP genes showed stage-specific expression during the asexual stages, where different MTP genes were expressed during the ring, late trophozoite and schizont stages. These

lipid-related MTPs may be involved in the uptake of the phospholipid precursors required for membrane biogenesis, which is at its peak during the trophozoite stages (Pessi *et al.*, 2004). Thus, the presence of these MTPs during each asexual stage suggests that the parasite is possibly ensuring that the transporter proteins are present prior to when the lipid molecules need to be transported for membrane biogenesis during the schizont stages, which is required for enclosing each new daughter parasite with a plasma membrane (Ben Mamoun *et al.*, 2010; Gulati *et al.*, 2015; Palacpac *et al.*, 2004). However, the substrate specificities of these MTPs should be investigated to confirm whether they transport either fatty acids, serine, ethanolamine or choline as the specific MTPs involved in the uptake of the phospholipid precursors are yet to be identified (Kirk and Saliba, 2007; Ben Mamoun *et al.*, 2010).

During stage II – IV gametocyte stages, only two lipid-related MTP genes were expressed, which included the ABC transporter (PF3D7_1426500) and the aminophospholipid transporter (PF3D7_1468600). The presence of the ABC transporter correlated with a previous study that also identified this MTP predominantly in the gametocyte stages and reported to play an essential role in neutral lipid transport (Tran *et al.*, 2014), which is also required for membrane biogenesis. Therefore, this suggests that the gametocyte stages use both uptake of neutral lipids and synthesis of fatty acids (Young *et al.*, 2005) for membrane biogenesis. However, it cannot be excluded that the gametocyte stages require other phospholipid precursors for membrane biogenesis. The presence of these two MTP genes from stage II gametocytes onwards suggests that membrane biogenesis occurs in the later gametocyte stages as the gametocytes are preparing for the transition from the human host to the mosquito vector, and therefore sequester lipids obtained from the human host, which are less readily available in the mosquito (Tran *et al.*, 2014).

An interesting observation during this study is the stage-specific expression of ion transporting MTPs during both the asexual and gametocyte stages. Ion regulation has been extensively investigated in the asexual stages; however, the stage-specificity of ion transporting MTPs has not been investigated previously in both asexual and gametocyte stages.

In the asexual stages, Na⁺-related MTP genes and K⁺-related MTP genes showed stage-specific expression, as at any given point during asexual development there are a Na⁺- and K⁺-related MTP gene expressed. These MTPs may be required to maintain the low $[Na^+]_{cytosol}/[K^+]_{cytosol}$ ratio required for asexual parasites because there is an increase in the permeability of cations when the *P. falciparum* parasite infects the erythrocyte due to the formation of NPP (Ginsburg *et al.*, 1985; Kirk *et al.*, 1994), which mediate the movement of Na⁺ into and K⁺ out of the infected cell, causing an increase in erythrocyte $[Na^+]_{cytosol}$ and a decrease in erythrocyte $[K^+]_{cytosol}$, therefore, resulting in a high $[Na^+]_{cytosol}/[K^+]_{cytosol}$ ratio (Kirk, 2015). To maintain a low $[Na^+]_{cytosol}/[K^+]_{cytosol}$ ratio required by intraerythrocytic parasites, Na⁺ should be exported from the cytosol and K⁺ imported into the cytosol. P-type ATPases such as PfATP4 (PF3D7_1211900) serve as the major Na⁺ export

mechanism (Kirk, 2015; Spillman *et al.*, 2013b). However, PfATP4 is annotated as a Ca²⁺ ATPase (Krishna *et al.*, 2001), but the proposed Ca²⁺ transport function for this protein has not been demonstrated and it may still function as a Ca²⁺ pump. Nevertheless, PfATP4 and the other three Na⁺-related MTPs that may also contribute to the export of Na⁺ were expressed in each asexual stage, suggesting that the parasite is ensuring that these MTPs are present through all these stages to maintain this low cytosolic [Na⁺] through asexual development.

For the control of the high cytosolic [K⁺] in the intraerythrocytic parasite, the specific MTPs required for the import of K⁺ are yet to be determined. However, the K⁺-related MTP genes encoded by the parasite may be responsible for the import of K⁺. Here, K⁺-related MTP genes were expressed at any given point during the asexual stages, which may suggest that K⁺ import already starts in the ring stages to maintain the high cytosolic [K⁺] through all the asexual stages. Moreover, due to the presence of both Na⁺-related MTPs and K⁺-related MTP transcripts during all the asexual stages, it is suggested that the low [Na⁺]_{cytosol}/[K⁺]_{cytosol} ratio is therefore, maintained during asexual development.

The requirement of the low [Na⁺]_{cytosol}/[K⁺]_{cytosol} ratio in the gametocyte stages has never been suggested before; however, here it was observed that only one Na⁺-related MTP gene (PF3D7_0212800) and one K⁺-related MTP gene (F3D7_1465500) were expressed specifically in stage I – IV gametocytes. The presence of these MTPs may therefore, suggest that the gametocyte stages export Na⁺ and import K⁺ through the Na⁺/H⁺ antiporter and the PfK2. It was unexpected that the PfATP4 transcript was not expressed during the gametocyte stages as it has previously been shown that spiroindolones that target PfATP4 inhibit early and late gametocyte stages (van Pelt-Koops *et al.*, 2012), suggesting the presence of PfATP4 in the gametocyte stages. This indicates that future studies are required to investigate the protein presence of these MTPs as well as the protein presence of the MTPs, which showed decreased expression specifically in the gametocyte stages to confirm the presence of these MTP transcripts and confirm that these stages also require and maintain a low [Na⁺]_{cytosol}/[K⁺]_{cytosol} ratio.

During both asexual and gametocyte stages, the Ca²⁺-related MTP genes showed decreased transcript expression, which was unexpected as it has previously been shown that the intraerythrocytic parasite has a number of internal Ca²⁺ stores (Kirk, 2015), which requires the maintenance of a low resting [Ca²⁺], however, the mechanism by which it does so is unclear. The absence of these MTP transcripts suggests that the asexual and gametocyte stages do not use these MTPs to transport Ca²⁺, yet it cannot be excluded that the protein levels of these MTPs are not present in these stages or that other MTPs may be used to maintain [Ca²⁺]. Three zinc transporter genes showed stage-specific expression in the ring and trophozoite stages during asexual development, whereas in the gametocyte stages, only one zinc transporter showed stage-specific expression to stage I and IV gametocyte stages. These zinc transporters (zinc transporter -

PF3D7_1022300, zinc transporter - PF3D7_0715900 and Zn²⁺/Fe²⁺ permease - PF3D7_0609100) showed localisation to the PPM and to an acidocalcisome (<http://mpmp.huji.ac.il/maps/acidocalcisome.html>). Acidocalcisomes are the largest Ca²⁺ store in *T. gondii* and have been found in *P. falciparum* parasites, especially during the merozoite stages (Miranda *et al.*, 2008), confirming the regulation of [Ca²⁺] in the parasite. Therefore, the presence of zinc transporter transcripts that are localised to the acidocalcisome may suggest Ca²⁺ transport and therefore, regulation in both asexual and gametocyte stages.

The Mg²⁺ transporter genes showed stage-specific expression in each asexual stage, suggesting that the parasite ensures the transport of Mg²⁺ in these stages. This correlated with a previous study, which showed that Mg²⁺ ion regulation is required for parasite growth and survival, especially in the asexual stages, as inhibition of parasite growth were observed with the removal of magnesium from the extracellular medium (Maurois *et al.*, 1989). Thus, the presence of these Mg²⁺-related MTPs transcripts during the asexual stage associates to the parasite mechanisms that exerts a tight control over its intracellular magnesium level (Atamna and Ginsburg, 1997; Ginsburg, 2008). In the gametocyte stages, four of the five Mg²⁺ transporter genes showed stage-specific expression as these were expressed during different gametocyte stages (PF3D7_0827700, PF3D7_1427600, PF3D7_1304200 and PF3D7_0306700). The presence of these MTP transcripts suggests their importance and involvement in the gametocyte stages. This correlated with a previous study that observed that Mg²⁺ stimulates the exflagellation of stage V gametocytes when these stages are taken up by the mosquito (Guttery *et al.*, 2015). Thus, the presence of these MTPs during the gametocyte stages may suggests that the parasite is possibly ensuring that these MTPs are present prior to when Mg²⁺ need to be transported in the mosquito stages for exflagellation.

Taken together, it was observed that most of the MTPs involved in specific metabolic processes showed stage-specific expression, with a few individual MTPs that showed no stage-specific expression within asexual and gametocyte stages, suggesting their importance to either a specific stage or for all the developmental stages (constitutively expressed). When comparing the stage-specific expression between the asexual and gametocyte stages, it was observed that during the gametocyte stages, there was an absence of some MTP genes (decreased expression) that were expressed during the asexual stages, correlating with the strategy-specific expression also observed. The presence of only specific MTP genes during the gametocyte stages may suggests that the gametocyte stages require only certain metabolites for the investigated metabolic processes, yet enough MTPs were expressed to carry out the metabolic processes. This was suggested for amino acid transporters, PfNTs, lipid-related MTPs and ion transporting MTPs. Nevertheless, the investigation of the stage-specific expression of MTPs correlated well with literature regarding parasite biology and as such increases confidence of the presence of these MTPs transcripts during the asexual and gametocyte stages. Additionally, this is the first time that

ion transport was investigated in the gametocyte stages, therefore, giving insights into possible ion regulation processes in the gametocyte stages.

The identification of the presence of these MTP transcripts provides a foundation for highlighting potential *P. falciparum*-encoded MTPs as novel drug targets as either TCP-1 or TCP-5 targets (Burrows *et al.*, 2017), allowing for specific targeting of either asexual or gametocyte stages. However, the MTPs that showed stage-specific expression within both asexual and gametocytes should also be investigated further as potential drug targets. By targeting one of these MTPs with a single novel antimalarial compound, both asexual and gametocyte stages will be affected and will therefore, comply with TPP-1. MTPs that are specifically part of either the Channels class or ATP-powered pumps class should be investigated as these integral membrane protein classes showed the most essential MTP genes, suggesting that these classes may have less alternative MTPs for the gaining and utilisation of energy and the generation of ion gradients across membranes. Such MTPs include an ABC transporter (PF3D7_1426500) that has been identified as having an essential role in neutral lipid transport (Tran *et al.*, 2014), Pfk2, the Na⁺/H⁺ antiporter (PF3D7_0212800) and a zinc transporter (PF3D7_1022300), which were all expressed within both asexual and gametocyte stages. Therefore, by developing one novel compound targeting either one of these MTPs, both asexual and gametocyte stages will then be affected, ultimately decreasing developmental costs and pharmacological complexities as only one compound is then required to be further tested and developed (Birkholtz *et al.*, 2016).

In conclusion, the permeome showed strategy- and stage-specific expression, which indicated that the permeome is differentially expressed between and within the asexual and gametocyte stages. This study resulted in identifying the presence of MTPs transcripts specific to the asexual stages as the whole complement of parasite-encoded MTPs were expressed in the asexual stages, whereas less than half of the permeome were expressed in the gametocyte stages, as well as the identification of the presence of MTPs transcripts that were expressed within both asexual and gametocyte stages, which may be novel drug targets as these will affect both stages (TPP-1). Additionally, this is the first transcriptome data of MTPs in the gametocyte stages that suggested for the first time ion transport during these stages. These transcriptomic data may aid in the future investigation of transport in the gametocyte stages.

Although a substantial amount of data was generated during this study for the investigation of transcript expression of the permeome, a few constraints have arisen during these findings. First, it was observed that in the gametocyte stages, some MTPs did not show increased transcript expression, but their protein presence was confirmed with previous proteomics studies (Lasonder *et al.*, 2016). This highlights the importance of time-dependent transcription, where the presence of the transcript does not always overlap with the translation of the protein (Bozdech and Ginsburg, 2005), which was also previously reported by Le Roch *et al.* (Le Roch *et al.*, 2004). Therefore,

transcriptomics can at best set a time for possible translation, but not for its actual presence, which confirms that for the identification of the actual MTPs, the protein levels should also be investigated. Previous proteomics studies did not specifically investigate MTPs as proteomic analysis investigated mostly the soluble proteins and therefore, the protein levels of all the MTPs have not been identified previously. This can be investigated in future studies, where the protein levels of insoluble proteins, specifically MTPs encoded by *P. falciparum* parasites, are determined to confirm the transcriptome data that will also aid in ultimately identifying possible novel drug targets.

Secondly, for most of the MTPs, the substrate specificity is either unknown or is predicted, based on orthology models. Therefore, for these MTPs such as the amino acid transporters, sugar transporters and lipid-related MTPs, the substrate specificities can be determined by expressing these MTP genes in *X. laevis* oocytes (Penny *et al.*, 1998) that may help elucidate underlying biological mechanisms during the asexual and gametocyte stages.

Lastly, metabolite uptake has not been experimentally investigated in the gametocyte stages to date due to the lengthy process of gametocyte cultivation that takes ~14 days as well as the large number of gametocytes that need to be cultivated to obtain $5 \times 10^7 - 1 \times 10^8$ cells/ml, making large-scale production of these gametocytes expensive. While the expression of MTPs in the gametocyte stages identified in this study needs to be confirmed with the biochemical characterisation of uptake studies, such experiments will require advances in the large-scale production of gametocytes. There are efforts in developing high throughput gametocyte production protocols that include (i) the use of magnetic separation for isolation of haemozoin-containing parasites to increase parasitaemia, decrease haematocrit and introduce higher levels of young RBC in a culture for optimum induction of gametocytogenesis (Duffy *et al.*, 2016), (ii) the use of a HP1 strain, where the heterochromatin protein 1 (HP1) regulates PfAP2 - G, a transcription factor required for gametocyte conversion and therefore, with depletion of PfHP1, derepression of PfAP2 - G takes place and then results in a dramatic increase in gametocyte production (Flueck *et al.*, 2009; Brancucci *et al.*, 2014) and (iii) the use of lysophosphatidylcholine, which regulates gametocyte stage differentiation by limiting lysophosphatidylcholine (membrane biogenesis) availability, reducing the number of daughter cells produced by asexual stages and therefore, stimulating the differentiation and development of the gametocyte stages (Brancucci *et al.*, 2017). Thus, these avenues should be pursued and the number of gametocytes obtained through the various methods as indicated, should be compared to decide, which protocol would be the most optimal for gametocyte production in high numbers, as well as the production of viable gametocytes for future gametocyte uptake studies.

Chapter 5: Concluding Discussion

Malaria is a devastating disease with 216 million malaria cases reported in 2016, which led to 445 000 deaths globally, mostly affecting children under 5 years of age (World Health Organisation, 2017). The WHO developed the GTS for Malaria 2016 - 2030 together with the RBM Partnership to accelerate progress towards malaria elimination (Hemingway *et al.*, 2016). However, the effective treatment of malaria infections is under threat due to the increase in resistance against the majority of antimalarial compounds. Therefore, the development of novel antimalarial agents that would target a novel biological activity in the parasite is of utmost importance. The targeting of *P. falciparum*-encoded MTPs has been shown to be promising novel drug targets as there are new potent antimalarial drugs (spiroindolones and dihydroisoquinolones), which target the PfATP4 (Spillman *et al.*, 2013b). However, ongoing studies of the parasite-encoded MTPs are still required to investigate the presence and absence of these MTPs in the asexual and gametocyte stages as limited knowledge is available about these MTPs in the gametocyte stages. The different strategy- and stage-specific metabolic requirements of the asexual and gametocytes suggest that the parasite-encoded MTPs may be differentially expressed between these stages. Therefore, the identification of the presence of MTPs in the asexual and gametocyte will result in a better understanding of the physiological roles of MTPs in these stages and ultimately highlight potential novel drug targets that comply with TPP-1.

The aim of this study was to get a comprehensive overview of the whole permeome strategy- and stage-specific expression in the asexual and gametocyte stages. The *P. falciparum*-encoded permeome is well characterised in the asexual stages (Kirk and Lehane, 2014; Martin *et al.*, 2005; Martin *et al.*, 2009). However, limited knowledge is available about the *P. falciparum*-encoded permeome in the gametocyte stages. Therefore, by investigating the strategy- and stage-specific expression of the entire complement of parasite-encoded MTPs in the asexual and gametocyte stages, the presence of these MTP transcripts in these stages were inferred in the absence of biochemical uptake data. The transcript presence of the MTPs during the asexual and gametocyte stages also allowed for the identification of novel drug targets.

Here, the permeome showed a strategy-specific expression between the asexual and gametocyte stages, where the entire complement of parasite-encoded MTP genes were expressed during the asexual stages, correlating to the highly proliferative asexual stages that require constant exchange of metabolites. By contrast, less than half of the entire complement of parasite-encoded MTP genes was expressed during the non-proliferative gametocyte stages, indicating a reduced range of MTPs active in the gametocyte stages and therefore, switches to limited metabolite uptake (MacRae *et al.*, 2013; Daily *et al.*, 2007; White *et al.*, 1983). These different expression profiles of the entire permeome in the asexual and gametocyte stage correlate with previous studies that showed these stages are metabolically different (Lamour *et al.*, 2014).

The stage-specific expression of MTPs associated to specific metabolic processes within the asexual and gametocyte stages indicated that most of these MTP genes showed stage-specific expression, with a few individual MTP genes that showed no stage-specific expression within the asexual and gametocyte stages, respectively. When comparing the stage-specific expression between the asexual and gametocyte stages, it was observed that during the gametocyte stages, there was an absence of some MTP genes that were expressed during the asexual stages, suggesting that the gametocyte stages are more specific in the metabolites transported to maintain the investigated metabolic processes.

In conclusion, the strategy- and stage-specific expression of the permeome between and within the asexual and gametocyte stages suggested that the permeome is differentially expressed in these stages, therefore, implying different metabolite exchange, which is indicative of the different maturation processes of the asexual and gametocyte stages (Bannister and Mitchell, 2003; Salcedo-Sora *et al.*, 2014; Talman *et al.*, 2004; Dixon *et al.*, 2008). However, the presence of MTP transcripts during the gametocyte stages rejects the idea that gametocytes are generally perceived as metabolically quiescent (Shute, 1960; Sinden and Smalley, 1979; Delves *et al.*, 2013). Therefore, the hypothesis of this study was accepted that the permeome is differentially expressed in the asexual and the gametocyte stages of *P. falciparum* parasites.

This study contributed by providing the MTPs transcript expression profiles for both the *P. falciparum* asexual and the gametocyte stages as well as to infer the presence of these MTPs in the asexual and gametocyte stages, which may aid in highlighting potential novel drug targets. Additionally, this is the first transcriptome data of MTP genes in the gametocyte stages, which specifically suggested for the first time the presence of ion transport in the gametocyte stages. These transcript data of MTPs in the gametocyte stages therefore, serve as a blueprint for future investigation of transport in these stages.

However, many questions have arisen during these findings. First, it will be important to determine, whether the transcript expression is translated into the proteomic expression of these MTPs as previous proteomic analysis investigated mostly the soluble proteins and did not identify protein levels for all the MTPs (Florens *et al.*, 2002; Lasonder *et al.*, 2002; Lasonder *et al.*, 2016). Therefore, future studies may firstly include proteome analysis for the insoluble protein fractions to provide confirmatory results of the MTPs being expressed during the different stages. Second, it will be necessary to investigate the substrate specificities of MTPs that have not previously been investigated as this will help elucidate underlying biological mechanisms during the asexual and gametocyte stages. Researchers will also need to investigate and characterise metabolite uptake in the gametocyte stages, and additionally, investigate the ion regulation based on ion transport in the gametocyte stages as this has not been done to date. The results of these studies will ultimately contribute to a greater understanding of the *P. falciparum* biology.

References

Allen, R. J. and Kirk, K. 2004a. Cell volume control in the *Plasmodium*-infected erythrocyte. Trends in Parasitology, 20, 7-10.

Allen, R. J. and Kirk, K. 2004b. The membrane potential of the intraerythrocytic malaria parasite *Plasmodium falciparum*. Journal of Biological Chemistry, 279, 11264-11272.

Alonso, P. L., Brown, G., Arevalo-Herrera, M., Binka, F., Chitnis, C., Collins, F., Doumbo, O. K., Greenwood, B., Hall, B. F. and Levine, M. M. 2011. A research agenda to underpin malaria eradication. PLOS Medicine, 8, e1000406.

Ancelin, M. L., Parant, M., Thuet, M. J., Philippot, J. R. and Vial, H. J. 1991. Increased permeability to choline in simian erythrocytes after *Plasmodium knowlesi* infection. Biochemical Journal, 273, 701-709.

Anders, J., Chung, H. and Theoharides, A. 1988. Methemoglobin formation resulting from administration of candidate 8-aminoquinoline antiparasitic drugs in the dog. Toxicological Sciences, 10, 270-275.

Atamna, H. and Ginsburg, H. 1997. The malaria parasite supplies glutathione to its host cell—investigation of glutathione transport and metabolism in human erythrocytes infected with *Plasmodium falciparum*. European Journal of Biochemistry, 250, 670-679.

Augagneur, Y., Jaubert, L., Schiavoni, M., Pachikara, N., Garg, A., Usmani-Brown, S., Wesolowski, D., Zeller, S., Ghosal, A. and Cornillot, E. 2013. Identification and functional analysis of the primary pantothenate transporter, PfPAT, of the human malaria parasite *Plasmodium falciparum*. Journal of Biological Chemistry, 288, 20558-20567.

Aurrecoechea, C., Brestelli, J., Brunk, B. P., Dommer, J., Fischer, S., Gajria, B., Gao, X., Gingle, A., Grant, G. and Harb, O. S. 2008. PlasmoDB: a functional genomic database for malaria parasites. Nucleic Acids Research, 37, D539-D543.

Bannister, L. and Mitchell, G. 2003. The ins, outs and roundabouts of malaria. Trends in Parasitology, 19, 209-213.

Barrand, M. A., Winterberg, M., Ng, F., Nguyen, M., Kirk, K. and Hladky, S. B. 2012. Glutathione export from human erythrocytes and *Plasmodium falciparum* malaria parasites. Biochemical Journal, 448, 389-400.

- Basore, K., Cheng, Y., Kushwaha, A. K., Nguyen, S. T. and Desai, S. A. 2015. How do antimalarial drugs reach their intracellular targets? *Frontiers in Pharmacology*, 6.
- Bayliss, R., Leung, S. W., Baker, R. P., Quimby, B. B., Corbett, A. H. and Stewart, M. 2002. Structural basis for the interaction between NTF2 and nucleoporin FxFG repeats. *The EMBO Journal*, 21, 2843-2853.
- Beitz, E. 2005. Aquaporins from pathogenic protozoan parasites: structure, function and potential for chemotherapy. *Biology of the Cell*, 97, 373-383.
- Beitz, E., Pavlovic-Djuranovic, S., Yasui, M., Agre, P. and Schultz, J. E. 2004. Molecular dissection of water and glycerol permeability of the aquaglyceroporin from *Plasmodium falciparum* by mutational analysis. *Proceedings of the National Academy of Sciences of the United States of America*, 101, 1153-1158.
- Ben Mamoun, C., Prigge, S. T. and Vial, H. 2010. Targeting the lipid metabolic pathways for the treatment of malaria. *Drug Development Research*, 71, 44-55.
- Bhatt, S., Weiss, D., Cameron, E., Bisanzio, D., Mappin, B., Dalrymple, U., Battle, K., Moyes, C., Henry, A. and Eckhoff, P. 2015. The effect of malaria control on *Plasmodium falciparum* in Africa between 2000 and 2015. *Nature*, 526, 207.
- Bholowalia, P. and Kumar, A. 2014. EBK-means: A clustering technique based on elbow method and K-means in WSN. *International Journal of Computer Applications*, 105.
- Biagini, G. A., Bray, P. G., Spiller, D. G., White, M. R. and Ward, S. A. 2003. The digestive food vacuole of the malaria parasite is a dynamic intracellular Ca^{2+} store. *Journal of Biological Chemistry*, 278, 27910-27915.
- Biagini, G. A., Pasini, E. M., Hughes, R., De Koning, H. P., Vial, H. J., O'Neill, P. M., Ward, S. A. and Bray, P. G. 2004. Characterization of the choline carrier of *Plasmodium falciparum*: a route for the selective delivery of novel antimalarial drugs. *Blood*, 104, 3372-3377.
- Birkholtz, L.-M., Bornman, R., Focke, W., Mutero, C. and De Jager, C. 2012. Sustainable malaria control: transdisciplinary approaches for translational applications. *Malaria Journal*, 11, 431.
- Birkholtz, L.-M., Coetzer, T. L., Mancama, D., Leroy, D. and Alano, P. 2016. Discovering new transmission-blocking antimalarial compounds: challenges and opportunities. *Trends in Parasitology*, 32, 669-681.

Black, B. E., Holaska, J. M., Lévesque, L., Ossareh-Nazari, B., Gwizdek, C., Dargemont, C. and Paschal, B. M. 2001. NXT1 is necessary for the terminal step of Crm1-mediated nuclear export. *The Journal of Cell Biology*, 152, 141-156.

Boisson, B., Lacroix, C., Bischoff, E., Gueirard, P., Bargieri, D. Y., Franke-Fayard, B., Janse, C. J., Ménard, R. and Baldacci, P. 2011. The novel putative transporter NPT1 plays a critical role in early stages of *Plasmodium berghei* sexual development. *Molecular Microbiology*, 81, 1343-1357.

Bolchoz, L. J., Budinsky, R. A., Mcmillan, D. C. and Jollow, D. J. 2001. Primaquine-induced hemolytic anemia: formation and hemotoxicity of the arylhydroxylamine metabolite 6-methoxy-8-hydroxylaminoquinoline. *Journal of Pharmacology and Experimental Therapeutics*, 297, 509-515.

Bousquet, I., Dujardin, G. and Slonimski, P. P. 1991. ABC1, a novel yeast nuclear gene has a dual function in mitochondria: it suppresses a cytochrome b mRNA translation defect and is essential for the electron transfer in the bc 1 complex. *The EMBO Journal*, 10, 2023.

Bouvier, L. A., Silber, A. M., Lopes, C. G., Canepa, G. E., Miranda, M. R., Tonelli, R. R., Colli, W., Alves, M. J. M. and Pereira, C. A. 2004. Post genomic analysis of permeases from the amino acid/auxin family in protozoan parasites. *Biochemical and Biophysical Research Communications*, 321, 547-556.

Bozdech, Z. and Ginsburg, H. 2005. Data mining of the transcriptome of *Plasmodium falciparum*: the pentose phosphate pathway and ancillary processes. *Malaria Journal*, 4, 17.

Bozdech, Z., Llinás, M., Pulliam, B. L., Wong, E. D., Zhu, J. and Derisi, J. L. 2003. The transcriptome of the intraerythrocytic developmental cycle of *Plasmodium falciparum*. *PLOS Biology*, 1, e5.

Brancucci, N. M., Bertschi, N. L., Zhu, L., Niederwieser, I., Chin, W. H., Wampfler, R., Freymond, C., Rottmann, M., Felger, I. and Bozdech, Z. 2014. Heterochromatin protein 1 secures survival and transmission of malaria parasites. *Cell Host & Microbe*, 16, 165-176.

Brancucci, N. M., Gerdt, J. P., Wang, C., De Niz, M., Philip, N., Adapa, S. R., Zhang, M., Hitz, E., Niederwieser, I. and Boltryk, S. D. 2017. Lysophosphatidylcholine Regulates Sexual Stage Differentiation in the Human Malaria Parasite *Plasmodium falciparum*. *Cell*, 171, 1532-1544.e15.

Bricker, D. K., Taylor, E. B., Schell, J. C., Orsak, T., Boutron, A., Chen, Y.-C., Cox, J. E., Cardon, C. M., Van Vranken, J. G. and Dephoure, N. 2012. A mitochondrial pyruvate carrier required for pyruvate uptake in yeast, *Drosophila*, and humans. *Science*, 337, 96-100.

- Brown, J. and Smalley, M. 1981. Inhibition of the *in vitro* growth of *Plasmodium falciparum* by human polymorphonuclear neutrophil leucocytes. *Clinical and Experimental Immunology*, 46, 106.
- Burrows, J. N., Duparc, S., Gutteridge, W. E., Van Huijsduijnen, R. H., Kaszubska, W., Macintyre, F., Mazzuri, S., Möhrle, J. J. and Wells, T. N. 2017. New developments in anti-malarial target candidate and product profiles. *Malaria Journal*, 16, 26.
- Busch, W. and Saier, M. H. 2003. The IUBMB-endorsed transporter classification system. *Membrane Transporters: Methods and Protocols*, 21-36.
- Bushell, E., Gomes, A. R., Sanderson, T., Anar, B., Girling, G., Herd, C., Metcalf, T., Modrzynska, K., Schwach, F. and Martin, R. E. 2017. Functional profiling of a *Plasmodium* genome reveals an abundance of essential genes. *Cell*, 170, 260-272. e8.
- Butterworth, A. S., Skinner-Adams, T. S., Gardiner, D. L. and Trenholme, K. R. 2013. *Plasmodium falciparum* gametocytes: with a view to a kill. *Parasitology*, 140, 1718-1734.
- Carson, P. E., Flanagan, C. L., Ickes, C. and Alving, A. S. 1956. Enzymatic deficiency in primaquine-sensitive erythrocytes. *Science*, 124, 484-485.
- Cassera, B. M., Zhang, Y., Hazleton, K. Z. and Schramm, V. L. 2011. Purine and pyrimidine pathways as targets in *Plasmodium falciparum*. *Current Topics in Medicinal Chemistry*, 11, 2103-2115.
- Catterall, W. A. 1995. Structure and function of voltage-gated ion channels. *Annual Review of Biochemistry*, 64, 493-531.
- Celada, A., Cruchaud, A. and Perrin, L. H. 1983. Phagocytosis of *Plasmodium falciparum*-parasitized erythrocytes by human polymorphonuclear leukocytes. *The Journal of Parasitology*, 49-53.
- Cho, H., Dhillon, I. S., Guan, Y. and Sra, S. Minimum sum-squared residue co-clustering of gene expression data. *Proceedings of the 2004 SIAM International Conference on Data Mining*, 2004. SIAM, 114-125.
- Choveaux, D. L., Przyborski, J. M. and Goldring, J. D. 2012. A *Plasmodium falciparum* copper-binding membrane protein with copper transport motifs. *Malaria Journal*, 11, 397.

- Ciborowski, P. and Silberring, J. 2016. Proteomic profiling and analytical chemistry: the crossroads, United States, Elsevier.
- Cobbold, S. A., Martin, R. E. and Kirk, K. 2011. Methionine transport in the malaria parasite *Plasmodium falciparum*. *International Journal for Parasitology*, 41, 125-135.
- Cobbold, S. A. and Mcconville, M. J. 2014. The *Plasmodium* Tricarboxylic Acid Cycle and Mitochondrial Metabolism. *Encyclopedia of Malaria*, 1-18.
- Cobbold, S. A., Vaughan, A. M., Lewis, I. A., Painter, H. J., Camargo, N., Perlman, D. H., Fishbaugher, M., Healer, J., Cowman, A. F. and Kappe, S. H. 2013. Kinetic flux profiling elucidates two independent acetyl-CoA biosynthetic pathways in *Plasmodium falciparum*. *Journal of Biological Chemistry*, 288, 36338-36350.
- Corbel, V., N'guessan, R., Brengues, C., Chandre, F., Djogbenou, L., Martin, T., Akogbeto, M., Hougard, J.-M. and Rowland, M. 2007. Multiple insecticide resistance mechanisms in *Anopheles gambiae* and *Culex quinquefasciatus* from Benin, West Africa. *Acta Tropica*, 101, 207-216.
- Cowman, A. F. and Crabb, B. S. 2006. Invasion of red blood cells by malaria parasites. *Cell*, 124, 755-766.
- Cowman, A. F., Karcz, S., Galatis, D. and Culvenor, J. G. 1991. A P-glycoprotein homologue of *Plasmodium falciparum* is localized on the digestive vacuole. *The Journal of Cell Biology*, 113, 1033-1042.
- Cranmer, S. L., Conant, A. R., Gutteridge, W. E. and Halestrap, A. P. 1995. Characterization of the enhanced transport of L- and D-lactate into human red blood cells infected with *Plasmodium falciparum* suggests the presence of a novel saturable lactate proton cotransporter. *Journal of Biological Chemistry*, 270, 15045-15052.
- Crompton, P. D., Pierce, S. K. and Miller, L. H. 2010. Advances and challenges in malaria vaccine development. *The Journal of Clinical Investigation*, 120, 4168-4178.
- Daily, J. Á., Scandfeld, D., Pochet, N., Le Roch, K., Plouffe, D., Kamal, M., Sarr, O., Mboup, S., Ndir, O. and Wypij, D. 2007. Distinct physiological states of *Plasmodium falciparum* in malaria-infected patients. *Nature*, 450, 1091.

De Koning-Ward, T. F., Gilson, P. R., Boddey, J. A., Rug, M., Smith, B. J., Papenfuss, A. T., Sanders, P. R., Lundie, R. J., Maier, A. G. and Cowman, A. F. 2009. A novel protein export machine in malaria parasites. *Nature*, 459, 945.

De Koning, H. P., Bridges, D. J. and Burchmore, R. J. 2005. Purine and pyrimidine transport in pathogenic protozoa: from biology to therapy. *FEMS Microbiology Reviews*, 29, 987-1020.

Dearnley, M. K., Yeoman, J. A., Hanssen, E., Kenny, S., Turnbull, L., Whitchurch, C. B., Tilley, L. and Dixon, M. W. 2012. Origin, composition, organization and function of the inner membrane complex of *Plasmodium falciparum* gametocytes. *Journal of Cell Science*, 125, 2053-2063.

Delves, M., Plouffe, D., Scheurer, C., Meister, S., Wittlin, S., Winzeler, E. A., Sinden, R. E. and Leroy, D. 2012. The activities of current antimalarial drugs on the life cycle stages of *Plasmodium*: a comparative study with human and rodent parasites. *PLOS Medicine*, 9, e1001169.

Delves, M. J., Ruecker, A., Straschil, U., Lelièvre, J., Marques, S., López-Barragán, M. J., Herreros, E. and Sinden, R. E. 2013. Male and female *Plasmodium falciparum* mature gametocytes show different responses to antimalarial drugs. *Antimicrobial Agents and Chemotherapy*, 57, 3268-3274.

Desai, S. A., Krogstad, D. J. and McCleskey, E. W. 1993. A nutrient-permeable channel on the intraerythrocytic malaria parasite. *Nature*, 362, 643-646.

Desai, S. A., Rayavara, K., Sharma, P., Syed, S. K., Nguitrageol, W. and Nina, P. B. 2016. *Advances in Malaria Research: Membrane transport proteins as therapeutic targets in malaria*, United States, John Wiley & Sons.

Desai, S. A. and Rosenberg, R. L. 1997. Pore size of the malaria parasite's nutrient channel. *Proceedings of the National Academy of Sciences*, 94, 2045-2049.

Divo, A. A., Geary, T. G., Davis, N. L. and Jensen, J. B. 1985. Nutritional requirements of *Plasmodium falciparum* in culture. I. Exogenously supplied dialyzable components necessary for continuous growth. *The Journal of Protozoology*, 32, 59-64.

Dixon, M. W., Dearnley, M. K., Hanssen, E., Gilberger, T. and Tilley, L. 2012. Shape-shifting gametocytes: how and why does *P. falciparum* go banana-shaped? *Trends in Parasitology*, 28, 471-478.

- Dixon, M. W., Thompson, J., Gardiner, D. L. and Trenholme, K. R. 2008. Sex in *Plasmodium*: a sign of commitment. *Trends in Parasitology*, 24, 168-175.
- Downie, M. J., Saliba, K. J., Bröer, S., Howitt, S. M. and Kirk, K. 2008. Purine nucleobase transport in the intraerythrocytic malaria parasite. *International Journal for Parasitology*, 38, 203-209.
- Downie, M. J., Saliba, K. J., Howitt, S. M., Bröer, S. and Kirk, K. 2006. Transport of nucleosides across the *Plasmodium falciparum* parasite plasma membrane has characteristics of PfENT1. *Molecular Microbiology*, 60, 738-748.
- Drakeley, C., Sutherland, C., Bousema, J. T., Sauerwein, R. W. and Targett, G. A. 2006. The epidemiology of *Plasmodium falciparum* gametocytes: weapons of mass dispersion. *Trends in Parasitology*, 22, 424-430.
- Duffy, S., Loganathan, S., Holleran, J. P. and Avery, V. M. 2016. Large-scale production of *Plasmodium falciparum* gametocytes for malaria drug discovery. *Nature Protocols*, 11, 976-993.
- Dyer, M., Jackson, M., Mcwhinney, C., Zhao, G. and Mikkelsen, R. 1996. Analysis of a cation-transporting ATPase of *Plasmodium falciparum*. *Molecular and Biochemical Parasitology*, 78, 1-12.
- Eksi, S., Czesny, B., Van Gemert, G. J., Sauerwein, R. W., Eling, W. and Williamson, K. C. 2006. Malaria transmission-blocking antigen, Pfs230, mediates human red blood cell binding to exflagellating male parasites and oocyst production. *Molecular Microbiology*, 61, 991-998.
- Elford, B. C., Haynes, J. D., Chulay, J. D. and Wilson, R. J. 1985. Selective stage-specific changes in the permeability to small hydrophilic solutes of human erythrocytes infected with *Plasmodium falciparum*. *Molecular and Biochemical Parasitology*, 16, 43-60.
- Elliott, D. A., McIntosh, M. T., Hosgood, H. D., Chen, S., Zhang, G., Baevova, P. and Joiner, K. A. 2008. Four distinct pathways of hemoglobin uptake in the malaria parasite *Plasmodium falciparum*. *Proceedings of the National Academy of Sciences*, 105, 2463-2468.
- Elliott, J. L., Saliba, K. J. and Kiaran, K. 2001. Transport of lactate and pyruvate in the intraerythrocytic malaria parasite, *Plasmodium falciparum*. *Biochemical Journal*, 355, 733-739.
- Enayati, A. and Hemingway, J. 2010. Malaria management: past, present, and future. *Annual Review of Entomology*, 55, 569-591.

Ferdig, M. T., Cooper, R. A., Mu, J., Deng, B., Joy, D. A., Su, X. Z. and Wellems, T. E. 2004. Dissecting the loci of low-level quinine resistance in malaria parasites. *Molecular Microbiology*, 52, 985-997.

Fitch, C. D., Chevli, R., Kanjanangulpan, P., Dutta, P., Chevli, K. and Chou, A. C. 1983. Intracellular ferriprotoporphyrin IX is a lytic agent. *Blood*, 62, 1165-1168.

Fitch, C. D. and Kanjanangulpan, P. 1987. The state of ferriprotoporphyrin IX in malaria pigment. *Journal of Biological Chemistry*, 262, 15552-15555.

Florens, L., Washburn, M. P., Raine, J. D., Anthony, R. M., Grainger, M., Haynes, J. D., Moch, J. K., Muster, N., Sacci, J. B. and Tabb, D. L. 2002. A proteomic view of the *Plasmodium falciparum* life cycle. *Nature*, 419, 520-526.

Flueck, C., Bartfai, R., Volz, J., Niederwieser, I., Salcedo-Amaya, A. M., Alako, B. T., Ehlgren, F., Ralph, S. A., Cowman, A. F. and Bozdech, Z. 2009. *Plasmodium falciparum* heterochromatin protein 1 marks genomic loci linked to phenotypic variation of exported virulence factors. *PLOS Pathogens*, 5, e1000569.

Foley, M. and Tilley, L. 1997. Quinoline antimalarials: mechanisms of action and resistance. *International Journal for Parasitology*, 27, 231-240.

Frame, I., Merino, E. F., Schramm, V. L., Cassera, M. B. and Akabas, M. H. 2012. Malaria parasite type 4 equilibrative nucleoside transporters (ENT4) are purine transporters with distinct substrate specificity. *Biochemical Journal*, 446, 179-190.

Francis, S. E., Sullivan Jr, D. J., Goldberg and E, D. 1997. Hemoglobin metabolism in the malaria parasite *Plasmodium falciparum*. *Annual Reviews in Microbiology*, 51, 97-123.

Gardner, M. J., Hall, N., Fung, E., White, O., Berriman, M., Hyman, R. W., Carlton, J. M., Pain, A., Nelson, K. E. and Bowman, S. 2002. Genome sequence of the human malaria parasite *Plasmodium falciparum*. *Nature*, 419, 498-511.

Gene Ontology Consortium 2014. Gene ontology consortium: going forward. *Nucleic Acids Research*, 43, D1049-D1056.

Ginsburg, H. 2006. Progress in *in silico* functional genomics: the malaria Metabolic Pathways database. *Trends in Parasitology*, 22, 238-240.

- Ginsburg, H. 2008. The permeability properties of the parasite cell membrane. *Transport and Trafficking in the Malaria-Infected Erythrocyte*, 798, 99.
- Ginsburg, H. and Krugliak, M. 1983. Uptake of L-tryptophan by erythrocytes infected with malaria parasites (*Plasmodium falciparum*). *Biochimica et Biophysica Acta (BBA)-Biomembranes*, 729, 97-103.
- Ginsburg, H., Kutner, S., Krugliak, M. and Cabantchik, Z. I. 1985. Characterization of permeation pathways appearing in the host membrane of *Plasmodium falciparum* infected red blood cells. *Molecular and Biochemical Parasitology*, 14, 313-322.
- Gregson, A. and Plowe, C. V. 2005. Mechanisms of resistance of malaria parasites to antifolates. *Pharmacological Reviews*, 57, 117-145.
- Gulati, S., Ekland, E. H., Ruggles, K. V., Chan, R. B., Jayabalasingham, B., Zhou, B., Mantel, P.-Y., Lee, M. C., Spottiswoode, N. and Coburn-Flynn, O. 2015. Profiling the essential nature of lipid metabolism in asexual blood and gametocyte stages of *Plasmodium falciparum*. *Cell Host & Microbe*, 18, 371-381.
- Gunasekera, A. M., Patankar, S., Schug, J., Eisen, G. and Wirth, D. F. 2003. Drug-induced alterations in gene expression of the asexual blood forms of *Plasmodium falciparum*. *Molecular Microbiology*, 50, 1229-1239.
- Guttery, D. S., Roques, M., Holder, A. A. and Tewari, R. 2015. Commit and transmit: molecular players in *Plasmodium* sexual development and zygote differentiation. *Trends in Parasitology*, 31, 676-685.
- Hansen, B. D., Sleeman, H. K. and Pappas, P. W. 1980. Purine base and nucleoside uptake in *Plasmodium berghei* and host erythrocytes. *The Journal of Parasitology*, 205-212.
- Hanssen, E., Knoechel, C., Dearnley, M., Dixon, M. W., Le Gros, M., Larabell, C. and Tilley, L. 2012. Soft X-ray microscopy analysis of cell volume and hemoglobin content in erythrocytes infected with asexual and sexual stages of *Plasmodium falciparum*. *Journal of Structural Biology*, 177, 224-232.
- Hartigan, J. A. and Wong, M. A. 1979. Algorithm AS 136: A k-means clustering algorithm. *Journal of the Royal Statistical Society. Series C (Applied Statistics)*, 28, 100-108.

- Hatin, I., Jambou, R., Ginsburg, H. and Jaureguiberry, G. 1992. Single or multiple localization of ADP/ATP transporter in human malarial *Plasmodium falciparum*. *Biochemical Pharmacology*, 43, 71-75.
- Hayashi, M., Yamada, H., Mitamura, T., Horii, T., Yamamoto, A. and Moriyama, Y. 2000. Vacuolar H⁺-ATPase localized in plasma membranes of malaria parasite cells, *Plasmodium falciparum*, is involved in regional acidification of parasitized erythrocytes. *Journal of Biological Chemistry*, 275, 34353-34358.
- Hemingway, J., Shretta, R., Wells, T. N., Bell, D., Djimdé, A. A., Achee, N. and Qi, G. 2016. Tools and Strategies for Malaria Control and Elimination: What Do We Need to Achieve a Grand Convergence in Malaria? *PLOS Biol*, 14, e1002380.
- Henry, R. I., Martin, R. E., Howitt, S. M. and Kirk, K. 2007. Localisation of a candidate anion transporter to the surface of the malaria parasite. *Biochemical and Biophysical Research Communications*, 363, 288-291.
- Herzig, S., Raemy, E., Montessuit, S., Veuthey, J.-L., Zamboni, N., Westermann, B., Kunji, E. R. and Martinou, J.-C. 2012. Identification and functional expression of the mitochondrial pyruvate carrier. *Science*, 337, 93-96.
- Hiller, S. and Wagner, G. 2009. The role of solution NMR in the structure determinations of VDAC-1 and other membrane proteins. *Current Opinion in Structural Biology*, 19, 396-401.
- Huber, S. M., Duranton, C., Henke, G., Van De Sand, C., Heussler, V., Shumilina, E., Sandu, C. D., Tanneur, V., Brand, V. and Kasinathan, R. S. 2004. *Plasmodium* induces swelling-activated ClC-2 anion channels in the host erythrocyte. *Journal of Biological Chemistry*, 279, 41444-41452.
- Jacot, D., Waller, R. F., Soldati-Favre, D., Macpherson, D. A. and Macrae, J. I. 2016. Apicomplexan energy metabolism: carbon source promiscuity and the quiescence hyperbole. *Trends in Parasitology*, 32, 56-70.
- Janse, C., Ponnudurai, T., Lensen, A., Meuwissen, J. T., Ramesar, J., Van Der Ploeg, M. and Overdulve, J. 1988. DNA synthesis in gametocytes of *Plasmodium falciparum*. *Parasitology*, 96, 1-7.
- Jensen, M. D., Conley, M. and Helstowski, L. D. 1983. Culture of *Plasmodium falciparum*: the role of pH, glucose, and lactate. *The Journal of Parasitology*, 1060-1067.

Jiang, H., Patel, J. J., Yi, M., Mu, J., Ding, J., Stephens, R., Cooper, R. A., Ferdig, M. T. and Su, X.-Z. 2008. Genome-wide compensatory changes accompany drug-selected mutations in the *Plasmodium falciparum* crt gene. PLOS One, 3, e2484.

Jiménez-Díaz, M. B., Ebert, D., Salinas, Y., Pradhan, A., Lehane, A. M., Myrand-Lapierre, M.-E., O'loughlin, K. G., Shackleford, D. M., De Almeida, M. J. and Carrillo, A. K. 2014. (+)-SJ733, a clinical candidate for malaria that acts through ATP4 to induce rapid host-mediated clearance of *Plasmodium*. Proceedings of the National Academy of Sciences, 111, E5455-E5462.

Joet, T., Morin, C., Fischbarg, J., Louw, A. I., Eckstein-Ludwig, U., Woodrow, C. and Krishna, S. 2003. Why is the *Plasmodium falciparum* hexose transporter a promising new drug target? Expert Opinion on Therapeutic Targets, 7, 593-602.

Jongwutiwes, S., Putaporntip, C., Iwasaki, T., Sata, T. and Kanbara, H. 2004. Naturally acquired *Plasmodium knowlesi* malaria in human, Thailand. Emerging Infectious Diseases, 10, 2211-2213.

Kanaani, J. and Ginsburg, H. 1989. Metabolic interconnection between the human malarial parasite *Plasmodium falciparum* and its host erythrocyte. Regulation of ATP levels by means of an adenylate translocator and adenylate kinase. Journal of Biological Chemistry, 264, 3194-3199.

Kanaani, J. and Ginsburg, H. 1991. Transport of lactate in *Plasmodium falciparum*-infected human erythrocytes. Journal of Cellular Physiology, 149, 469-476.

Kanehisa, M. and Goto, S. 2000. KEGG: kyoto encyclopedia of genes and genomes. Nucleic Acids Research, 28, 27-30.

Kavishe, R. A., Van Den Heuvel, J. M., Van De Vegte-Bolmer, M., Luty, A. J., Russel, F. G. and Koenderink, J. B. 2009. Localization of the ATP-binding cassette (ABC) transport proteins PfMRP1, PfMRP2, and PfMDR5 at the *Plasmodium falciparum* plasma membrane. Malaria Journal, 8, 205.

Kelly-Hope, L., Ranson, H. and Hemingway, J. 2008. Lessons from the past: managing insecticide resistance in malaria control and eradication programmes. The Lancet Infectious Diseases, 8, 387-389.

Kenthirapalan, S., Waters, A. P., Matuschewski, K. and Kooij, T. W. 2016. Functional profiles of orphan membrane transporters in the life cycle of the malaria parasite. Nature Communications, 7, 10519.

- Kirk, K. 2001. Membrane transport in the malaria-infected erythrocyte. *Physiological Reviews*, 81, 495-537.
- Kirk, K. 2015. Ion Regulation in the Malaria Parasite. *Annual Review of Microbiology*, 69, 341-359.
- Kirk, K., Ashworth, K. J., Elford, B. C., Pinches, R. A. and Ellory, J. C. 1991a. Characteristics of 86Rb^+ transport in human erythrocytes infected with *Plasmodium falciparum*. *Biochimica et Biophysica Acta (BBA)-Biomembranes*, 1061, 305-308.
- Kirk, K. and Horner, H. A. 1995. In search of a selective inhibitor of the induced transport of small solutes in *Plasmodium falciparum*-infected erythrocytes: effects of arylaminobenzoates. *Biochemical Journal*, 311, 761-768.
- Kirk, K., Horner, H. A., Elford, B. C., Ellory, J. C. and Newbold, C. I. 1994. Transport of diverse substrates into malaria-infected erythrocytes via a pathway showing functional characteristics of a chloride channel. *Journal of Biological Chemistry*, 269, 3339-3347.
- Kirk, K., Horner, H. A. and Kirk, J. 1996. Glucose uptake in *Plasmodium falciparum*-infected erythrocytes is an equilibrative not an active process. *Molecular and Biochemical Parasitology*, 82, 195-205.
- Kirk, K. and Lehane, A. M. 2014. Membrane transport in the malaria parasite and its host erythrocyte. *Biochemical Journal*, 457, 1-18.
- Kirk, K. and Saliba, K. J. 2007. Targeting nutrient uptake mechanisms in *Plasmodium*. *Current Drug Targets*, 8, 75-88.
- Kirk, K., Wong, H., Elford, B., Newbold, C. and Ellory, J. 1991b. Enhanced choline and Rb^+ transport in human erythrocytes infected with the malaria parasite *Plasmodium falciparum*. *Biochemical Journal*, 278, 521-525.
- Klokouzas, A., Tiffert, T., Van Schalkwyk, D., Wu, C.-P., Van Veen, H. W., Barrand, M. A. and Hladky, S. B. 2004. *Plasmodium falciparum* expresses a multidrug resistance-associated protein. *Biochemical and Biophysical Research Communications*, 321, 197-201.
- Köhler, S., Delwiche, C. F., Denny, P. W., Tilney, L. G., Webster, P., Wilson, R., Palmer, J. D. and Roos, D. S. 1997. A plastid of probable green algal origin in Apicomplexan parasites. *Science*, 275, 1485-1489.

- Krishna, S., Cowan, G., Meade, J. C., Wells, R. A., Stringer, J. R. and Robson, K. J. 1993. A family of cation ATPase-like molecules from *Plasmodium falciparum*. *The Journal of Cell Biology*, 120, 385-398.
- Krishna, S., Woodrow, C., Burchmore, R., Saliba, K. and Kirk, K. 2000. Hexose transport in asexual stages of *Plasmodium falciparum* and kinetoplastidae. *Parasitology Today*, 16, 516-521.
- Krishna, S., Woodrow, C., Webb, R., Penny, J., Takeyasu, K., Kimura, M. and East, J. M. 2001. Expression and functional characterization of a *Plasmodium falciparum* Ca²⁺-ATPase (PfATP4) belonging to a subclass unique to apicomplexan organisms. *Journal of Biological Chemistry*, 276, 10782-10787.
- Krogh, A., Larsson, B., Von Heijne, G. and Sonnhammer, E. L. 2001. Predicting transmembrane protein topology with a hidden Markov model: application to complete genomes. *Journal of Molecular Biology*, 305, 567-580.
- Krugliak, M. and Ginsburg, H. 2006. The evolution of the new permeability pathways in *Plasmodium falciparum*—infected erythrocytes—a kinetic analysis. *Experimental Parasitology*, 114, 253-258.
- Krugliak, M., Zhang, J. and Ginsburg, H. 2002. Intraerythrocytic *Plasmodium falciparum* utilizes only a fraction of the amino acids derived from the digestion of host cell cytosol for the biosynthesis of its proteins. *Molecular and Biochemical Parasitology*, 119, 249-256.
- Kuhn, Y., Sanchez, C. P., Ayoub, D., Saridaki, T., Van Dorsselaer, A. and Lanzer, M. 2010. Trafficking of the phosphoprotein PfCRT to the digestive vacuolar membrane in *Plasmodium falciparum*. *Traffic*, 11, 236-249.
- Kyte, J. and Doolittle, R. F. 1982. A simple method for displaying the hydropathic character of a protein. *Journal of Molecular Biology*, 157, 105-132.
- Lagerberg, R. E. 2008. Malaria in pregnancy: a literature review. *Journal of Midwifery & Women's Health*, 53, 209-215.
- Lambros, C. and Vanderberg, J. P. 1979. Synchronization of *Plasmodium falciparum* erythrocytic stages in culture. *The Journal of Parasitology*, 418-420.
- Lamour, S. D., Straschil, U., Saric, J. and Delves, M. J. 2014. Changes in metabolic phenotypes of *Plasmodium falciparum* *in vitro* cultures during gametocyte development. *Malaria Journal*, 13, 1-10.

Lasonder, E., Ishihama, Y., Andersen, J. S., Vermunt, A. M., Pain, A., Sauerwein, R. W., Eling, W. M., Hall, N., Waters, A. P. and Stunnenberg, H. G. 2002. Analysis of the *Plasmodium falciparum* proteome by high-accuracy mass spectrometry. *Nature*, 419, 537-542.

Lasonder, E., Rijpma, S. R., Van Schaijk, B. C., Hoeijmakers, W. A., Kensche, P. R., Gresnigt, M. S., Italiaander, A., Vos, M. W., Woestenenk, R. and Bousema, T. 2016. Integrated transcriptomic and proteomic analyses of *P. falciparum* gametocytes: molecular insight into sex-specific processes and translational repression. *Nucleic Acids Research*, 44, 6087-6101.

Lauer, S. A., Rathod, P. K., Ghori, N. and Haldar, K. 1997. A membrane network for nutrient import in red cells infected with the malaria parasite. *Science*, 276, 1122-1125.

Le Roch, K. G., Johnson, J. R., Florens, L., Zhou, Y., Santrosyan, A., Grainger, M., Yan, S. F., Williamson, K. C., Holder, A. A. and Carucci, D. J. 2004. Global analysis of transcript and protein levels across the *Plasmodium falciparum* life cycle. *Genome research*, 14, 2308-2318.

Lew, V. L., Macdonald, L., Ginsburg, H., Krugliak, M. and Tiffert, T. 2004. Excess haemoglobin digestion by malaria parasites: a strategy to prevent premature host cell lysis. *Blood Cells, Molecules, and Diseases*, 32, 353-359.

Lian, L.-Y., Al-Helal, M., Roslani, A. M., Fisher, N., Bray, P. G., Ward, S. A. and Biagini, G. A. 2009. Glycerol: an unexpected major metabolite of energy metabolism by the human malaria parasite. *Malaria Journal*, 8, 1-4.

Lim, L. and Mcfadden, G. I. 2010. The evolution, metabolism and functions of the apicoplast. *Philosophical Transactions of the Royal Society B: Biological Sciences*, 365, 749-763.

Lim, L., Sayers, C. P., Goodman, C. D. and Mcfadden, G. I. 2016. Targeting of a transporter to the outer apicoplast membrane in the human malaria parasite *Plasmodium falciparum*. *PLOS One*, 11, e0159603.

Liu, J., Istvan, E. S., Gluzman, I. Y., Gross, J. and Goldberg, D. E. 2006. *Plasmodium falciparum* ensures its amino acid supply with multiple acquisition pathways and redundant proteolytic enzyme systems. *Proceedings of the National Academy of Sciences*, 103, 8840-8845.

Liu, Y., Promeneur, D., Rojek, A., Kumar, N., Frøkiær, J., Nielsen, S., King, L. S., Agre, P. and Carbrey, J. M. 2007. Aquaporin 9 is the major pathway for glycerol uptake by mouse erythrocytes, with implications for malarial virulence. *Proceedings of the National Academy of Sciences*, 104, 12560-12564.

- Lodish, H., Berk, A., Kaiser, C. A., Krieger, M., Bretscher, A., Ploegh, H., Amon, A. and Martin, K. C. 2016. *Molecular Cell Biology*, W. H. Freeman.
- Lodish, H., Berk, A., Zipursky, S. L., Matsudaira, P., Baltimore, D. and Darnell, J. 2000. *Molecular Cell Biology*, New York, W. H. Freeman and Company.
- Lodish, H., Kaiser, C. A., Bretscher, A., Amon, A., Berk, A., Krieger, M., Ploegh, H. and Scott, M. P. 2013. *Molecular Cell Biology*, New York, Scientific American Books.
- Luo, S., Marchesini, N., Moreno, S. N. and Docampo, R. 1999. A plant-like vacuolar H⁺-pyrophosphatase in *Plasmodium falciparum*. *FEBS Letters*, 460, 217-220.
- Mackinnon, R. 1995. Pore loops: an emerging theme in ion channel structure. *Neuron*, 14, 889-892.
- Macrae, J. I., Dixon, M. W., Dearnley, M. K., Chua, H. H., Chambers, J. M., Kenny, S., Bottova, I., Tilley, L. and Mcconville, M. J. 2013. Mitochondrial metabolism of sexual and asexual blood stages of the malaria parasite *Plasmodium falciparum*. *BMC Biology*, 11, 1.
- Makowski, G. S. 2017. *Advances in clinical chemistry*, United States, Academic Press.
- Malera, C. G. O. V. C. 2011. A research agenda for malaria eradication: vector control. *PLOS Med*, 8, e1000401.
- Marchesini, N., Shuhong, L., Rodrigues, C. O., Moreno, S. N. and Docampo, R. 2000. Acidocalcisomes and a vacuolar H⁺-pyrophosphatase in malaria parasites. *Biochemical Journal*, 347, 243-253.
- Marchesini, N., Vieira, M., Luo, S., Moreno, S. N. and Docampo, R. 2005. A malaria parasite-encoded vacuolar H⁺-ATPase is targeted to the host erythrocyte. *Journal of Biological Chemistry*, 280, 36841-36847.
- Marchetti, R. V., Lehane, A. M., Shafik, S. H., Winterberg, M., Martin, R. E. and Kirk, K. 2015. A lactate and formate transporter in the intraerythrocytic malaria parasite, *Plasmodium falciparum*. *Nature Communications*, 6, ncomms7721.
- Marcus, B. and Babcock, H. 2009. *Malaria, (Deadly Diseases and Epidemics)*, New York, Chelsea House.

- Martin, R. E., Ginsburg, H. and Kirk, K. 2009. Membrane transport proteins of the malaria parasite. *Molecular Microbiology*, 74, 519-528.
- Martin, R. E., Henry, R. I., Abbey, J. L., Clements, J. D. and Kirk, K. 2005. The 'permeome' of the malaria parasite: an overview of the membrane transport proteins of *Plasmodium falciparum*. *Genome Biology*, 6, R26.
- Martin, R. E. and Kirk, K. 2004. The malaria parasite's chloroquine resistance transporter is a member of the drug/metabolite transporter superfamily. *Molecular Biology and Evolution*, 21, 1938-1949.
- Martin, R. E. and Kirk, K. 2007. Transport of the essential nutrient isoleucine in human erythrocytes infected with the malaria parasite *Plasmodium falciparum*. *Blood*, 109, 2217-2224.
- Maurois, P., Gueux, E. and Rayssiguier, Y. 1989. Protective effect of severe magnesium deficiency on *Plasmodium chabaudi* infection. *Magnesium Research: Official Organ of the International Society for the Development of Research on Magnesium*, 2, 183-187.
- McIntosh, M. T., Drozdowicz, Y. M., Laroia, K., Rea, P. A. and Vaidya, A. B. 2001. Two classes of plant-like vacuolar-type H⁺-pyrophosphatases in malaria parasites. *Molecular and Biochemical Parasitology*, 114, 183-195.
- McIntosh, M. T. and Vaidya, A. B. 2002. Vacuolar type H⁺ pumping pyrophosphatases of parasitic protozoa. *International Journal for Parasitology*, 32, 1-14.
- Meibalan, E. and Marti, M. 2017. Biology of malaria transmission. *Cold Spring Harbor Perspectives in Medicine*, 7, a025452.
- Meier, A., Erler, H. and Beitz, E. 2018. Targeting channels and transporters in protozoan parasite infections. *Frontiers in Chemistry*, 6, 88.
- Mi-Ichi, F., Kita, K. and Mitamura, T. 2006. Intraerythrocytic *Plasmodium falciparum* utilize a broad range of serum-derived fatty acids with limited modification for their growth. *Parasitology*, 133, 399-410.
- Miller, L. H., Baruch, D. I., Marsh, K. and Doumbo, O. K. 2002. The pathogenic basis of malaria. *Nature*, 415, 673-679.

- Miranda, K., De Souza, W., Plattner, H., Hentschel, J., Kawazoe, U., Fang, J. and Moreno, S. N. 2008. Acidocalcisomes in Apicomplexan parasites. *Experimental Parasitology*, 118, 2-9.
- Mullin, K. A., Lim, L., Ralph, S. A., Spurck, T. P., Handman, E. and Mcfadden, G. I. 2006. Membrane transporters in the relict plastid of malaria parasites. *Proceedings of the National Academy of Sciences*, 103, 9572-9577.
- Nájera, J. A., González-Silva, M. and Alonso, P. L. 2011. Some lessons for the future from the Global Malaria Eradication Programme (1955–1969). *PLOS Medicine*, 8, e1000412.
- Nguitragool, W., Bokhari, A. A., Pillai, A. D., Rayavara, K., Sharma, P., Turpin, B., Aravind, L. and Desai, S. A. 2011. Malaria parasite *clag3* genes determine channel-mediated nutrient uptake by infected red blood cells. *Cell*, 145, 665-677.
- Nina, P. B., Morrissey, J. M., Ganesan, S. M., Ke, H., Pershing, A. M., Mather, M. W. and Vaidya, A. B. 2011. ATP Synthase Complex of *Plasmodium falciparum* dimeric assembly in mitochondrial membranes and resistance to genetic disruption. *Journal of Biological Chemistry*, 286, 41312-41322.
- Noedl, H., Se, Y., Sriwichai, S., Schaecher, K., Teja-Isavadharm, P., Smith, B., Rutvisuttinunt, W., Bethell, D., Surasri, S. and Fukuda, M. M. 2010. Artemisinin resistance in Cambodia: a clinical trial designed to address an emerging problem in Southeast Asia. *Clinical Infectious Diseases*, 51, e82-e89.
- Nozawa, A., Fujimoto, R., Matsuoka, H., Tsuboi, T. and Tozawa, Y. 2011. Cell-free synthesis, reconstitution, and characterization of a mitochondrial dicarboxylate–tricarboxylate carrier of *Plasmodium falciparum*. *Biochemical and Biophysical Research Communications*, 414, 612-617.
- Olszewski, K. L. and Llinás, M. 2011. Central carbon metabolism of *Plasmodium* parasites. *Molecular and Biochemical Parasitology*, 175, 95-103.
- Olszewski, K. L., Morrissey, J. M., Wilinski, D., Burns, J. M., Vaidya, A. B., Rabinowitz, J. D. and Llinás, M. 2009. Host-parasite interactions revealed by *Plasmodium falciparum* metabolomics. *Cell Host & Microbe*, 5, 191-199.
- Oppenheim, R. D., Creek, D. J., Macrae, J. I., Modrzynska, K. K., Pino, P., Limenitakis, J., Polonais, V., Seeber, F., Barrett, M. P. and Billker, O. 2014. BCKDH: the missing link in apicomplexan mitochondrial metabolism is required for full virulence of *Toxoplasma gondii* and *Plasmodium berghei*. *PLOS Pathogens*, 10, e1004263.

Otto, T. D., Wilinski, D., Assefa, S., Keane, T. M., Sarry, L. R., Böhme, U., Lemieux, J., Barrell, B., Pain, A. and Berriman, M. 2010. New insights into the blood-stage transcriptome of *Plasmodium falciparum* using RNA-Seq. *Molecular Microbiology*, 76, 12-24.

Overington, J. P., Al-Lazikani, B. and Hopkins, A. L. 2006. How many drug targets are there? *Nature Reviews Drug Discovery*, 5, 993-996.

Painter, H. J., Carrasquilla, M. and Llinás, M. 2017. Capturing *in vivo* RNA transcriptional dynamics from the malaria parasite *P. falciparum*. *Genome Research*, 099549.

Palacpac, N. M. Q., Hiramine, Y., Mi-Ichi, F., Torii, M., Kita, K., Hiramatsu, R., Horii, T. and Mitamura, T. 2004. Developmental-stage-specific triacylglycerol biosynthesis, degradation and trafficking as lipid bodies in *Plasmodium falciparum*-infected erythrocytes. *Journal of Cell Science*, 117, 1469-1480.

Pavlovic-Djuranovic, S., Kun, J. F., Schultz, J. E. and Beitz, E. 2006. Dihydroxyacetone and methylglyoxal as permeants of the *Plasmodium* aquaglyceroporin inhibit parasite proliferation. *Biochimica et Biophysica Acta (BBA)-Biomembranes*, 1758, 1012-1017.

Penny, J. I., Hall, S. T., Woodrow, C. J., Cowan, G. M., Gero, A. M. and Krishna, S. 1998. Expression of substrate-specific transporters encoded by *Plasmodium falciparum* in *Xenopus laevis* oocytes. *Molecular and Biochemical Parasitology*, 93, 81-89.

Pessi, G., Kociubinski, G. and Mamoun, C. B. 2004. A pathway for phosphatidylcholine biosynthesis in *Plasmodium falciparum* involving phosphoethanolamine methylation. *Proceedings of the National Academy of Sciences of the United States of America*, 101, 6206-6211.

Pillai, A. D., Addo, R., Sharma, P., Nguitragool, W., Srinivasan, P. and Desai, S. A. 2013. Malaria parasites tolerate a broad range of ionic environments and do not require host cation remodelling. *Molecular Microbiology*, 88, 20-34.

Pillai, A. D., Nguitragool, W., Lyko, B., Dolinta, K., Butler, M. M., Nguyen, S. T., Peet, N. P., Bowlin, T. L. and Desai, S. A. 2012. Solute restriction reveals an essential role for clag3-associated channels in malaria parasite nutrient acquisition. *Molecular Pharmacology*, 82, 1104-1114.

Poole, R. C. and Halestrap, A. P. 1993. Transport of lactate and other monocarboxylates across mammalian plasma membranes. *American Journal of Physiology-Cell Physiology*, 264, C761-C782.

Quashie, N. B., Ranford-Cartwright, L. C. and De Koning, H. P. 2010. Uptake of purines in *Plasmodium falciparum*-infected human erythrocytes is mostly mediated by the human equilibrative nucleoside transporter and the human facilitative nucleobase transporter. *Malaria Journal*, 9, 1-10.

Raabe, A. C., Billker, O., Vial, H. J. and Wengelnik, K. 2009. Quantitative assessment of DNA replication to monitor microgametogenesis in *Plasmodium berghei*. *Molecular and Biochemical Parasitology*, 168, 172-176.

Rager, N., Mamoun, C. B., Carter, N. S., Goldberg, D. E. and Ullman, B. 2001. Localization of the *Plasmodium falciparum* PfNT1 Nucleoside Transporter to the Parasite Plasma Membrane. *Journal of Biological Chemistry*, 276, 41095-41099.

Raibaud, A., Lupetti, P., Paul, R. E., Mercati, D., Brey, P. T., Sinden, R. E., Heuser, J. E. and Dallai, R. 2001. Cryofracture electron microscopy of the ookinete pellicle of *Plasmodium gallinaceum* reveals the existence of novel pores in the alveolar membranes. *Journal of Structural Biology*, 135, 47-57.

Raj, D. K., Mu, J., Jiang, H., Kabat, J., Singh, S., Sullivan, M., Fay, M. P., Mccutchan, T. F. and Su, X. Z. 2009. Disruption of a *Plasmodium falciparum* multidrug resistance-associated protein (PfMRP) alters its fitness and transport of antimalarial drugs and glutathione. *Journal of Biological Chemistry*, 284, 7687-7696.

Rajendran, E., Hapuarachchi, S. V., Miller, C. M., Fairweather, S. J., Cai, Y., Smith, N. C., Cockburn, I. A., Bröer, S., Kirk, K. and Van Dooren, G. G. 2017. Cationic amino acid transporters play key roles in the survival and transmission of apicomplexan parasites. *Nature Communications*, 8.

Ralph, S. A., Van Dooren, G. G., Waller, R. F., Crawford, M. J., Fraunholz, M. J., Foth, B. J., Tonkin, C. J., Roos, D. S. and Mcfadden, G. I. 2004. Metabolic maps and functions of the *Plasmodium falciparum* apicoplast. *Nature Reviews Microbiology*, 2, 203.

Ranson, H., Abdallah, H., Badolo, A., Guelbeogo, W. M., Kerah-Hinzoumbé, C., Yangalbé-Kalnoné, E., Sagnon, N. F., Simard, F. and Coetzee, M. 2009. Insecticide resistance in *Anopheles gambiae*: data from the first year of a multi-country study highlight the extent of the problem. *Malaria Journal*, 8, 299.

Rasoloson, D., Lirong, S., Chong, C. R., Kafsack, B. F. and Sullivan, D. J. 2004. Copper pathways in *Plasmodium falciparum* infected erythrocytes indicate an efflux role for the copper P-ATPase. *Biochemical Journal*, 381, 803-811.

Reader, J., Botha, M., Theron, A., Lauterbach, S. B., Rossouw, C., Engelbrecht, D., Wepener, M., Smit, A., Leroy, D. and Mancama, D. 2015. Nowhere to hide: interrogating different metabolic parameters of *Plasmodium falciparum* gametocytes in a transmission blocking drug discovery pipeline towards malaria elimination. *Malaria Journal*, 14, 213.

Reed, M. B., Saliba, K. J., Caruana, S. R., Kirk, K. and Cowman, A. F. 2000. Pgh1 modulates sensitivity and resistance to multiple antimalarials in *Plasmodium falciparum*. *Nature*, 403, 906-909.

Ren, Q., Chen, K. and Paulsen, I. T. 2007. TransportDB: a comprehensive database resource for cytoplasmic membrane transport systems and outer membrane channels. *Nucleic Acids Research*, 35, D274-D279.

Ribbeck, K., Lipowsky, G., Kent, H. M., Stewart, M. and Görlich, D. 1998. NTF2 mediates nuclear import of Ran. *The EMBO Journal*, 17, 6587-6598.

Rodrigo, C., Rajapakse, S. and Fernando, S. D. 2016. Primaquine or tafenoquine for preventing malaria in people travelling to or living in endemic areas. *The Cochrane Library*.

Roth, E. 1989. *Plasmodium falciparum* carbohydrate metabolism: a connection between host cell and parasite. *Blood Cells*, 16, 453-60; discussion 461-6.

Roth, E., Calvin, M.-C., Max-Audit, I., Rosa, J. and Rosa, R. 1988. The enzymes of the glycolytic pathway in erythrocytes infected with *Plasmodium falciparum* malaria parasites. *Blood*, 72, 1922-1925.

Rotmann, A., Sanchez, C., Guiguemde, A., Rohrbach, P., Dave, A., Bakouh, N., Planelles, G. and Lanzer, M. 2010. PfCHA is a mitochondrial divalent cation/H⁺ antiporter in *Plasmodium falciparum*. *Molecular microbiology*, 76, 1591-1606.

Rottmann, M., Mcnamara, C., Yeung, B. K., Lee, M. C., Zou, B., Russell, B., Seitz, P., Plouffe, D. M., Dharia, N. V. and Tan, J. 2010. Spiroindolones, a potent compound class for the treatment of malaria. *Science*, 329, 1175-1180.

Saeed, A., Sharov, V., White, J., Li, J., Liang, W., Bhagabati, N., Braisted, J., Klapa, M., Currier, T. and Thiagarajan, M. 2003. TM4: a free, open-source system for microarray data management and analysis. *Biotechniques*, 34, 374.

Saier, M. H., Reddy, V. S., Tsu, B. V., Ahmed, M. S., Li, C. and Moreno-Hagelsieb, G. 2016. The Transporter Classification Database (TCDB): recent advances. *Nucleic Acids Research*, 44, D372-D379.

Saifi, M. A., Beg, T., Harrath, A. H., Altayalan, F. S. H. and Al Quraishy, S. 2013. Antimalarial drugs: Mode of action and status of resistance. *African Journal of Pharmacy and Pharmacology*, 7, 148-156.

Salcedo-Sora, J. E., Caamano-Gutierrez, E., Ward, S. A. and Biagini, G. A. 2014. The proliferating cell hypothesis: a metabolic framework for *Plasmodium* growth and development. *Trends in Parasitology*, 30, 170-175.

Salcedo-Sora, J. E., Ochong, E., Beveridge, S., Johnson, D., Nzila, A., Biagini, G. A., Stocks, P. A., O'Neill, P. M., Krishna, S. and Bray, P. G. 2011. The molecular basis of folate salvage in *Plasmodium falciparum* characterization of two folate transporters. *Journal of Biological Chemistry*, 286, 44659-44668.

Saliba, K. J., Horner, H. A. and Kirk, K. 1998. Transport and Metabolism of the Essential Vitamin Pantothenic Acid in Human Erythrocytes Infected with the Malaria Parasite *Plasmodium falciparum*. *Journal of Biological Chemistry*, 273, 10190-10195.

Saliba, K. J. and Kirk, K. 2001. H⁺-coupled pantothenate transport in the intracellular malaria parasite. *Journal of Biological Chemistry*, 276, 18115-18121.

Saliba, K. J., Krishna, S. and Kirk, K. 2004. Inhibition of hexose transport and abrogation of pH homeostasis in the intraerythrocytic malaria parasite by an O-3-hexose derivative. *FEBS letters*, 570, 93-96.

Saliba, K. J., Martin, R. E., Bröer, A., Henry, R. I., Mccarthy, C. S., Downie, M. J., Allen, R. J., Mullin, K. A., Mcfadden, G. I. and Bröer, S. 2006. Sodium-dependent uptake of inorganic phosphate by the intracellular malaria parasite. *Nature*, 443, 582-585.

Sana, T. R., Gordon, D. B., Fischer, S. M., Tichy, S. E., Kitagawa, N., Lai, C., Gosnell, W. L. and Chang, S. P. 2013. Global mass spectrometry based metabolomics profiling of erythrocytes infected with *Plasmodium falciparum*. *PLOS One*, 8, e60840.

Sanchez, C. P., Dave, A., Stein, W. D. and Lanzer, M. 2010. Transporters as mediators of drug resistance in *Plasmodium falciparum*. *International Journal for Parasitology*, 40, 1109-1118.

- Sanderson, T. and Rayner, J. C. 2017. PhenoPlasm: a database of disruption phenotypes for malaria parasite genes. Wellcome Open Research, 2.
- Sayers, C. P., Mollard, V., Buchanan, H. D., Mcfadden, G. I. and Goodman, C. D. 2018. A genetic screen in rodent malaria parasites identifies five new apicoplast putative membrane transporters, one of which is essential in human malaria parasites. *Cellular Microbiology*, 20.
- Schwab, J., Beckers, C. J. and Joiner, K. 1994. The parasitophorous vacuole membrane surrounding intracellular *Toxoplasma gondii* functions as a molecular sieve. *Proceedings of the National Academy of Sciences*, 91, 509-513.
- Schwach, F., Bushell, E., Gomes, A. R., Anar, B., Girling, G., Herd, C., Rayner, J. C. and Billker, O. 2015. Plasmo GEM, a database supporting a community resource for large-scale experimental genetics in malaria parasites. *Nucleic Acids Research*, 43, D1176-D1182.
- Sherman, I. 1977. Transport of amino acids and nucleic acid precursors in malarial parasites. *Bulletin of the World Health Organization*, 55, 211.
- Sherman, I. W. 1979. Biochemistry of *Plasmodium* (malarial parasites). *Microbiological reviews*, 43, 453.
- Shoemaker, D. G., Bender, C. A. and Gunn, R. B. 1988. Sodium-phosphate cotransport in human red blood cells. Kinetics and role in membrane metabolism. *The Journal of General Physiology*, 92, 449-474.
- Shortt, H. E., Fairley, N. H., Covell, G., Shute, P. and Garnham, P. 1949. Pre-erythrocytic stage of *Plasmodium falciparum*. *British Medical Journal*, 2, 1006.
- Shute, P. 1960. Quiescent Malaria Parasites. *British Medical Journal*, 1, 730.
- Sidhu, A. B. S., Verdier-Pinard, D. and Fidock, D. A. 2002. Chloroquine resistance in *Plasmodium falciparum* malaria parasites conferred by pfcrt mutations. *Science*, 298, 210-213.
- Silvestrini, F., Alano, P. and Williams, J. 2000. Commitment to the production of male and female gametocytes in the human malaria parasite *Plasmodium falciparum*. *Parasitology*, 121, 465-471.
- Sinden, R. 1982. Gametocytogenesis of *Plasmodium falciparum in vitro*: an electron microscopic study. *Parasitology*, 84, 1-11.

- Sinden, R. and Smalley, M. 1979. Gametocytogenesis of *Plasmodium falciparum* *in vitro*: the cell-cycle. *Parasitology*, 79, 277-296.
- Slavic, K., Delves, M. J., Prudêncio, M., Talman, A. M., Straschil, U., Derbyshire, E. T., Xu, Z., Sinden, R. E., Mota, M. M. and Morin, C. 2011. Use of a selective inhibitor to define the chemotherapeutic potential of the *plasmodial* hexose transporter in different stages of the parasite's life cycle. *Antimicrobial Agents and Chemotherapy*, 55, 2824-2830.
- Slavic, K., Straschil, U., Reininger, L., Doerig, C., Morin, C., Tewari, R. and Krishna, S. 2010. Life cycle studies of the hexose transporter of *Plasmodium* species and genetic validation of their essentiality. *Molecular Microbiology*, 75, 1402-1413.
- Smith, R. C., Vega-Rodríguez, J. and Jacobs-Lorena, M. 2014. The *Plasmodium* bottleneck: malaria parasite losses in the mosquito vector. *Memorias Do Instituto Oswaldo Cruz*, 109, 644-661.
- Smith, T., Lourenco, P., Carter, R., Walliker, D. and Ranford-Cartwright, L. 2000. Commitment to sexual differentiation in the human malaria parasite, *Plasmodium falciparum*. *Parasitology*, 121, 127-133.
- Sonnhammer, E. L., Von Heijne, G. and Krogh, A. 1998. A hidden Markov model for predicting transmembrane helices in protein sequences. *Intelligent Systems for Molecular Biology*, 6, 175-182.
- Spillman, N. J., Allen, R. J. and Kirk, K. 2013a. Na⁺ extrusion imposes an acid load on the intraerythrocytic malaria parasite. *Molecular and Biochemical Parasitology*, 189, 1-4.
- Spillman, N. J., Allen, R. J., Mcnamara, C. W., Yeung, B. K., Winzeler, E. A., Diagona, T. T. and Kirk, K. 2013b. Na⁺ regulation in the malaria parasite *Plasmodium falciparum* involves the cation ATPase PfATP4 and is a target of the spiroindolone antimalarials. *Cell Host & Microbe*, 13, 227-237.
- Staines, H. M., Derbyshire, E. T., Slavic, K., Tattersall, A., Vial, H. and Krishna, S. 2010. Exploiting the therapeutic potential of *Plasmodium falciparum* solute transporters. *Trends in Parasitology*, 26, 284-296.
- Staines, H. M., Ellory, J. C. and Kirk, K. 2001. Perturbation of the pump-leak balance for Na⁺ and K⁺ in malaria-infected erythrocytes. *American Journal of Physiology-Cell Physiology*, 280, C1576-C1587.

- Talman, A. M., Domarle, O., Mckenzie, F. E., Arie, F. and Robert, V. 2004. Gametocytogenesis: the puberty of *Plasmodium falciparum*. *Malaria Journal*, 3, 24.
- Teng, R., Junankar, P. R., Bubb, W. A., Rae, C., Mercier, P. and Kirk, K. 2009. Metabolite profiling of the intraerythrocytic malaria parasite *Plasmodium falciparum* by ¹H NMR spectroscopy. *NMR in Biomedicine*, 22, 292-302.
- Theander, T. G. and Lusingu, J. P. A. 2015. Efficacy and safety of RTS, S/AS01 malaria vaccine with or without a booster dose in infants and children in Africa: final results of a phase 3, individually randomised, controlled trial. *The Lancet*, 386, 31-45.
- Tibshirani, R., Walther, G. and Hastie, T. 2001. Estimating the number of clusters in a data set via the gap statistic. *Journal of the Royal Statistical Society: Series B (Statistical Methodology)*, 63, 411-423.
- Touré, Y. Malaria Vector Control in Africa: Strategies and Challenges. Report from a symposium held at the 2001 American Association for the Advancement of Science Annual Meeting, 2001 San Francisco.
- Tran, P. N., Brown, S. H., Mitchell, T. W., Matuschewski, K., Mcmillan, P. J., Kirk, K., Dixon, M. W. and Maier, A. G. 2014. A female gametocyte-specific ABC transporter plays a role in lipid metabolism in the malaria parasite. *Nature Communications*, 5.
- Trang, D. T., Huy, N. T., Kariu, T., Tajima, K. and Kamei, K. 2004. One-step concentration of malarial parasite-infected red blood cells and removal of contaminating white blood cells. *Malaria Journal*, 3, 7.
- Tuteja, R. and Mehta, J. 2010. A genomic glance at the components of the mRNA export machinery in *Plasmodium falciparum*. *Communicative & Integrative Biology*, 3, 318-326.
- Upston, J. M. and Gero, A. M. 1995. Parasite-induced permeation of nucleosides in *Plasmodium falciparum* malaria. *Biochimica et Biophysica Acta (BBA)-Biomembranes*, 1236, 249-258.
- Van Dooren, G. G., Stimmler, L. M. and Mcfadden, G. I. 2006. Metabolic maps and functions of the *Plasmodium* mitochondrion. *FEMS Microbiology Reviews*, 30, 596-630.
- Van Pelt-Koops, J., Pett, H., Graumans, W., Van Der Vegte-Bolmer, M., Van Gemert, G., Rottmann, M., Yeung, B., Diagana, T. and Sauerwein, R. 2012. The spiroindolone drug candidate

NITD609 potently inhibits gametocytogenesis and blocks *Plasmodium falciparum* transmission to *Anopheles* mosquito vector. *Antimicrobial Agents and Chemotherapy*, 56, 3544-3548.

Van Schaijk, B. C., Kumar, T. S., Vos, M. W., Richman, A., Van Gemert, G.-J., Li, T., Eappen, A. G., Williamson, K. C., Morahan, B. J. and Fishbaugher, M. 2014. Type II fatty acid biosynthesis is essential for *Plasmodium falciparum* sporozoite development in the midgut of *Anopheles* mosquitoes. *Eukaryotic Cell*, 13, 550-559.

Van Schalkwyk, D. A., Priebe, W. and Saliba, K. J. 2008. The inhibitory effect of 2-halo derivatives of D-glucose on glycolysis and on the proliferation of the human malaria parasite *Plasmodium falciparum*. *Journal of Pharmacology and Experimental Therapeutics*, 327, 511-517.

Verloo, P., Kocken, C. H., Van Der Wel, A., Tilly, B. C., Hogema, B. M., Sinaasappel, M., Thomas, A. W. and De Jonge, H. R. 2004. *Plasmodium falciparum*-activated chloride channels are defective in erythrocytes from cystic fibrosis patients. *Journal of Biological Chemistry*, 279, 10316-10322.

Wagner, C. A., Lang, F. and Bröer, S. 2001. Function and structure of heterodimeric amino acid transporters. *American Journal of Physiology-Cell Physiology*, 281, C1077-C1093.

Waller, K. L., McBride, S. M., Kim, K. and McDonald, T. V. 2008. Characterization of two putative potassium channels in *Plasmodium falciparum*. *Malaria Journal*, 7, 19.

Weiner, J. and Kooij, T. W. 2016. Phylogenetic profiles of all membrane transport proteins. *Microbial Cell*, 3, 511.

Wells, T. N., Burrows, J. N. and Baird, J. K. 2010. Targeting the hypnozoite reservoir of *Plasmodium vivax*: the hidden obstacle to malaria elimination. *Trends in Parasitology*, 26, 145-151.

White, N. J., Warrell, D. A., Chanthavanich, P., Looareesuwan, S., Warrell, M., Krishna, S., Williamson, D. H. and Turner, R. C. 1983. Severe hypoglycemia and hyperinsulinemia in falciparum malaria. *New England Journal of Medicine*, 309, 61-66.

Winter, C. G. and Christensen, H. N. 1964. Migration of amino acids across the membrane of the human erythrocyte. *Journal of Biological Chemistry*, 239, 872-878.

Winterberg, M., Rajendran, E., Baumeister, S., Bietz, S., Kirk, K. and Lingelbach, K. 2012. Chemical activation of a high-affinity glutamate transporter in human erythrocytes and its implications for malaria-parasite-induced glutamate uptake. *Blood*, 119, 3604-3612.

- Wipasa, J., Elliott, S., Xu, H. and Good, M. F. 2002. Immunity to asexual blood stage malaria and vaccine approaches. *Immunology and cell biology*, 80, 401-414.
- Woodrow, C. J., Burchmore, R. J. and Krishna, S. 2000. Hexose permeation pathways in *Plasmodium falciparum*-infected erythrocytes. *Proceedings of the National Academy of Sciences*, 97, 9931-9936.
- World Health Organisation 1973. Handbook of resolutions and decisions of the World Health Assembly and the Executive Board, Geneva, Switzerland, World Health Organisation.
- World Health Organisation 2015a. Global Technical Strategy for Malaria 2016–2030, Geneva, Switzerland, World Health Organisation.
- World Health Organisation 2015b. World Malaria Report 2015, Geneva, Switzerland, World Health Organisation.
- World Health Organisation 2017. World Malaria Report 2017, Geneva, Switzerland, World Health Organisation.
- Wu, B., Rambow, J., Bock, S., Holm-Bertelsen, J., Wiechert, M., Soares, A. B., Spielmann, T. and Beitz, E. 2015. Identity of a *Plasmodium* lactate/H⁺ symporter structurally unrelated to human transporters. *Nature Communications*, 6, 6284.
- Xu, X., Yamasaki, H., Feng, Z. and Aoki, T. 2002. Molecular cloning and characterization of *Plasmodium falciparum* transportin. *Parasitology Research*, 88, 391-394.
- Young, J. A., Fivelman, Q. L., Blair, P. L., De La Vega, P., Le Roch, K. G., Zhou, Y., Carucci, D. J., Baker, D. A. and Winzeler, E. A. 2005. The *Plasmodium falciparum* sexual development transcriptome: a microarray analysis using ontology-based pattern identification. *Molecular and Biochemical Parasitology*, 143, 67-79.
- Zalis, M. G., Wilson, C. M., Zhang, Y. and Wirth, D. F. 1993. Characterization of the pfmdr 2 gene for *Plasmodium falciparum*. *Molecular and Biochemical Parasitology*, 62, 83-92.
- Zeuthen, T., Wu, B., Pavlovic-Djuranovic, S., Holm, L. M., Uzcategui, N. L., Duszenko, M., Kun, J. F., Schultz, J. E. and Beitz, E. 2006. Ammonia permeability of the aquaglyceroporins from *Plasmodium falciparum*, *Toxoplasma gondii* and *Trypanosoma brucei*. *Molecular Microbiology*, 61, 1598-1608.

Zolg, J. W., Macleod, A. J., Scaife, J. G. and Beaudoin, R. L. 1984. The accumulation of lactic acid and its influence on the growth of *Plasmodium falciparum* in synchronized cultures. *In vitro Cellular and Developmental Biology*, 20, 205-215.

Supplementary material

Supplementary Table 1: An overview of the endogenous erythrocyte MTPs, NPP and the MTPs across the PVM in the asexual parasites. The endogenous erythrocyte MTPs that are still active after parasite infection are shown. The metabolites of the parasite-induced NPP and of the PVM channel are also included.

EPM			
Endogenous erythrocyte MTPs (still active after infection)			
Transporter	Metabolite	Function	Reference
Band 3	Anions (bicarbonate and chloride), Glycine, Cysteine, Serine, Lactate export, P _i	Parasite growth Protein incorporation Removal of glucose metabolism by-products	(Kirk and Lehane, 2014)
Monocarboxylate transporter (MCT1)	Lactate export	Removal of glucose metabolism by-products	(Kirk and Lehane, 2014; Poole and Halestrap, 1993)
Aquaglyceroporin	Glycerol	By-product of glucose metabolism	(Liu <i>et al.</i> , 2007; Lian <i>et al.</i> , 2009)
GLUT1	Glucose	Provide erythrocyte with primary energy substrate	(Krishna <i>et al.</i> , 2000; Kirk and Lehane, 2014)
Na ⁺ /K ⁺ ATPase	Na ⁺ and K ⁺	Generates and maintains inward Na ⁺ gradient and outward K ⁺ gradient across EPM	(Kirk <i>et al.</i> , 1991a; Staines <i>et al.</i> , 2001; Kirk and Lehane, 2014)
Ca ²⁺ ATPase	Ca ²⁺	Maintains low [Ca ²⁺] in the erythrocyte cytosol	(Kirk and Lehane, 2014)
L-system	Amino acids, Isoleucine, Methionine	Incorporation into proteins	(Wagner <i>et al.</i> , 2001; Cobbold <i>et al.</i> , 2011)
T-system	Aromatic amino acids: Tryptophan	Protein incorporation?	(Ginsburg and Krugliak, 1983)
Glutamate transporter: Transporter belonging to the excitatory amino acid transporter (EAAT) family	Amino acid: Glutamate	Incorporation into proteins	(Winterberg <i>et al.</i> , 2012; Lauer <i>et al.</i> , 1997)
ClC-2 Anion channel	Anions: Cl ⁻	Maintain cell volume and alter permeability of erythrocyte	(Huber <i>et al.</i> , 2004)
Anion channels	Anions	Maintain cell volume, alter permeability of erythrocyte and mediate anion conductance	(Verloo <i>et al.</i> , 2004)
Human equilibrative nucleoside transporter (hENT1) Human facilitative nucleobase transporter (hFNT1)	Purines	Growth and multiplication of parasite	(Quashie <i>et al.</i> , 2010)
MRP (multidrug resistance proteins)	Glutathione	Antioxidant role and redox defence	(Kirk and Lehane, 2014; Barrand <i>et al.</i> , 2012)
Choline carrier	Choline	<i>De novo</i> synthesis of phosphatidylcholine (PC)	(Kirk <i>et al.</i> , 1991b; Biagini <i>et al.</i> , 2004; Ancelin <i>et al.</i> , 1991)
Na ⁺ :P _i symporter	Na ⁺ and P _i	Parasite growth	(Shoemaker <i>et al.</i> , 1988; Kirk and Lehane, 2014)
NPP			
NPP	Monosaccharides: Glucose	Provide parasite with essential metabolite	(Kirk and Lehane, 2014)
	Amino acids: Isoleucine (together with L system), Methionine, Glutamate, Aspartate, Neutral amino acids	Incorporated into proteins (protein synthesis)	(Kirk and Lehane, 2014; Cobbold <i>et al.</i> , 2011; Ginsburg <i>et al.</i> , 1985; Martin and Kirk, 2007)
	Nucleosides	Provide parasite with essential metabolite	(Upston and Gero, 1995; Kirk and Lehane, 2014)
	Ions: Na ⁺ import and K ⁺ export	Increase in Na ⁺ and decrease in K ⁺ in erythrocyte cytosol (similar to concentrations in blood plasma)	(Staines <i>et al.</i> , 2001; Pillai <i>et al.</i> , 2013)
	Pantothenic acid	Provide parasite with essential metabolite	(Kirk and Lehane, 2014)
	Glutathione export	Provide parasite with essential metabolite	(Kirk and Lehane, 2014)
	Larger peptides: antiplasmodial pentapeptide pepstatin	Provide parasite with essential metabolite	(Saliba and Kirk, 1998)
	Choline	Provide parasite with essential metabolite	(Kirk <i>et al.</i> , 1991b)
PVM			
Non - selective pore	Low molecular weight solutes: Purine nucleotides Cations and anions: Cs ⁺ , Tris ⁺ , Ca ²⁺ , Mg ²⁺ , Cl ⁻ Amino acids: Lysine ⁺ , Glucuronate- Molecules (<.4 kDa)	Provide parasite access to small metabolite molecules	(Desai <i>et al.</i> , 1993; Desai and Rosenberg, 1997; Schwab <i>et al.</i> , 1994; Hansen <i>et al.</i> , 1980; Sherman, 1977)
Aquaporin3	Glycerol and Water	Use glycerol for lipid backbone. Decrease rapidly the parasite water volume.	(Bietz <i>et al.</i> , 2009; Beitz, 2005)

Supplementary Table 2: Classification of *P. falciparum*-encoded MTPs. The *P. falciparum*-encoded MTPs were classified into integral membrane protein classes and sub membrane protein families using TCDB dataset. The 11 newly identified parasite-encoded MTPs are indicated with (*).

Protein Gene ID	TMD	Chromosome	Annotation	Size (aa)	Size (Da)	Putative function
α-Type channels (TC 1.A)						
Voltage-gated Ion channel Superfamily (1.A.1)						
PF3D7_1227200	8	12	PfK1	1966	232190	Potassium channel
PF3D7_1436100	5	14	Hypothetical protein	1949	235199	Conserved Plasmodium membrane protein, unknown function
PF3D7_1465500	7	14	PfK2	1461	174224	Potassium channel
The Major Intrinsic Protein family (1.A.8)						
PF3D7_1132800	6	11	Aquaglyceroporin, putative	258	28297	Aquaglyceroporin
The Formate-Nitrite Transporter (FNT) Family (1.A.16)						
PF3D7_0316600	6	3	PfFNT	309	34459	Formate-nitrite transporter
The Calcium-Dependent Chloride Channel (Ca-ClC) Family (1.A.17)						
PF3D7_1250200	9	12	Conserved membrane protein, unknown function	1039	121332	Conserved membrane protein, unknown function
Small Conductance Mechanosensitive Ion Channel Family (1.A.23)						
PF3D7_1107900	5	11	Mechanosensitive ion channel, putative	1812	213624	Mechanosensitive ion channel protein
CorA Metal Ion Transporter Family (1.A.35)						
PF3D7_1120300	2	11	PfMIT1	529	63253	CorA-like Mg ²⁺ transporter protein, putative
PF3D7_1304200	2	13	PfMIT2	468	55011	CorA-like Mg ²⁺ transporter protein, putative
PF3D7_1427600	2	14	PfMIT3	478	56683	CorA-like Mg ²⁺ transporter protein, putative
Copper Transporter Family (1.A.56)						
PF3D7_1421900	4	14	Copper transporter, putative	160	18752	Copper channel
PF3D7_1439000	2	14	Copper transporter	235	27151	Copper transporter
The Membrane Mg²⁺ Transporter (MMgT) Family (1.A.67)						
PF3D7_0306700*	2	3	Membrane magnesium transporter, putative	116	13267	Membrane magnesium transporter
The Human Coronavirus 229E Viroporin (229E Viroporin) Family (1.A.89)						
PF3D7_0312500	12	3	Hypothetical protein/transporter, putative	579	67770	Transporter
β -Type channels (TC 1.B)						
Mitochondrial and Plastid Porin Family (1.B. 8)						
PF3D7_1432100	0	14	Voltage-dependent anion-selective channel protein, putative	289	33267	Hypothetical protein/voltage-dependent anion-selective channel protein
The Outer Membrane Receptor (OMR) Family (1.B. 14)						
PF3D7_0315700	12	3	Conserved membrane protein, unknown function	936	112219	Conserved membrane protein, unknown function
Pore-Forming Toxins (Proteins and Peptides) (TC 1.C)						
The Bacillus thuringiensis Vegetative Insecticidal Protein-3 (Vip3) Family (1.C.105)						
PF3D7_0614300	12	6	Hypothetical protein/organic anion transporter, putative	583	96981	Organic anion transporter
PF3D7_1231400	9	12	Amino acid transporter, putative	1944	228963	Amino acid transporter
PF3D7_0813700*	0	8	ABC transporter F family member 1, putative (ABCF1)	1419	170110	ABC transporter
Membrane-bounded Channels (TC 1.I)						
The Nuclear Pore Complex (NPC) Family (1.I.1)						
PF3D7_0905100*	4	9	Nucleoporin NUP100/NSP100, putative (NUP100)	2112	235541	Nucleoporin NUP100/NSP100

Protein Gene ID	TMD	Chromosome	Annotation	Size (aa)	Size (Da)	Putative function
Electrochemical Potential driven Transporter (TC 2.A)						
Major Facilitator Superfamily (TC 2.A.1)						
Sugar Porter family (2.A.1.1)						
PF3D7_0919500	11	9	Hypothetical protein/sugar transporter, putative	476	56073	Sugar transporter
PF3D7_0916000	11	9	Major facilitator superfamily protein/sugar transporter, putative	1379	160371	Sugar transporter
PF3D7_0204700	12	2	PfHT	504	56417	Hexose transporter
Drug: H⁺ Antiporter-1 Family (2.A.1.2)						
PF3D7_1440800	12	14	Hypothetical protein/major facilitator superfamily, putative	582	68091	Metabolite/drug transporter
PF3D7_0516500	10	5	Metabolite/drug transporter, putative	442	49073	Metabolite/drug transporter
The Oxalate:Formate Antiporter (OFA) Family (2.A.1.11)						
PF3D7_0926400	11	9	Hypothetical protein/monocarboxylate transporter, putative	529	60709	Monocarboxylate transporter
Monocarboxylate Porter Family (2.A.1.13)						
PF3D7_0210300	12	2	Hypothetical protein/monocarboxylate transporter, putative	457	51862	Monocarboxylate transporter
Peptide-Acetyl-Coenzyme A transporter family (2.A.1.25)						
PF3D7_1036800	10	10	PfACT	590	69797	Acetyl-CoA transporter
The Unidentified Major Facilitator-12 (UMF12) Family (2.A.1.63)						
PF3D7_1104800	9	11	Hypothetical protein/metabolite/drug transporter, putative	417	49281	Metabolite/drug transporter
The Unidentified Major Facilitator-15 (UMF15) Family (2.A.1.66)						
PF3D7_1428200	12	14	Hypothetical protein/metabolite/drug transporter, putative	809	96055	Metabolite/drug transporter
PF3D7_0206200	11	2	Major facilitator superfamily protein/pantothenate transporter	565	62663	Pantothenate:H ⁺ symport
Glycoside-Pentoside-Hexuronide: Cation Symporter Family (related to MFS) (sugar: cation symporter) (2.A.2)						
PF3D7_0529200	12	5	Sugar transporter, putative	548	63770	Sugar:cation symporter
PF3D7_0914700	11	9	Hypothetical protein/transporter, putative	516	58421	Transporter
Cation Diffusion Facilitator Family (2.A.4)						
PF3D7_0715900	6	7	Zinc transporter, putative	556	62945	Zinc transporter
Zinc (Zn²⁺)-iron (Fe²⁺) Permease family (2.A.5)						
PF3D7_0609100	8	6	Hypothetical protein/Zn ²⁺ or Fe ²⁺ permease/permease, putative	358	40260	Zn ²⁺ or Fe ²⁺ permease
PF3D7_1022300	7	10	ZIP domain-containing protein, putative	325	37165	Zinc transporter
Resistance-Nodulation-Cell Division Superfamily (2.A.6)						
Eukaryotic (putative) Sterol Transporter family (2.A.6.6)						
PF3D7_0107500	12	1	Patched family protein, putative/lipid/sterol:H ⁺ symporter	1470	170303	Lipid/sterol:H ⁺ symporter
The Drug/Metabolite Transporter (DMT) Superfamily (2.A.7)						
10 TMS Drug/Metabolite Exporter Family (2.A.7.3)						
PF3D7_0715800	9	7	Drug metabolite transporter, putative	434	50250	Drug/metabolite exporter
Triose-phosphate Transporter Family (2.A.7.9)						
PF3D7_0508300	9	5	PfTPT	342	39041	Triose phosphate transporter
PF3D7_0530200	7	5	PfPPT	524	59790	Phosphoenolpyruvate/phosphate translocator
PF3D7_1218400	10	12	Hypothetical protein/phosphate translocator, putative/triose or hexose phosphate/phosphate translocator	478	54723	Triose or hexose phosphate/phosphate translocator, putative

Protein Gene ID	TMD	Chromosome	Annotation	Size (aa)	Size (Da)	Putative function
The UDP-N-Acetylglucosamine:UMP Antiporter (UAA) Family (2.A.7.10)						
PF3D7_0709000	10	7	PfCRT	424	48676	Chloroquine resistance transporter
UDP-galactose: UMP Antiporter Family (2.A.7.11)						
PF3D7_1113300	8	11	Protein tyrosine phosphatase, putative/UDP-galactose transporter, putative	343	39425	UDP-galactose transporter
The CMP-Sialate: CMP Antiporter (CSA) Family (2.A.7.12)						
PF3D7_0505300	9	5	Hypothetical protein/UDP-N-acetyl glucosamine:UMP antiporter, putative	611	74042	UDP-N-acetyl glucosamine:UMP antiporter
The GDP-fucose Transporter (GFT) Family (2.A.7.16)						
PF3D7_0515700	10	5	Hypothetical protein/glideosome-associated protein 40	456	51800	Glideosome-associated protein 40
PF3D7_0212000	7	2	Hypothetical protein/GDP-fructose:GMP antiporter, putative	311	36668	GDP-fructose:GMP antiporter
The Putative Tryptophan Efflux (Trp-E) Family (2.A.7.23)						
PF3D7_0716900	9	7	Hypothetical protein/drug metabolite transporter, putative	322	37277	Drug metabolite transporter
The NIPA Mg²⁺ Uptake Permease (NIPA) Family (2.A.7.25)						
PF3D7_0522600	8	5	IMC protein, putative	483	55665	IMC protein
PF3D7_0827700	9	8	Magnesium transporter, putative	943	109653	Magnesium transporter
Amino acid/Auxin Permease family (2.A.18)						
PF3D7_0629500	9	6	Transmembrane amino acid transporter protein, putative	606	68859	Amino acid transporter
PF3D7_1208400	10	12	Hypothetical protein/amino acid transporter, putative	1564	185933	Amino acid transporter
Ca²⁺: Cation Antiporter Family (2.A.19)						
PF3D7_0603500	11	6	Cation/H ⁺ antiporter, putative	441	48920	Cation/H ⁺ antiporter
Inorganic Phosphate Transporter Family (2.A.20)						
PF3D7_1340900	10	13	PfPiT	687	75296	Na ⁺ -dependent Pi transporter
Neurotransmitter: Na⁺ Symporter Family (2.A.22)						
PF3D7_0209600	13	2	Transporter, putative	1132	133699	Amino acid transporter
PF3D7_0515500	14	5	Amino acid transporter, putative	960	115455	Amino acid transporter
PF3D7_1132500	15	11	Amino acid transporter, putative	1439	174055	Amino acid transporter
The Mitochondrial Carrier (MC) Family (2.A.29)						
PF3D7_0108400.1	5	1	Mitochondrial carrier protein, putative	330	38977	Mitochondrial carrier protein
PF3D7_0108800	0	1	Conserved protein, unknown function	360	42502	Hypothetical protein; mitochondrial carrier family
PF3D7_0407500	3	4	Mitochondrial carrier protein, putative	380	45300	Mitochondrial carrier protein
PF3D7_0823900	1	8	PfDTC	318	35387	Dicarboxylate/tricarboxylate antiporter
PF3D7_0811100	4	8	Mitochondrial carrier protein, putative	540	64925	Mitochondrial carrier protein
PF3D7_0905200	0	9	Mitochondrial carrier protein, putative	1199	142074	Mitochondrial carrier protein
PF3D7_0908800	4	9	Transporter, putative	590	70056	Transporter
PF3D7_1004800	5	10	ADP/ATP carrier protein, putative	340	41010	ADP/ATP antiporter
PF3D7_1037300	3	10	ADP/ATP transporter on adenylate translocase	301	33727	ADP/ATP antiporter
PF3D7_1202200	1	12	Mitochondrial phosphate carrier protein	324	36802	Pi : H ⁺ symporter
PF3D7_1223800	0	12	Mitochondrial carrier protein, putative	308	34887	Transporter
PF3D7_1241600	4	12	Mitochondrial carrier protein, putative	256	28774	Transporter

Protein Gene ID	TMD	Chromosome	Annotation	Size (aa)	Size (Da)	Putative function
PF3D7_1368700	2	13	Mitochondrial carrier protein, putative	576	67861	Transporter
The Monovalent Cation:Proton Antiporter-1 (CPA1) Family (2.A.36)						
PF3D7_0613300	11	6	Rhoptry protein ROP14	1422	172017	Rhoptry protein
PF3D7_1303500	14	13	PfNHE	1920	226085	Na ⁺ :H ⁺ exchanger
The Sulfate Pemease (SulP) family (2.A.53)						
PF3D7_1471200	11	14	PfSulP	664	75469	Inorganic anion antiporter
The Metal ion (Mn²⁺ - iron) Transporter (Nramp) family (2.A.55)						
PF3D7_0523800	11	5	Transporter, putative	684	78743	Divalent cation (metal) :H ⁺ symporter
The Equilibrative Nucleoside Transporter (ENT) family (2.A.57)						
PF3D7_0103200	11	1	PfNT4	434	50011	Nucleoside transporter
PF3D7_0824400	10	8	PfNT2	585	67643	Nucleoside transporter
PF3D7_1347200	9	13	PfNT1	422	47632	Nucleoside transporter
PF3D7_1469400	11	14	PfNT3, putative	437	50941	Nucleoside transporter
Folate-Biopterin Transporter family (related to MFS) (2.A.71)						
PF3D7_0828600	12	8	Hypothetical protein/folate transporter 1	505	58061	Folate transporter 1
PF3D7_1116500	11	11	Hypothetical protein/folate transporter 2, putative	455	51355	Folate transporter 2
The Vacuolar Iron Transporter (VIT) Family (2.A.89)						
PF3D7_1223700	5	12	Iron transporter, putative	273	30984	Fe ²⁺ transporter
The Mitochondrial Pyruvate Carrier (MPC) Family (2.A.105)						
PF3D7_0628400	7	6	Conserved membrane protein, unknown function	339	40641	Conserved membrane protein, unknown function
PF3D7_1340800	1	13	Mitochondrial pyruvate carrier protein 1, putative	106	12259	Pyruvate:H ⁺ symporter
PF3D7_1470400	0	14	Mitochondrial pyruvate carrier protein 2, putative	129	15255	Pyruvate:H ⁺ symporter
P-P-bond-hydrolysis-driven transporters (TC 3.A)						
The ATP-binding Cassette (ABC) Superfamily (3.A.1)						
The Cobalamin Precursor (B12-P) Family (3.A.1.32)						
PF3D7_1368200	0	13	ABC transporter E family member 1, putative (ABCE1)	619	70271	ATPase activity
The (Putative) Drug Resistance ATPase-2 (Drug RA2) Family (3.A.1.121)						
PF3D7_1121700	0	11	ABC transporter F family member 2, putative (GCN20)	815	95376	ABC transporter GCN20
The 3-component Peptide-5 exporter (Pep5E) Family (3.A.1.124)						
PF3D7_0319700	13	3	ABC transporter I family member 1, putative (ABC13)	3133	375812	ABC transporter
The Multidrug Resistance exporter (MDR) Family (ABCB) (3.A.1.201)						
PF3D7_1209900	5	12	ABC transporter B family member 7, putative (ABCB7)	855	98830	ABC transporter
PF3D7_0523000	11	5	PfMDR1	1419	162254	Multidrug resistance protein
The Eye Pigment Precursor Transporter (EPP) Family (ABCG) (3.A.1.204)						
PF3D7_1426500	6	14	ABC transporter G family member 2 (ABCG2)	660	75479	ABC transporter
The a-Factor Sex Pheromone Exporter (STE) Family (ABCB) (3.A.1.206)						
PF3D7_1339900	4	13	ABC transporter B family member 5, putative (ABCB5)	925	108514	ABC transporter

Protein Gene ID	TMD	Chromosome	Annotation	Size (aa)	Size (Da)	Putative function
The Drug Conjugate Transporter (DCT) Family (ABCC) (3.A.1.208)						
PF3D7_0104800	12	1	PfNPT1	577	65426	Novel putative transporter 1
PF3D7_1129900	12	11	Hypothetical protein/transporter, putative	609	70139	Transporter
PF3D7_0112200	11	1	PfMRP1	1822	214443	ABC transporter
PF3D7_1229100	11	12	PfMRP2	2108	248305	ABC transporter
PF3D7_0216800	14	2	Conserved membrane protein, unknown function	1122	132222	Conserved membrane protein, unknown function
The Heavy metal Transporter (HMT) Family (3.A.1.210)						
PF3D7_0302600	6	3	ABC transporter B family member 4, putative (ABCB4)	1365	161244	ABC transporter
PF3D7_1145500	6	11	ABC transporter B family member 3, putative (ABCB3)	833	99350	ABC transporter
PF3D7_1352100	5	13	ABC transporter B family member 6, putative (ABCB6)	1049	123664	ABC transporter
PF3D7_1447900	10	14	PfMDR2	1024	119014	Multidrug resistance protein 2
The H⁺- or Na⁺-translocating F-type, V-type and A-type ATPase (F-ATPase) Superfamily (3.A.2)						
PF3D7_1147700	0	11	Mitochondrial ATP synthase delta subunit, putative	154	17617	Mitochondrial ATP synthase delta subunit
PF3D7_0217100	0	2	ATP synthase F1, alpha subunit	551	61771	ATP synthase F1, alpha subunit
PF3D7_1235700	0	12	ATP synthase subunit beta, mitochondrial	535	58395	ATP synthase beta chain, mitochondrial
PF3D7_1310000	0	13	Mitochondrial ATP synthase delta subunit, putative	253	30199	Mitochondrial ATP synthase delta subunit
PF3D7_1311300	0	13	ATP synthase subunit gamma, mitochondrial	311	35756	ATP synthase gamma chain, mitochondrial
PF3D7_0715500	0	7	Mitochondrial ATP synthase F1, epsilon subunit, putative	71	8496	Mitochondrial ATP synthase F1, epsilon subunit
PF3D7_0519200	4	5	V-type proton ATPase proteolipid subunit	165	17066	Vacuolar ATP synthetase, putative
PF3D7_0806800	6	8	Vacuolar proton translocating ATPase subunit A, putative	1053	123000	Vacuolar proton translocating ATPase subunit A
PF3D7_1354400	4	13	V-type proton ATPase proteolipid subunit, putative	181	19124	V-type ATPase
PF3D7_1464700	0	14	ATP synthase subunit, putative	382	44532	ATP synthase subunit
PF3D7_1140100	0	11	V-type proton ATPase subunit F, putative	128	14624	Vacuolar ATP synthase subunit F
PF3D7_0406100	0	4	V-type proton ATPase subunit B	494	55790	Vacuolar ATP synthase subunit B
PF3D7_0106100	0	1	V-type proton ATPase subunit C, putative	383	45260	V-type ATPase, subunit C
PF3D7_1311900	0	13	V-type proton ATPase catalytic subunit A	611	68577	Vacuolar ATP synthase, catalytic subunit A
PF3D7_1323200	0	13	V-type proton ATPase subunit G, putative	123	14192	Vacuolar ATP synthase subunit G
PF3D7_1341900	0	13	V-type proton ATPase subunit D, putative	247	27801	Vacuolar ATP synthase subunit D
PF3D7_1306600	0	13	V-type proton ATPase subunit H, putative	455	53830	Vacuolar ATP synthase subunit H, putative
PF3D7_0934500	0	9	V-type proton ATPase subunit E, putative	235	27191	Vacuolar ATP synthase subunit E, putative
PF3D7_0705900*	2	7	ATP synthase subunit C, putative	166	18559	ATP synthase subunit c, putative; F0 (ATP9) proteolipid subunit
The P-type ATPase (P-ATPase) Superfamily (3.A.3)						
PF3D7_0106300	8	1	Calcium-transporting ATPase (ATP6)	1228	139416	SERCA-type Ca ²⁺ -transporting P-ATPase
PF3D7_1211900	8	12	Non-SERCA-type Ca ²⁺ -transporting P-ATPase (ATP4)	1264	140264	Non-SERCA-type Ca ²⁺ -transporting PATPase
PF3D7_1348800	9	13	E1-E2 ATPase, putative	1834	219275	E1-E2 ATPase
PF3D7_0904900	7	9	Copper-transporting ATPase	2568	299393	Cu ²⁺ -transporting P-ATPase

Protein Gene ID	TMD	Chromosome	Annotation	Size (aa)	Size (Da)	Putative function
PF3D7_0504000	12	5	Cation transporting P-ATPase (ATPase3)	2393	283040	Cation transporting P-ATPase
PF3D7_0516100	10	5	Cation-transporting ATPase 1 (ATPase1)	2400	283603	Cation-transporting P-ATPase
PF3D7_0727800	12	7	Cation transporting ATPase, putative	1918	225080	Cation transporting ATPase
PF3D7_1138400	19	11	Guanylyl cyclase (GCalpha)	4226	496026	Guanylyl cyclases Gca and GCb
PF3D7_1360500	21	13	Guanylyl cyclase beta (GCbeta)	3179	376995	Guanylyl cyclase
PF3D7_0319000	10	3	P-type ATPase, putative (ATPase7)	1864	218022	Aminophospho-lipid-transporting P-ATPase
PF3D7_1219600	10	12	Aminophospho-lipid-transporting P-ATPase (ATPase2)	1555	179137	Aminophospho-lipid-transporting P-ATPase
PF3D7_1223400	10	12	Phospholipid-transporting ATPase, putative	1618	190448	Aminophospho-lipid-transporting P-ATPase
PF3D7_1468600	10	14	Aminophospho-lipid transporter, putative	2008	240465	Aminophospho-lipid transporting P-ATPase
PF3D7_0806200	9	8	Conserved membrane protein, unknown function	1018	122107	Conserved membrane protein, unknown function
The H⁺, Na⁺-translocating Pyrophosphatase (M+-PPase) Family (3.A.10)						
PF3D7_1235200	16	12	PfVP2	1057	117107	V-type K ⁺ -independent H ⁺ -translocating inorganic pyrophosphatase
PF3D7_1456800	16	14	PfVP1	717	76417	V-type H ⁺ -translocating pyrophosphatase
The endoplasmic Reticular Retrotranslocon (ER-RT) Family (3.A.16)						
PF3D7_0212800	11	2	Multidrug efflux pump, putative	1224	144034	Organic solutes/Na ⁺ or H ⁺ antiporter
The TMS Recognition/Insertion Complex (TRC) Family (3.A.19)						
PF3D7_0415000*	0	4	ATPase, putative	379	43318	Arsenical pump-driving ATPase
The Symbiont-specific ERAD-like Machinery (SELMA) Family (3.A.25)						
PF3D7_0104700	12	1	Hypothetical protein/ transporter, putative	711	83693	Transporter
PF3D7_0924500	14	9	Conserved membrane protein, unknown function	1298	154492	Conserved membrane protein, unknown function
PF3D7_0614900	11	6	Conserved membrane protein, unknown function	1096	130936	Conserved membrane protein, unknown function
PF3D7_0305300	11	3	Conserved membrane protein, unknown function	956	114504	Conserved membrane protein, unknown function
PF3D7_0530500	13	5	Conserved membrane protein, unknown function	1009	123360	Conserved membrane protein, unknown function
Auxiliary transport proteins (TC 8.A)						
The SLC and TCST-Associated Component (STAC-A) Family (8.A.59)						
PF3D7_1404600.1	4	14	Adenylyl cyclase alpha (ACalpha)	865	104216	Protein with ion channel and adenylate cyclase domains
Putative transport proteins (TC 9.B)						
The Putative Heme Handling Protein (HHP) Family (9.B.14)						
PF3D7_1022200	12	10	Hypothetical protein/ Metabolite/ vitamin transporter	629	74846	Conserved membrane protein, unknown function
PF3D7_0824700	10	8	Lipase maturation factor, putative	590	71244	Conserved membrane protein, unknown function
PF3D7_1332100	11	13	Conserved membrane protein, unknown function	522	61248	Conserved membrane protein, unknown function
PF3D7_1135300	8	11	Conserved membrane protein, unknown function	409	48430	Conserved membrane protein, unknown function
No Class						
PF3D7_1203400	12	12	Hypothetical protein/ transporter, putative	1250	149197	Transporter

Supplementary Table 3: The phenotypic data of the MTP genes identified in *P. berghei* and *P. falciparum*. The phenotypic data of 112 MTP genes in *P. berghei* and *P. falciparum* are listed and was obtained from PhenoPlasm and PlasmogEM. The phenotypic data include the identification of essential and dispensable genes as well as the MTP genes which affected the asexual or gametocyte stages after the knock-out studies.

GeneID		Known or putative function	Phenotype		
<i>P. falciparum</i>	<i>P. berghei</i> orthologs		PhenoPlasm	PlasmogEM	Attenuation on asexual or gametocyte stages
Channels					
PF3D7_1227200	PBANKA_1442000	K1	Essential in <i>P. falciparum</i>	Dispensable in <i>P. berghei</i>	Asexual and gametocytes (<i>P. berghei</i>)
PF3D7_1465500	PBANKA_1328900	K2	Essential in <i>P. falciparum</i>	Dispensable in <i>P. berghei</i>	-
PF3D7_1436100	PBANKA_1008700	Conserved Plasmodium membrane protein	Dispensable in <i>P. berghei</i>	Dispensable in <i>P. berghei</i>	-
PF3D7_1132800	PBANKA_0915600	Aquaglyceroporin	Dispensable in <i>P. berghei</i>	Not determined	Asexual stages (<i>P. berghei</i>)
PF3D7_1107900	PBANKA_0939000	Mechanosensitive ion channel protein	Dispensable in <i>P. berghei</i>	Not determined	-
PF3D7_0312500	PBANKA_0410500	Transporter	Dispensable in <i>P. berghei</i>	Dispensable in <i>P. berghei</i>	Asexual stages (<i>P. berghei</i>)
PF3D7_1432100	PBANKA_1012800	Voltage-dependent anion-selective channel protein	Essential in <i>P. berghei</i>	Essential in <i>P. berghei</i>	-
PF3D7_0905100	PBANKA_0416300	Nucleoporin NUP100/NSP100	Essential in <i>P. berghei</i>	Essential in <i>P. berghei</i>	-
ATP-powered pumps					
PF3D7_1368200	PBANKA_1144100	ABC transporter E family member 1	Essential in <i>P. berghei</i>	Essential in <i>P. berghei</i>	-
PF3D7_1121700	PBANKA_0926600	ABC transporter F family member 2 (GCN20)	Dispensable in <i>P. berghei</i>	Dispensable in <i>P. berghei</i>	-
PF3D7_0302600	PBANKA_0401200	ABC transporter B family member 4	Essential in <i>P. berghei</i>	Dispensable in <i>P. berghei</i>	-
PF3D7_0813700	PBANKA_1423800	ABC transporter F family member 1	Essential in <i>P. berghei</i>	Essential in <i>P. berghei</i>	-
PF3D7_1352100	PBANKA_1364800	ABC transporter B family member 6	Essential in <i>P. berghei</i>	Essential in <i>P. berghei</i>	Asexual stages (<i>P. berghei</i>)
PF3D7_0319700	PBANKA_1218800	ABC transporter I family member 1 (ABC13)	Essential in <i>P. berghei</i>	Essential in <i>P. berghei</i>	-
PF3D7_1209900	PBANKA_0608300	ABC transporter B family member 7	Essential in <i>P. berghei</i>	Not determined	-
PF3D7_0523000	PBANKA_1237800	MDR1	Essential in <i>P. falciparum</i> and <i>P. berghei</i>	Essential in <i>P. berghei</i>	-
PF3D7_1426500	PBANKA_1018100	ABC transporter G family member 2	Dispensable in <i>P. falciparum</i> and <i>P. berghei</i>	Slow phenotype in <i>P. berghei</i>	Asexual stages (<i>P. berghei</i>)
PF3D7_1339900	PBANKA_1353300	ABC transporter B family member 5	Essential in <i>P. berghei</i>	Slow phenotype in <i>P. berghei</i>	Asexual stages (<i>P. berghei</i>)
PF3D7_0104800	PBANKA_0208300	NPT1	Dispensable in <i>P. berghei</i>	Dispensable in <i>P. berghei</i>	Asexual and gametocytes (<i>P. berghei</i>)
PF3D7_1129900	PBANKA_0918300	Transporter	Dispensable in <i>P. berghei</i>	Not determined	Asexual and gametocytes (<i>P. berghei</i>)
PF3D7_0112200	-	MRP1	Dispensable in <i>P. falciparum</i>	Not determined	-
PF3D7_1229100	PBANKA_1443800	MRP2	Dispensable in <i>P. falciparum</i> and <i>P. berghei</i>	Slow phenotype in <i>P. berghei</i>	Asexual and gametocytes (<i>P. berghei</i>)
PF3D7_1145500	PBANKA_0903500	ABC transporter B family member 3	Dispensable in <i>P. falciparum</i> and <i>P. berghei</i>	Not determined	Asexual stages (<i>P. berghei</i>)
PF3D7_1447900	PBANKA_1311700	MDR2	Dispensable in <i>P. falciparum</i> and <i>P. berghei</i>	Slow phenotype in <i>P. berghei</i>	Asexual stages (<i>P. berghei</i>)
PF3D7_1147700	PBANKA_0901400	Mitochondrial ATP synthase delta subunit	Dispensable in <i>P. berghei</i>	Slow phenotype in <i>P. berghei</i>	Asexual stages (<i>P. berghei</i>)

PF3D7_0217100	PBANKA_0313800	ATP synthase F1, alpha subunit	Dispensible in <i>P. berghei</i>	Slow phenotype in <i>P. berghei</i>	Asexual stages (<i>P. berghei</i>)
PF3D7_1235700	PBANKA_1450300	ATP synthase subunit beta, mitochondrial	Dispensible in <i>P. berghei</i>	Slow phenotype in <i>P. berghei</i>	Asexual and gametocytes (<i>P. berghei</i>)
PF3D7_1311300	PBANKA_1409800	ATP synthase subunit gamma, mitochondrial	Essential in <i>P. falciparum</i>	Slow phenotype in <i>P. berghei</i>	Asexual stages (<i>P. berghei</i>)
PF3D7_0519200	PBANKA_1234000	V-type proton ATPase proteolipid subunit	Essential in <i>P. berghei</i>	Essential in <i>P. berghei</i>	-
PF3D7_1354400	PBANKA_1131000	V-type proton ATPase proteolipid subunit	Essential in <i>P. berghei</i>	Essential in <i>P. berghei</i>	-
PF3D7_1464700	PBANKA_1328100	ATP synthase subunit	Essential in <i>P. berghei</i>	Essential in <i>P. berghei</i>	-
PF3D7_0406100	PBANKA_1003800	V-type proton ATPase subunit B	Essential in <i>P. berghei</i>	Essential in <i>P. berghei</i>	-
PF3D7_0106100	PBANKA_0207200	V-type proton ATPase subunit C	Essential in <i>P. berghei</i>	Essential in <i>P. berghei</i>	-
PF3D7_1311900	PBANKA_1410400	V-type proton ATPase catalytic subunit A	Essential in <i>P. berghei</i>	Essential in <i>P. berghei</i>	-
PF3D7_1323200	PBANKA_1338400	V-type proton ATPase subunit G	Essential in <i>P. berghei</i>	Essential in <i>P. berghei</i>	-
PF3D7_1306600	PBANKA_1405100	V-type proton ATPase subunit H	Essential in <i>P. berghei</i>	Essential in <i>P. berghei</i>	-
PF3D7_0934500	PBANKA_0835300	V-type proton ATPase subunit E	Essential in <i>P. berghei</i>	Essential in <i>P. berghei</i>	-
PF3D7_0106300	PBANKA_0207000	Calcium-transporting ATPase	Essential in <i>P. berghei</i>	Essential in <i>P. berghei</i>	-
PF3D7_1211900	PBANKA_0610400	ATP4	Dispensible in <i>P. berghei</i>	Slow phenotype in <i>P. berghei</i>	Asexual stages (<i>P. berghei</i>)
PF3D7_0904900	PBANKA_0416500	Copper-transporting ATPase	Dispensible in <i>P. berghei</i>	Not determined	Asexual and gametocytes (<i>P. berghei</i>)
PF3D7_0504000	PBANKA_1103600	Cation transporting P-ATPase (ATPase3)	Essential in <i>P. berghei</i>	Essential in <i>P. berghei</i>	-
PF3D7_0727800	PBANKA_0211900	Cation transporting ATPase	Essential in <i>P. berghei</i>	Essential in <i>P. berghei</i>	-
PF3D7_1138400	PBANKA_0910300	Guanylyl cyclase (GCalpha)	Essential in <i>P. falciparum</i> and <i>P. berghei</i>	Slow phenotype in <i>P. berghei</i>	Asexual stages (<i>P. berghei</i>)
PF3D7_1360500	PBANKA_1136700	Guanylyl cyclase beta (GCbeta)	Dispensible in <i>P. falciparum</i> and <i>P. berghei</i>	Slow phenotype in <i>P. berghei</i>	Asexual stages (<i>P. berghei</i>)
PF3D7_0319000	PBANKA_0806300	P-type ATPase	Essential in <i>P. berghei</i>	Dispensible in <i>P. berghei</i>	-
PF3D7_1219600	PBANKA_1434800	Aminophospholipid-transporting P-ATPase (ATPase2)	Essential in <i>P. berghei</i>	Essential in <i>P. berghei</i>	-
PF3D7_1223400	PBANKA_1438300	Phospholipid-transporting ATPase	Essential in <i>P. berghei</i>	Slow phenotype in <i>P. berghei</i>	Asexual stages (<i>P. berghei</i>)
PF3D7_1235200	PBANKA_1449800	VP2	Dispensible in <i>P. falciparum</i> and <i>P. berghei</i>	Dispensible in <i>P. berghei</i>	-
PF3D7_0212800	PBANKA_0309700	Multidrug efflux pump	Dispensible in <i>P. berghei</i>	Dispensible in <i>P. berghei</i>	-
PF3D7_0415000	PBANKA_0717000	Arsenical pump-driving ATPase	Dispensible in <i>P. berghei</i>	Slow phenotype in <i>P. berghei</i>	Asexual stages (<i>P. berghei</i>)
PF3D7_0104700	PBANKA_0208400	Transporter	Dispensible in <i>P. berghei</i>	Dispensible in <i>P. berghei</i>	Gametocyte stages (<i>P. berghei</i>)
PF3D7_0924500	PBANKA_0825400	Conserved Plasmodium membrane protein, unknown function	Essential in <i>P. berghei</i>	Essential in <i>P. berghei</i>	-
PF3D7_0614900	PBANKA_1229600	Conserved Plasmodium membrane protein, unknown function	Dispensible in <i>P. berghei</i>	Slow phenotype in <i>P. berghei</i>	Asexual stages (<i>P. berghei</i>)
PF3D7_0305300	PBANKA_0403800	Conserved Plasmodium membrane protein, unknown function	Essential in <i>P. berghei</i>	Not determined	-

PF3D7_0530500	PBANKA_1244900	Conserved Plasmodium membrane protein, unknown function	Dispensible in <i>P. berghei</i>	Dispensible in <i>P. berghei</i>	-
Transporters					
PF3D7_1120300	PBANKA_0927900	MIT1	Dispensible in <i>P. berghei</i>	Not determined	-
PF3D7_1304200	PBANKA_1402700	MIT2	Dispensible in <i>P. berghei</i>	Dispensible in <i>P. berghei</i>	-
PF3D7_1427600	PBANKA_1017000	MIT3	Dispensible in <i>P. berghei</i>	Dispensible in <i>P. berghei</i>	-
PF3D7_0306700	PBANKA_0405100	Membrane magnesium transporter	Essential in <i>P. berghei</i>	Essential in <i>P. berghei</i>	-
PF3D7_0919500	PBANKA_0820400	Sugar transporter	Dispensible in <i>P. berghei</i>	Dispensible in <i>P. berghei</i>	-
PF3D7_0916000	PBANKA_0817000	Sugar transporter	Dispensible in <i>P. berghei</i>	Dispensible in <i>P. berghei</i>	Asexual stages (<i>P. berghei</i>)
PF3D7_0204700	PBANKA_0302500	HT	Essential in <i>P. falciparum</i> and <i>P. berghei</i>	Not determined	-
PF3D7_1440800	PBANKA_1304700	Metabolite/drug transporter	Dispensible in <i>P. berghei</i>	Slow phenotype in <i>P. berghei</i>	Asexual and gametocytes (<i>P. berghei</i>)
PF3D7_0516500	PBANKA_1231300	Metabolite/drug transporter	Dispensible in <i>P. berghei</i>	Not determined	Asexual stages (<i>P. berghei</i>)
PF3D7_1036800	PBANKA_0519800	ACT	Dispensible in <i>P. falciparum</i> and <i>P. berghei</i>	Slow phenotype in <i>P. berghei</i>	Asexual stages (<i>P. berghei</i> and <i>P. falciparum</i>)
PF3D7_1104800	PBANKA_0942100	Metabolite/drug transporter	Essential in <i>P. berghei</i>	Essential in <i>P. berghei</i>	-
PF3D7_1428200	PBANKA_1016400	Metabolite/drug transporter	Dispensible in <i>P. berghei</i>	Dispensible in <i>P. berghei</i>	Asexual stages (<i>P. berghei</i>)
PF3D7_0206200	PBANKA_0303900	Pantothenate transporter	Essential in <i>P. falciparum</i>	Not determined	Gametocyte stages (<i>P. berghei</i>)
PF3D7_0914700	PBANKA_0815700	Transporter	Dispensible in <i>P. berghei</i>	Not determined	-
PF3D7_0828600	PBANKA_0702100	Folate transporter 1	Dispensible in <i>P. berghei</i>	Dispensible in <i>P. berghei</i>	-
PF3D7_1116500	PBANKA_0931500	Folate transporter 2	Dispensible in <i>P. berghei</i>	Dispensible in <i>P. berghei</i>	-
PF3D7_0715900	PBANKA_1422200	Zinc transporter	Dispensible in <i>P. berghei</i>	Dispensible in <i>P. berghei</i>	Gametocyte stages (<i>P. berghei</i>)
PF3D7_0609100	PBANKA_0107700	Zinc transporter	Essential in <i>P. berghei</i>	Slow phenotype in <i>P. berghei</i>	Asexual and gametocytes (<i>P. berghei</i>)
PF3D7_1022300	PBANKA_0506500	Zinc transporter	Dispensible in <i>P. berghei</i>	Slow phenotype in <i>P. berghei</i>	Asexual stages (<i>P. berghei</i>)
PF3D7_0107500	PBANKA_0205900	Lipid/sterol:H ⁺ symporter	Essential in <i>P. berghei</i>	Essential in <i>P. berghei</i>	-
PF3D7_0715800	PBANKA_1422100	Drug/metabolite transporter	Dispensible in <i>P. berghei</i>	Dispensible in <i>P. berghei</i>	Asexual stages (<i>P. berghei</i>)
PF3D7_0508300	PBANKA_1107900	TPT	Essential in <i>P. berghei</i>	Not determined	-
PF3D7_0530200	PBANKA_1244600	PPT	Essential in <i>P. berghei</i>	Essential in <i>P. berghei</i>	-
PF3D7_1218400	PBANKA_1434000	Triose or hexose phosphate/phosphate translocator	Dispensible in <i>P. berghei</i>	Dispensible in <i>P. berghei</i>	-
PF3D7_0709000	PBANKA_1219500	CRT	Essential in <i>P. falciparum</i> and <i>P. berghei</i>	Essential in <i>P. berghei</i>	-
PF3D7_1113300	PBANKA_0934300	UDP-galactose transporter	Essential in <i>P. berghei</i>	Essential in <i>P. berghei</i>	-
PF3D7_0505300	PBANKA_1104900	UDP-N-acetylglucosamine transporter	Dispensible in <i>P. berghei</i>	Dispensible in <i>P. berghei</i>	-
PF3D7_0515700	PBANKA_1115300	Glideosome-associated protein 40 (GAP40)	Essential in <i>P. berghei</i>	Essential in <i>P. berghei</i>	-
PF3D7_0716900	PBANKA_0614600	Drug metabolite transporter	Essential in <i>P. berghei</i>	Essential in <i>P. berghei</i>	-

PF3D7_0522600	PBANKA_1237300	Inner membrane complex protein	Dispensible in <i>P. berghei</i>	Dispensible in <i>P. berghei</i>	-
PF3D7_1208400	PBANKA_0606900	Amino acid transporter	Dispensible in <i>P. berghei</i>	Dispensible in <i>P. berghei</i>	Asexual stages (<i>P. berghei</i>)
PF3D7_0209600	PBANKA_0306700	Amino acid transporter	Essential in <i>P. berghei</i>	Essential in <i>P. berghei</i>	-
PF3D7_0515500	PBANKA_1115100	Amino acid transporter	Dispensible in <i>P. berghei</i>	Dispensible in <i>P. berghei</i>	Asexual stages (<i>P. berghei</i>)
PF3D7_1231400	PBANKA_1446100	Amino acid transporter	Essential in <i>P. berghei</i>	Essential in <i>P. berghei</i>	Asexual stages (<i>P. berghei</i>)
PF3D7_0603500	PBANKA_0102300	Cation/H ⁺ antiporter	Dispensible in <i>P. berghei</i>	Not determined	-
PF3D7_0108400	PBANKA_0205100	Mitochondrial carrier protein	Dispensible in <i>P. berghei</i>	Dispensible in <i>P. berghei</i>	-
PF3D7_0811100	PBANKA_1426400	Mitochondrial carrier protein	-	Slow phenotype in <i>P. berghei</i>	Asexual stages (<i>P. berghei</i>)
PF3D7_0905200	PBANKA_0416200	Mitochondrial carrier protein	Essential in <i>P. berghei</i>	Essential in <i>P. berghei</i>	-
PF3D7_1004800	PBANKA_1203100	ADP/ATP carrier protein	Essential in <i>P. berghei</i>	Essential in <i>P. berghei</i>	-
PF3D7_1037300	PBANKA_0520200	ADP/ATP transporter	-	Slow phenotype in <i>P. berghei</i>	Asexual stages (<i>P. berghei</i>)
PF3D7_1202200	PBANKA_0601100	Mitochondrial phosphate carrier protein	Essential in <i>P. berghei</i>	Essential in <i>P. berghei</i>	-
PF3D7_1223800	PBANKA_1438700	Citrate/oxoglutarate carrier protein	Dispensible in <i>P. berghei</i>	Dispensible in <i>P. berghei</i>	-
PF3D7_1241600	PBANKA_1455000	Mitochondrial carrier protein	Essential in <i>P. berghei</i>	Essential in <i>P. berghei</i>	-
PF3D7_0613300	PBANKA_0111600	Rhoptry protein ROP14	Dispensible in <i>P. berghei</i>	Dispensible in <i>P. berghei</i>	-
PF3D7_0103200	PBANKA_0209900	NT4	Dispensible in <i>P. berghei</i>	Dispensible in <i>P. berghei</i>	-
PF3D7_0824400	PBANKA_0706200	NT2	Dispensible in <i>P. berghei</i>	Slow phenotype in <i>P. berghei</i>	Asexual stages (<i>P. berghei</i>)
PF3D7_1347200	PBANKA_1360100	NT1	Dispensible in <i>P. falciparum</i> and <i>P. berghei</i>	Slow phenotype in <i>P. berghei</i>	Asexual (<i>P. falciparum</i> and <i>P. berghei</i>) and gametocytes (<i>P. berghei</i>)
PF3D7_1223700	PBANKA_1438600	Iron transporter	Dispensible in <i>P. berghei</i>	Dispensible in <i>P. berghei</i>	Asexual stages (<i>P. berghei</i>)
PF3D7_0614300	PBANKA_0112500	Organic anion transporter	Dispensible in <i>P. berghei</i>	Dispensible in <i>P. berghei</i>	Asexual stages (<i>P. berghei</i>)
PF3D7_1421900	PBANKA_1021500	Copper transporter	Dispensible in <i>P. berghei</i>	Not determined	-
PF3D7_1439000	PBANKA_1302900	Copper transporter	Dispensible in <i>P. berghei</i>	Not determined	-
PF3D7_0628400	PBANKA_1127100	Conserved Plasmodium membrane protein, unknown function	Dispensible in <i>P. berghei</i>	Dispensible in <i>P. berghei</i>	-
Other transporters					
PF3D7_0315700	PBANKA_0413500	Conserved Plasmodium membrane protein, unknown function	Dispensible in <i>P. berghei</i>	Dispensible in <i>P. berghei</i>	-
PF3D7_1404600	PBANKA_1037500	Adenylyl cyclase alpha (ACalpha)	Dispensible in <i>P. berghei</i>	Not determined	-
PF3D7_0824700	PBANKA_0705900	Lipase maturation factor	Dispensible in <i>P. berghei</i>	Slow phenotype in <i>P. berghei</i>	Asexual stages (<i>P. berghei</i>)
PF3D7_1135300	PBANKA_0913200	Conserved Plasmodium membrane protein, unknown function	Essential in <i>P. berghei</i>	Essential in <i>P. berghei</i>	-
PF3D7_1203400	PBANKA_0602400	Transporter	Dispensible in <i>P. berghei</i>	Dispensible in <i>P. berghei</i>	Asexual stages (<i>P. berghei</i>)